(Trifluoromethyl)phenyldiazirines in Photoaffinity Labeling: Improved Synthesis, Functionalization, and Application

(トリフルオロメチルジアジリンによる光アフィニティーラベル：改良合成、機能化およびその利用)

Doctoral Thesis

(The Special Postgraduate Program in Biosphere Sustainability Science)

(生存基盤科学特別コース 博士後期課程)

Wang Lei

オウ ライ

Division of Applied Bioscience, Graduate School of Agriculture,

Hokkaido University, Japan

2016.09

TABLE OF CONTENTS

Acknowledgements

First, I really appreciate my supervisor, associate professor Dr. Makoto Hashimoto for the guidance for five years. Under his scrupulous instruction and scholastic guidance, I learned a lot. It is just his intellectual suggestion that help me to solve the problems existed during my daily research work. His creative viewpoint and comprehensive consideration are of great importance to direct me in the academic research. His enthusiastic and nice plans for the students' future benefit me a lot. Under the direction of him, all of the student can exert their own advantages.

I would like to show my thanks to Prof. Dr. Yasuyuki Hashidoko for his constructive advice and valuable comments that are valuable for me to solve problems and inspire good ideas. Furthermore, I really appreciate associate professor Dr. Xiufeng Wang for her kind help to my family. I am thankful to lecturer Dr. Yasuko Sakihama for her assistance during my study in my lab. Great thanks should be given to assistant professor Dr. Yuta Murai for his kind help and suggestion for my research work. I also thank Prof. Dr. Makoto Ubukata and associate professor Dr. Matsuura Hideyuki for checking my PhD thesis. Special appreciation should be given to Prof. Dr. Weijie Zhao (Dalian University of Technology, China) for his help during the application of study in Hokkaido University. Appreciation is also extended to all of the members in Lab of Molecular and Ecological Chemistry.

I really want to show my thanks to Japanese Government (Monbukagakusho) Scholarship for supporting me from master to doctor course. With this support, I can focus all my attention on my research work. Many thanks should be given to Chinese Government and Chinese Embassies in Japan.

I honestly present my gratitude to my family for their support, love and tolerance. Notably, I have to thank my wife for her understanding and support. Her comforts when I was in low mood, and her encourages after I got a little achievement are of great importance for my daily life and research work. Besides, I would like to talk to my daughter: you really give me so much happiness, thank you! With all of the bless and supports, I will continue to work harder and present a nice job in the next stage.

Abbreviations

d	Day
DMF	*N*, *N*-Dimethylformamide
DMSO	Dimethyl sulfoxide
et al.	And others (*et alii*)
ESI-MS	Electrospray ionization mass spectrometry
g	Gram
h	Hour
HPLC	High performance liquid chromatography
mM	0.001 Mole per liter
min	Minute
mL	Milliliter
NMR	Nuclear magnetic resonance
PAL	Photoaffinity labeling
RT	Room temperature
temp	Temperature
THF	Tetrahydrofuran
TLC	Thin layer chromatography
TPD	3-(Trifluoromethyl)-3-phenyldiazirine
(Tmd)Phe	Trifluoromethyldiazirinyl phenylalanine
UV	Ultraviolet

1. Introduction and Brief Summary

1.1 Photoaffinity labeling

The study of interactions between bioactive molecules and receptors has emerged as an important topic for understanding of the physiological activity of humans. Furthermore, the identification of targeted proteins and the corresponding binding sites are of great importance for drug discovery and design. For these purposes, a genetic method has been used as an indirect strategy to pinpoint the functional amino acids via deletion or mutation of the native amino acids alignments. 3D Structural determination involving homology modeling and NMR analysis are able to confirm the structures of proteins with a certain quantities. Chemical methods via the modification of ligands with a detection tag or functional group provide a direct strategy to identify the interactions between ligands and receptors. Among of them, photoaffinity labeling (PAL)[1] has emerged as an indispensable strategy to find out the corresponding interaction information in biochemistry field.

Figure 1.1 Photoaffinity labeling probe and photoaffinity labeling.

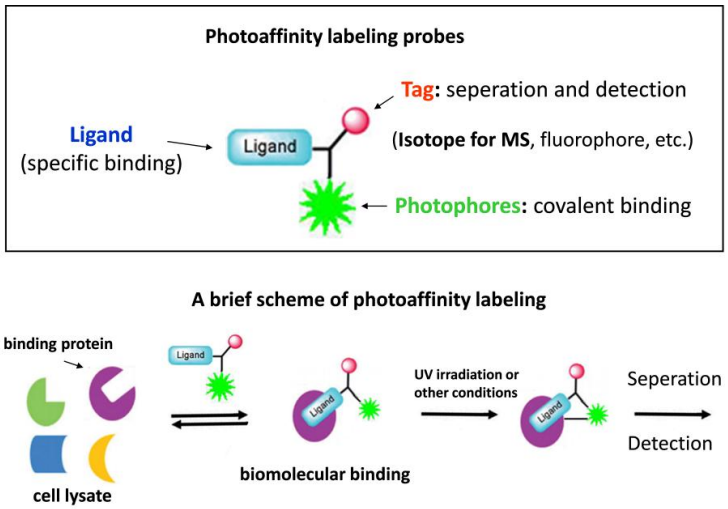

PAL was firstly introduced by Frank Westheimer in the 1960s. Since then, it has been greatly improved and used as an effective strategy to investigate the interactions between ligands and receptors. Generally, photoaffinity labeling probes consist of three components: the ligands or bioactive molecules, photophores, and the tags (Figure 1.1). The ligands can get to and react with receptors to form the desired binding. Photophores can be converted into highly reactive intermediates under the UV irradiation that can construct covalent binding between the ligands and proteins. Currently, there are three major types of photophores used in PAL field: arylazides[2], benzophenones[3] and diazirines[4]. The tags are used for the further separation and detection. Radioactive isotope[5], fluorophore[6], and affinity tag[7] are the widely detection tags for these purpose. Radioactive isotope has been used as a detection tag for many decades. Due to its relatively high radioactivity, radioactive isotope is able to detect labeled component. However, the limited radiolabeled reagents greatly make the synthetic procedure slight difficult. Recently, the combination of stable isotopes and MS analysis has been used as an effective strategy to identify the labeled component because of the significant difference of mass number for stable isotope-labeled and -unlabeled components.[8] Compared with radioactive isotope, stable isotopes are more easily to handle and to introduce into the desired skeletons. Fluorophores, or fluorochromes, are the compounds that are able to re-emit light under light excitation. With a fluorescence microscope, the labeled component can be imaged and detected. The biotin was widely used as the affinity tag due to its high affinity towards avidins (K_d=10^{-15}M).[9] As an alternative strategy, click reactions between alkynes and azides are widely used to decrease the huge structure of biotin that can affect the labeling efficiency. Recently, many kinds of interaction have been successfully identified by PAL such as ligand-protein (drug, inhibitor), proteins-proteins, protein-nucleic acid, or protein-cofactor.[10]

1.2 Photophores

To select an ideal photophore (Figure 1.2), many factors should be considered: close resemblence to biomolecule with similar affinity and less steric hindrance; stability in the dark at various pH conditions; suitable wavelengths that do minimal or no damage to the biomolecules and generation of highly reactive intermediate under UV irradiation; adaptability to react with different bonds without any preference and to form stable linking with receptor to survive the further detection. However, to get the right photophore that can meet all of the requirements is not easy.

Figure 1.2 Photophores used in the field of PAL.

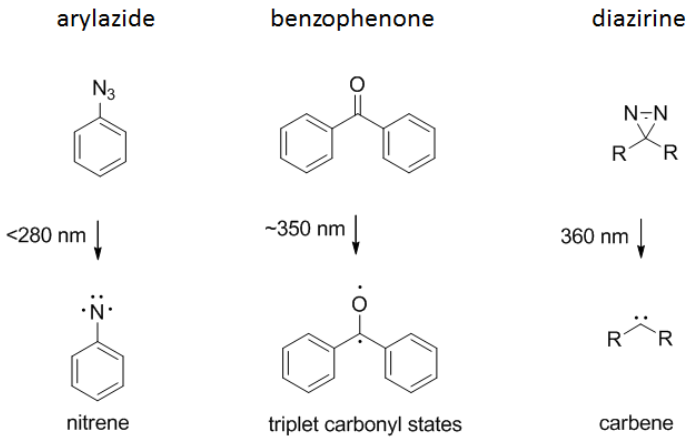

Arylazides are a kind of aromatic rings that were substituted with N_3 group. They are easily synthesized but they are activated under the wavelength of 300 nm which will result in the damage of biomolecules. Furthermore, nitrenes[11], its activated intermediate, can rearrange into keteimines as byproducts leading to undesired labeling in PAL field.[12]

Benzophenones generate reactive triplet carbonyl states upon irradiation around 350 nm. They are stable towards the solvents and its irradiation wavelength is longer.

However, photoreaction with benzophenones required longer times which is the major disadvantage limit their application.[13]

Diazirines are a kind of three-membered ring structures that containing two nitrogen and one carbon atoms.[14] Under the UV irradiation around 350 nm, it can be converted to carbenes that are more reactive compared with other photophores. The cross-linking with biomolecules can be constructed with shorter time. Viewed from the structures diazirines can be categorized as two types: aliphatic diazirines and aromatic diazirines (Figure 1.3). Among all of the photophores, 3-(trifluoromethyl)-3-phenyldiazirine (TPD)[15] is the most promising reagent used in the field of PAL.

Figure 1.3 Two types of diazirines and TPD.

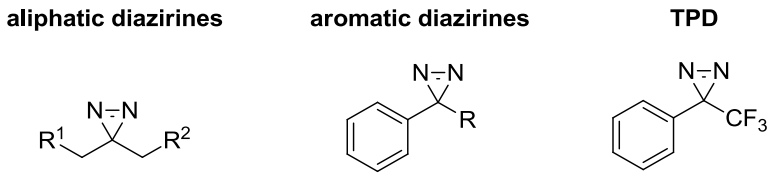

It was well known that aliphatic diazirines[16] are preferred in the field of PAL due to their relatively small size. Furthermore, under UV irradiation, diazirine can be converted to carbenes which are highly reactive.[17] The diazo isomerization is the major reason that leads to the undesired labeling for diazirine-based photoaffinity labeling. The diazos are less reactive and have longer lifetime. To solve this problem, in 1980, Brunner et al modified the aromatic diazirine by introducing a trifluoromethyl group to the carbon of diazirine to form TPD and the results indicated that the diazo isomerization are significantly inhibited.[15] The trifluoromethyl group can stabilize the carbene preventing it from further rearrangements. Furthermore, diazo isomer is so strongly stabilized in the presence of trifluoromethyl group as a

strong electron-withdrawing group. It has been estimated that around 65% of the diazirines can be converted to carbenes and other 35% were converted to 1-phenyl-2, 2, 2-trifluoromethyl-3-diazomethane by using UV-vis absorption spectra. In the field of photoorganic chemistry, the isomerizations to form diazo compounds are one of the major side reactions for irradiations of diazirines. While, it was found that the generation of carbene was greatly increased when the ligands concentration is less than 1 mM.[18] Many reports show that aromatic diazirines can generate more carbenes than aliphatic diazirines.[19-21]

1.3 3-(Trifluoromethyl)-3-phenyldiazirine (TPD)

Figure 1.4 TPD-based photoaffinity labeling.

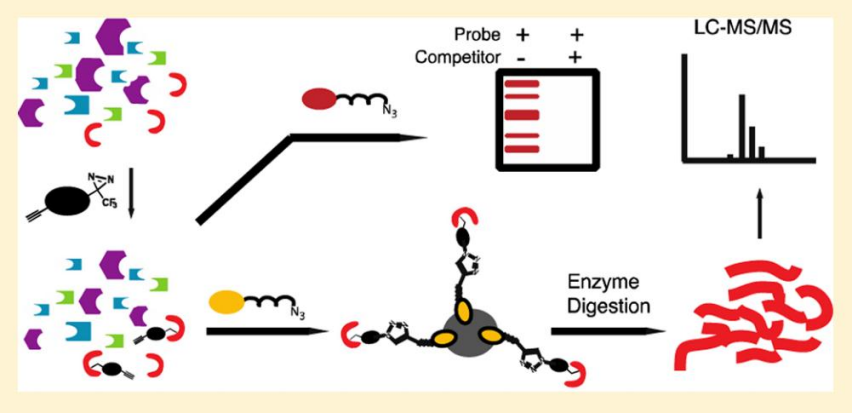

TPD has emerged as the most effective photoreactive group in photoaffinity labeling due to its thermal and chemical stability, long irradiation wavelength, low rate of rearrangement and high reactivity of its intermediate (Figure 1.4). However, compared with other photophores, the preparation of TPD required many steps.

As shown in Scheme 1.1, the preparation of aliphatic diazirine required two steps using ketone as the starting materials. The ketone precursor is initially treated with methanolic ammonia or liquid ammonia to form imine which is further converted to

diaziridine with the addition of hydroxylamine-*O*-sulfonic acid. Then, the diaziridine is subjected to oxidation by silver oxide or iodine in the presence of triethylamine to give the corresponding aliphatic diazirines.[22, 23] To prepare TPD, trifluoroacetophenones are commonly used as the precursors that are further subjected to four steps to afford TPD. Briefly, trifluoroacetophenones are firstly convent to oximes under Under the oximation with hydroxylammonium chloride at 60-85 °C. Then, tosylation[24] and mesylation[25] are used as the alternative strategies: in the presence of *p*-TsCl or MsCl, the tosyl or mesyl oximes were easily prepared. While, due to the unstability and relatively high toxicity of MsCl, tosylation with *p*-TsCl is the widely used strategy for this purpose. Next, tosyl or mesyl oximes were subjected to ammonia to afford diaziridine which are the key intermediate to construct diazirinyl ring. Finally, diazirines products were synthesized through the oxidation of the diaziridines with various oxidants such as Ag_2O[22], I_2/NEt_3[26], oxalyl chloride[27] or $(CH_3)_3COCl$[28].

Scheme 1.1 Synthetic procedure of aliphatic diazirines and TPD.

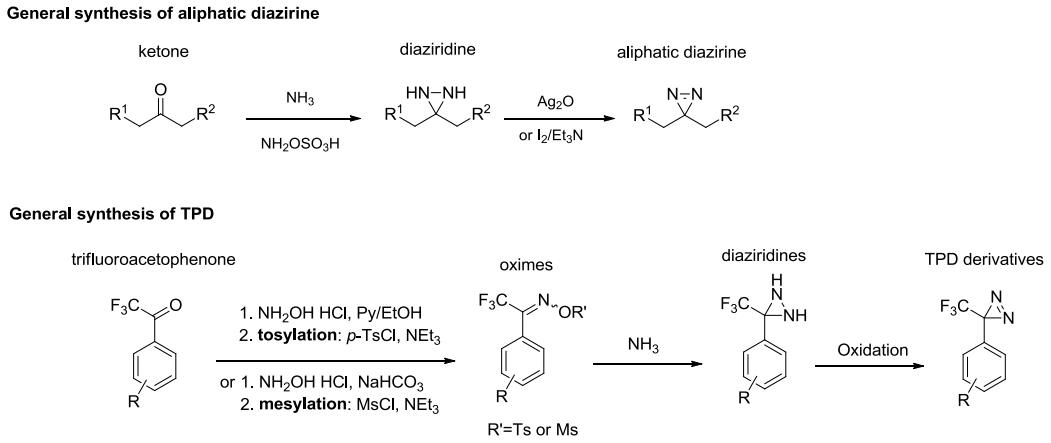

1.4 Brief summary

On the basis of the great importance of TPD or TPD-based photoaffinity labeling

probes in the field of PAL, my work were carried out around TPD including the improved synthesis, functionalization (deuteration and metabolic study) and further application.

1 Improved synthesis of TPD and corresponding application

Scheme 1.2 One-pot synthesis of TPD from tosyloxime and application.

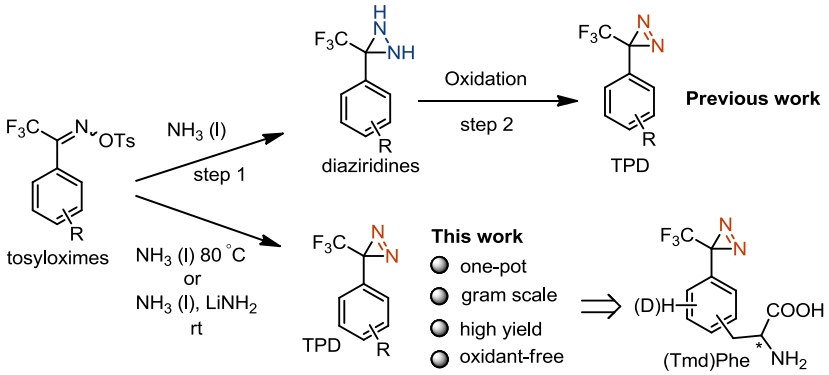

Lei Wang, *et al*. *Org. Lett*. **2015**, *17*, 616.

Despite of the advantages of TPD and TPD-based photoaffinity labeling probes, their long synthetic procedure are urgent to be solved to further broaden the application of TPD in the field of PAL. To shorten the synthesis of TPD and develop diverse synthetic method, we developed a one-pot synthesis of TPD derivatives from the corresponding tosyloximes (Scheme 1.2).[29] Under liquid ammonia at 80 °C or with addition of $LiNH_2$ at room temperature in a sealed tube, TPD can be readily constructed without the isolation of diaziridine. Mechanism investigation indicated that the NH_2^- generated from liquid ammonia or $LiNH_2$ are responsible for the formation of TPD from diaziridine. Involved which, a novel synthetic strategy of optically pure diazirinylphenylalanines for photoaffinity labeling were reported.

2 TfOD-mediated H/D exchange of cross-linkable aromatic α-amino acids

The combination of deuteration and MS analysis is an effective strategy for quantitative analysis of α-amino acids and peptides in the field of PAL. While, the low solubility of α-amino acids in conventional method for synthesis of deuterated derivatives have yet to be resolved. Furthermore, for many conventional methods, high temperature and high pressure are sometimes required to make the reaction frequent. Recently, our group reported a novel hydrogen/deuterium (H/D) exchange for preparing deuterated α-aromatic amino acids and the corresponding peptides in the presence of deuterated triflic acid (TfOD).[30] This method has many advantages such as reaction feasibility at low temperature and the controllability especially the good solubility for α-amino acid derivatives (Scheme 1.3). To further broaden its application, we carried out an H/D exchange study for cross-linkable aromatic α-amino acids in the presence of TfOD.[31]

Scheme 1.3 H/D exchange of aromatic α-amino acids by TfOD.

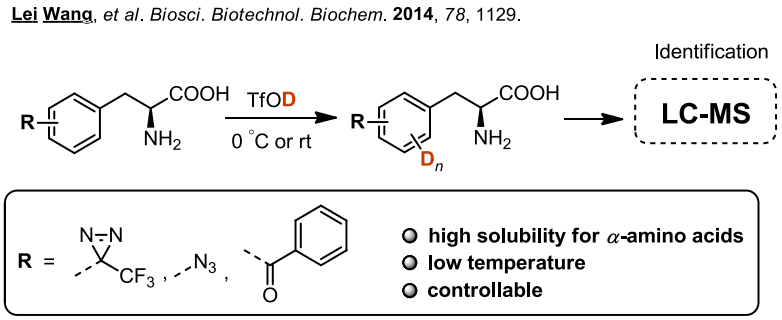

3 Metabolic studies of photoreactive aromatic α-amino acid derivatives with Klebsiella sp. CK6

Photophore-based L-phenylalanines are useful building blocks for biological functional analysis of peptides and the corresponding proteins. However, their metabolic studies with microorganism are rarely reported in previous work. As a basic work to extend photoaffinity labeling to microorganism, we reported comparative

analysis of metabolites from inoculation of photoreactive groups-based L-phenylalanine derivatives with *Klebsiella* sp. CK6 (Scheme 1.4).[32] The metabolites were identified and compared with that of normal L-phenylalanine and L-tryptophan and the influence factors for the metabolites formation were also discussed in this work.

Scheme 1.4 Metabolic investigation of photoreactive aromatic α-amino acids in *Klebsiella* sp. CK6.

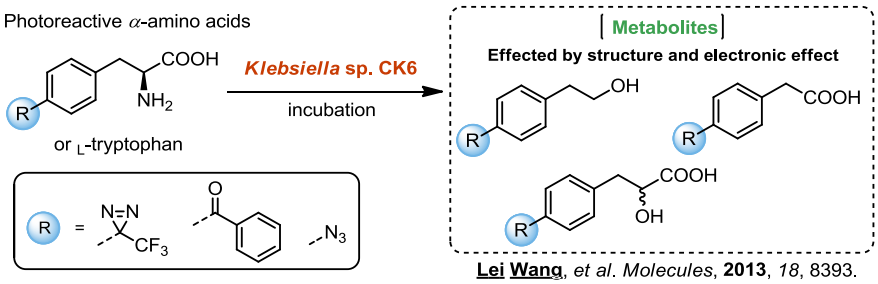

4 TPD-based photoreactive saccharins for photoaffinity labeling of gustatory receptors

Scheme 1.5 Preparation of diazirine-based photoreactive saccharin.

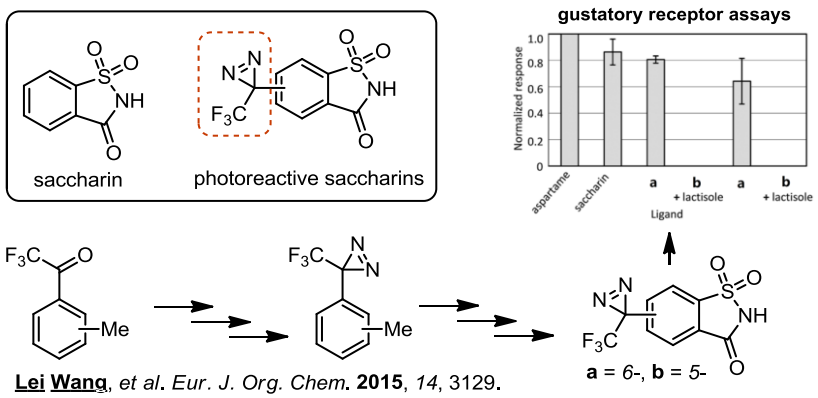

Saccharin is a common artificial sweetener that is hundred times sweeter than sucrose. While, its receptor binding conformations of the sweeteners remain unclear because of the limited structural information of the ligands complexes with their receptor. To prepare photoreactive saccharin is a kind of useful strategy to investigate corresponding binding information. In this work, we prepared photoreactive saccharin derivatives containing diazirinyl moiety at the 5- and 6- position involving the previous described one-pot reaction (Scheme 1.5).[33] The syntheses procedures are more convenient and efficient. Both of the photoreactive compounds have enough affinity for the investigation of the sweet and bitter receptors for photoaffinity labeling.

5 Preparation of photoreactive 1'-sucrose: a cosolvent-promoted O-benzylation strategy with silver(I) oxide

Scheme 1.6 Cosolvent-promoted O-benzylation of 1'-sucrose with silver(I) oxide.

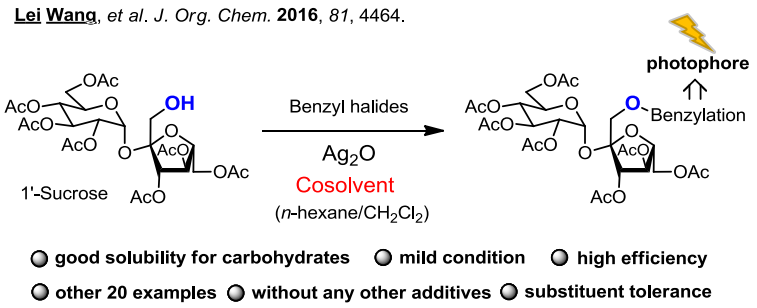

Sucrose, one of the widely used sweeteners, serves as a crucial component for the preparation of surfactants, macrocyclic derivatives, functional materials, food additives, and pharmaceutical compounds. The modification of the 1'-position to prepare nonnatural sucrose is the widely used strategy to investigate sucrose carrier protein and the physiology of sucrose transport. While, the 1'-hydroxyl presents the

lowest reactivity in many reactions, which brings many challenges for the further modification of 1'-position of sucrose. Silver(I) oxide (Ag_2O)-mediated O-benzylation has emerged as an indispensable strategy in carbohydrates field and synthetic chemistry. However, many reports meet the problems such as the excess use of reagents, preparation of fresh Ag_2O and low reaction yields. Furthermore, the poor solubility of the substrates is urgent to be solved. Hence, we developed a cosolvent-promoted O-benzylation strategy with Ag_2O that can not only improve the reaction solubility for carbohydrates but also increase the benzylation efficiency.[34] Notably, TPD skeleton was successfully introduced into the 1'-position to prepare a 1'-photoreactive sucrose derivative which acts as a promising reagent to investigate sucrose and its receptor in the field of PAL.

2. Improved Synthesis of TPD and Corresponding Application

2.1 Introduction

Scheme 2.1 Conventional preparation of TPD from tosyloxime and our finding.

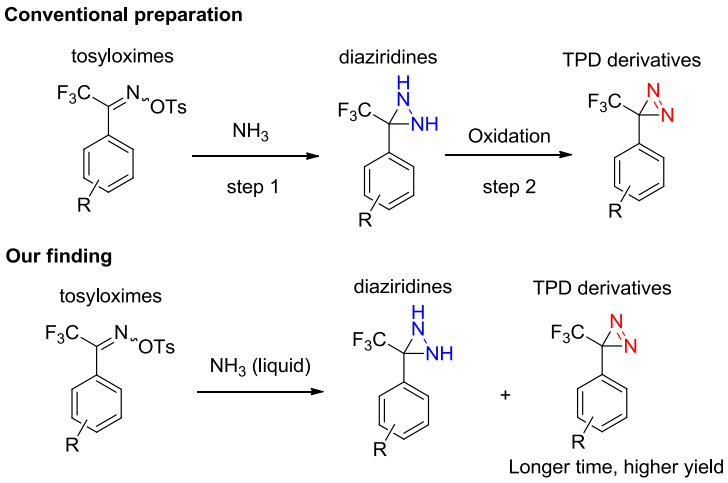

Viewed from the synthetic procedures of TPD, the construction of diaziridine from tosyloxime is a crucial step to afford the three-membered ring of diazirine. Under the further oxidation, the TPD can be prepared. To prepare diaziridine from tosyloxime, either methanolic ammonia or liquid ammonia is available. While, for the synthesis of diaziridine from tosyloxime in liquid ammonia system, we found that the TPD sometimes generated (Scheme 2.1). Thus, we supposed whether the formation of TPD can be improved in this reaction through the further reaction optimization. Many control experiments were carried out and the results showed that the generation of TPD is consistent with the reaction time which means that the reactions with longer time lead to more TPD. Inspired by this result, we would like to optimize the reaction to further improve the formation of TPD.

2.2 Results and Discussion

2.2.1 Optimization of the reaction conditions

Table 2.1 Reaction optimization of the one-pot synthesis of TPD.[a]

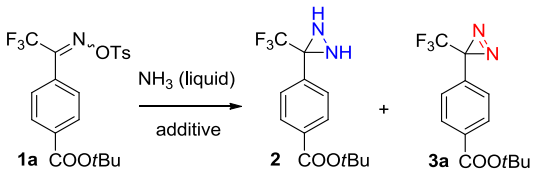

Entry	solvent	temp(°C)	time (h)	yield **2**/**3a** (%)
1	Et_2O	rt	1	100/0
2	Et_2O	rt	12	82/18
3	Et_2O	rt	96	3/97
4	Et_2O	60	8	0/100
5[c]	Et_2O	80	4	0/100 (97)
6[c]	CH_2Cl_2	80	4.5	0/100
7[c]	THF	80	5	0/100
8[c]		80	4	0/100
9[d]		80	4	100/0
10[ce]	Et_2O	80	4	84/16

[a]Reaction Conditions: **1a** (0.3 mmol), solvent (0.5 ml), liquid NH_3 (5 ml) in a sealed tube. [b]Yields were determined by ^{1}H-NMR spectroscopy, Isolated yield of **3a** in parenthese. [c]Liquid NH_3 (10 ml) was used. [d]**1a** was directly treated with gaseous NH_3 at 80 °C in a sealed tube. [e]NH_4Cl (5 equiv) was added.

Initially, tosyloxime **1a** was used as the model substrate. When it was reaction with liquid ammonia at room temperature for 1 h, no TPD **3a** detected (Table 2.1). Interestingly, prolong the reaction time to 12 h, 18% of TPD was found in the reaction

mixture, and 97% of TPD was formed in the reaction carried out for 96 h. Inspired by these results, we would like to perform the reaction at high temperature. The reaction performed at 60 °C significantly improved the formation of TPD and reaction completed within 8 h. Notably, optimal result was obtained for the reaction carried out 80 °C and the reaction came to completion with 4 h. While, the reaction performed at 100 °C lead to a complex mixtures which should be due to decomposition of diazirine

Figure 2.1 ^{19}F NMR of **1a**, **2**, **3a** and reaction mixtures at different temperature.

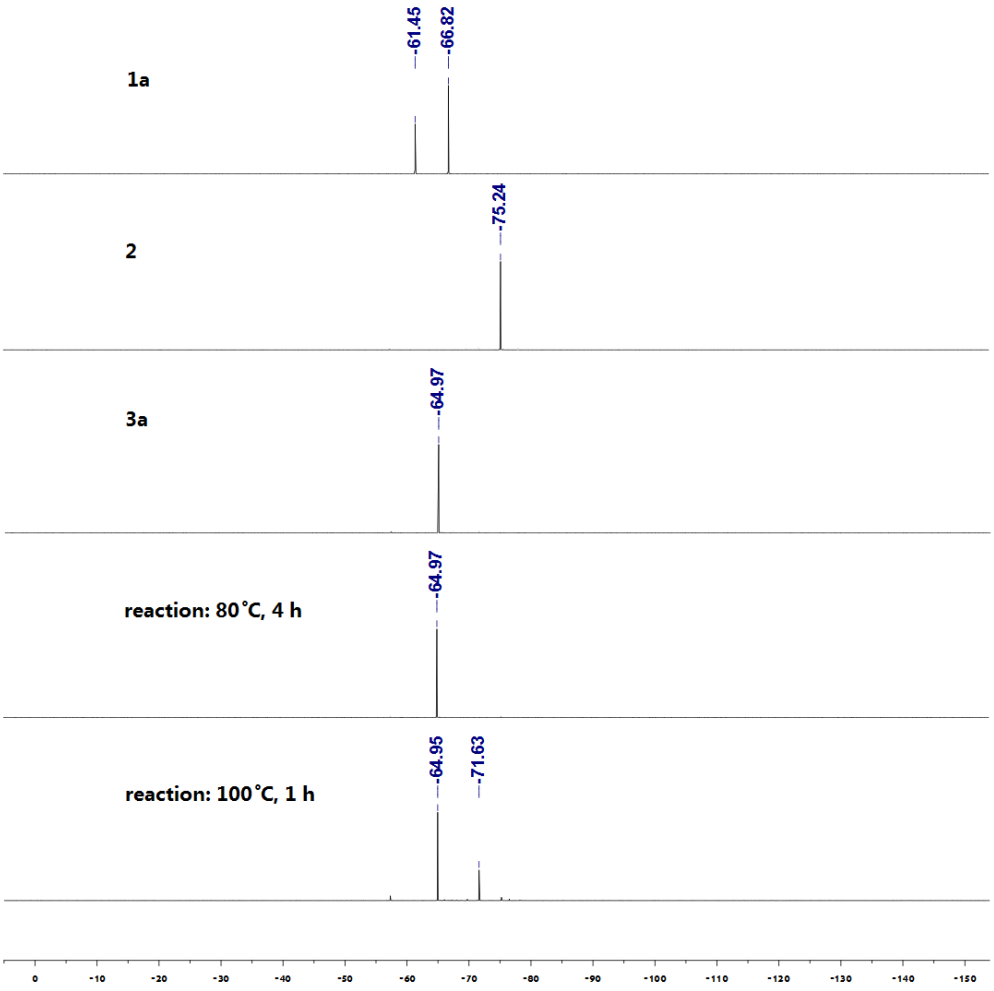

ring (Figure 2.1). To examine the solvent effect on the formation of TPD, several

experiments are carried out in CH_2Cl_2 and THF or without solvent. All of the reaction can afford to TPD in good yields. To find out the responsible species for the one-pot synthesis of TPD from tosyloxime, we performed two important control experiments. One is that tosyloxime was directly treated with ammonia gas at 80 °C. After 4 h, we found that no TPD **3a** generated and diaziridine was detected as the solo product indicating the liquid ammonia is essential for the formation of TPD. It was well known that self-ionization of liquid ammonia (Scheme 2.2) existed even though the self-ionization constant is low (pK_a=27.6 at 25 ℃)[35]. Therefore, we postulated that NH_2^- species generated form liquid ammonia[36] was responsible for the construction of TPD. A control experiment with NH_4Cl as an ion counter to inhibit the generation of NH_2^- also confirmed this hypothesis.

Scheme 2.2 Self-ionization of liquid ammonia.

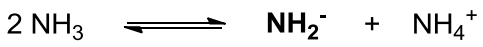

2.2.2 Kinetic investigation of one-pot synthesis of TPD

To clearly present the conversion of the substrates in the one-pot reaction and to find out the reaction process clearly, we performed a kinetic investigation of the model reaction and the ratios of the substrates were detected by ^{1}H NMR (Figure 2.2).

As shown in the kinetic curve plotas well as the ^{1}H NMR, the tosyloxime **1a** was consumed rapidly with the formation of diaziridine **2**. Within 10 min, all of tosyloxime was converted to diaziridine **2**. Next, TPD **3a** gradually generated from diaziridine and the conversion ratio reach to 100% with 4 h. These results indicated that in this one-pot reaction, diaziridine also act as the intermediate that can continuous afford to TPD in the same reaction.

Figure 2.2 Kinetic investigation of one-pot synthesis of **3a**.

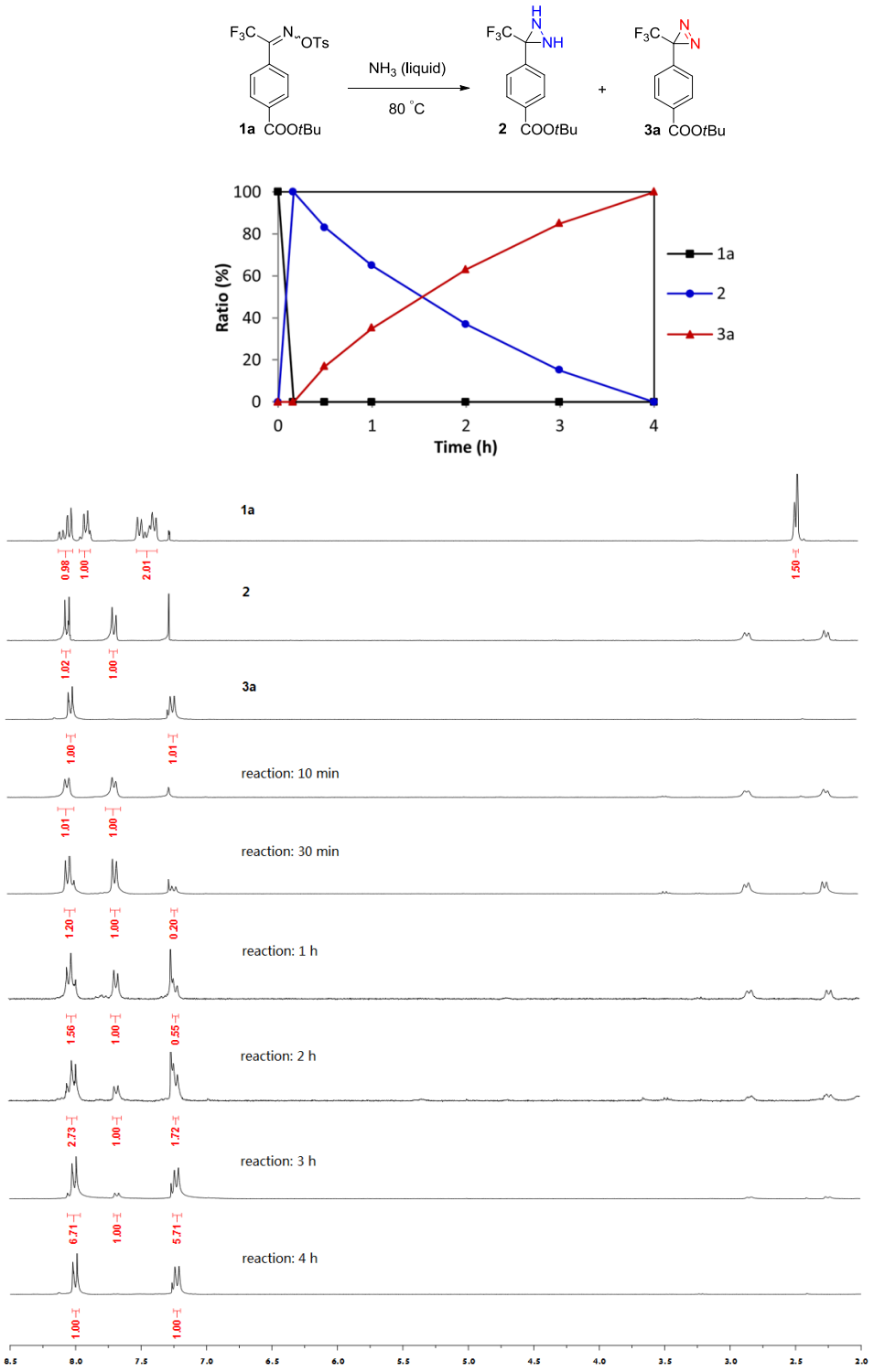

2.2.3 Alkali amide as NH_2^- supplier in liquid NH_3

To decrease the reaction temperature and broaden the application of this one-pot reaction, we carried out a serious of experiments with alkali amide as NH_2^- supplier in liquid ammonia. Lithium amide was firstly tested, but the reaction carried out -70 °C

Table 2.2 Alkali amide as NH_2^- supplier for the one-pot synthesis of TPD.[a]

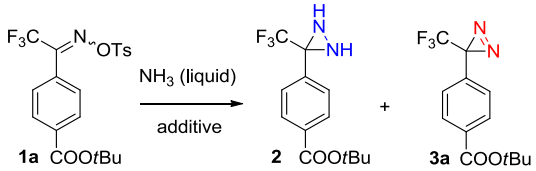

Entry	solvent	temp(°C)	additive (equiv)	time (h)	yield **2**/**3a** (%)
1	Et_2O	-78	$LiNH_2$ (5)	12	100/0
2	Et_2O	0	$LiNH_2$ (5)	10	0/100
3	Et_2O	rt	$LiNH_2$ (5)	4	0/100 (96)
4	Et_2O	0	$NaNH_2$ (5)	1	
5	Et_2O	0	NaH (5)	1	
6	Et_2O	rt	$LiNH_2$ (10)	4	0/100
7	Et_2O	rt	$LiNH_2$ (2)	8	80/20
8	CH_2Cl_2	rt	$LiNH_2$ (5)	7	0/100
9	THF	rt	$LiNH_2$ (5)	6	0/100
10		rt	$LiNH_2$ (5)	4.5	0/100

[a]Reaction Conditions: **1a** (0.3 mmol), solvent (0.5 ml), liquid NH_3 (5 ml) in a sealed tube. [b]Yields were determined by ^{1}H-NMR spectroscopy, Isolated yield of **3a** in parenthese. [c]Liquid NH_3 (10 ml) was used. [d]**1a** was directly treated with gaseous NH_3 at 80 °C in a sealed tube. [e]NH_4Cl (5 equiv) was added.

for 12 h failed to afford TPD **3a**. As expected, the reaction at 0 °C provided **3a** in 100%

yield within 12 h. Notably, the reaction was completed within 4 h at room temperature. Sodium amide and sodium hydride can not afford to desired product due to the ammonolysis of ester. The amount of lithium amide was set as 5 equiv to maintain the reaction efficiency. Solvent optimization indicated that other solvent also work well. Furthermore, the reaction carried out without solvent gave desired product in good yields. The above work shows that the reaction carried out at room temperature with the addition of $LiNH_2$ is an alternative strategy for the one-pot synthesis of TPD from tosyloximes.

2.2.4 One-pot synthesis of TPD derivatives

Inspired by the above-mentioned results, we would like to examine the one-pot synthesis of other TPD derivatives. As shown in Table 2.3, many tosyloxime derivatives were examined in these one-pot reactions. In the field of PAL, 'post-functional' adaptation of diazirinyl compounds[37, 38] are good strategy to successfully prepared TPD-based photoaffinity labeling probes. Under certain conditions, the mother skeletons are able to convert diverse structures such as *m*-methoxy substituted TPD (**1e**) which is the commonly used skeleton for this purpose.[39] In this work, we found that electron-deficient substituted tosyloximes show relatively high reactivity compared with that substituted with electron-rich groups indicating that the electron property of substituent are crucial for the reaction. Especially for the *m*-nitro substituted TPD (**1f**), the corresponding TPD can be constructed in excellent yield within 1 h. Furthermore, for these two strategies, byproducts can be easily removed by washing with water and there is no necessary for the purification by silica gel column chromatography. This is a great advantage for the synthesis of TPD derivatives as well as the TPD-based probes in the field of PAL.

Table 2.3 One-pot synthesis of TPD derivatives.[a]

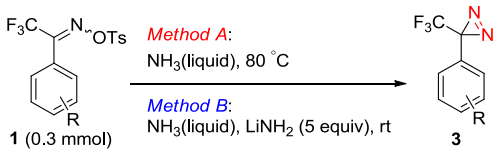

Entry	R	method	time (h)	yield **3** (%)
1	H (**1b**)	A	7	97
2	H (**1b**)	B	6	99
3	*p*-Me (**1c**)	A	11	98
4	*p*-Me (**1c**)	B	12	97
5	*m*-Me (**1d**)	A	6	99
6	*m*-Me (**1d**)	B	8	100
7	*p*-OMe (**1e**)	A	13	94
8	*p*-OMe (**1e**)	B	16	92
9	*m*-OMe (**1f**)	A	10	96
10	*m*-OMe (**1f**)	B	9	99
11	*m*-NO_2 (**1g**)	A	1	99
12	*m*-NO_2 (**1g**)	B	1	98
13	*m*-NHBoc (**1h**)	A	10	93
14	*m*-NHBoc (**1h**)	B	9	91

[a]Reaction Conditions: **1a** (0.3 mmol), solvent (0.5 ml), liquid NH_3 (5 ml) in a sealed tube. [b]Yields were determined by ^{1}H-NMR spectroscopy, Isolated yield of **3a** in parenthese. [c]Liquid NH_3 (10 ml) was used. [d]**1a** was directly treated with gaseous NH_3 at 80 °C in a sealed tube. [e]NH_4Cl (5 equiv) was added.

2.2.5 Plausible mechanism

On the basis of previous results, we outlined the plausible mechanism for the

one-pot reactions. Initially, the tosyloxime is attacked by NH_3 to construct the *gem*-diamine intermediate (I).[40] With the removal of tosyl group and proton, diaziridine **2** was formed. When the reaction was carried out at 80 °C, the NH_2^-, generated from the self-ionization of liquid NH_3, trigger the deprotonation of the diaziridine ring to afford intermediate (II). Then, the electron pair over nitrogen can attack the other one to construct TPD **3a** with the formation of NH_3 and hydrogen. For the reaction performed at RT in the presence of $LiNH_2$, the formation of TPD **3a** was triggered by the NH_2^- mainly generated form $LiNH_2$.

Scheme 2.3 Plausible mechanism of the one-pot reaction.

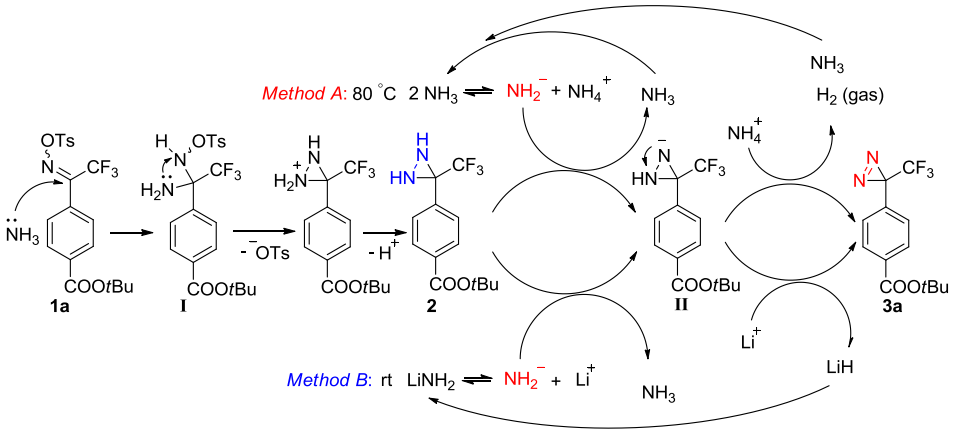

2.2.6 Preparation of optically pure (Tmd)Phe derivatives

2.2.6.1 Previous method to prepare optically pure (Tmd)Phe derivatives

Optically pure trifluoromethyldiazirinyl phenylalanine ((Tmd)Phe) derivatives are important building blocks for investigation of peptides, proteins and other biomacromolecule. Nassal, M. reported a synthesis of diazirinylphenylalanines from halogenaged TPD **4** (Scheme 2.4).[41] Via ligation with diethyl acetamido-malonate in

the presence of NaOEt, halogenaged TPD can be converted to TPD-based diester **5**. Following with the further deprotection and decarboxylation, $_{D}$, $_{L}$-*N*-acetyl(Tmd)Phe **7** were constructed. The racemates can be isolated with the enzymatic resolution of *N*-acyl amino acids. Under the treatment with acylase from *Aspergillus*, $_{L}$-(Tmd)Phe **8** and $_{D}$-*N*-acetyl(Tmd)Phe **9** were prepared.

Scheme 2.4 Synthesis of (Tmd)Phe via reaction of halogenaged TPD and diethyl acetamidomalonate.

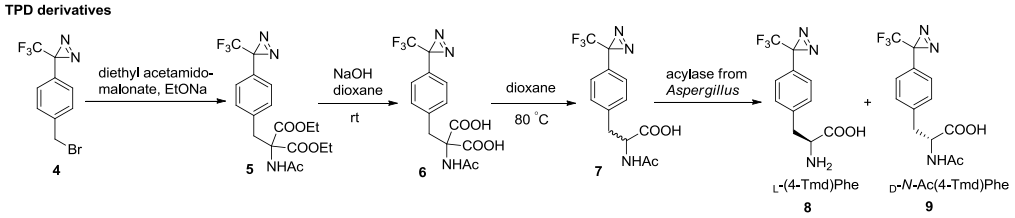

Asymmetric syntheses was also reported on the construction of (Tmd)Phe derivatives (Scheme 2.5). Fishwick, C. W. G. provided an effective method to prepare $_{L}$-(Tmd)Phe **8** via the treatment of halogenated TPD **13** and the chiral Ni complex (Scheme 2.5, a).[42] Halogenated TPD can be prepared from 4-bromobenzyl alcohol **10** through construction ketone skeleton on the benzene ring and the following procedure for TPD. The alkylation of Ni complex is the key step to prepare the stereoselective intermediate. Hydrolysis of the complex in refluxing HCl/MeOH readily afford to the desired product. Furthermore, another work was reported by Hashimoto, M.[43] It has been reported that through the reaction of halogenated TPD **4** and *tert*-butylglycinate benzophenone imine in the presence of cinchonidine-based asymmetric catalyst and 2-*tert*-butylimino-2-diethylamino-1,3-dimethylperhydro-1,3,2-diazaphosphorine (BEMP) as a base, $_{L}$-(Tmd)Phe can be easily constructed (Scheme 2.5, b).[44] In this work, Hatanaka, Y. presented a novel synthetic method for the preparation of aldehyde

TPD **16** by treating TPD **15** with dichloromethyl methyl ether in the presence of $TiCl_4$ and TfOH. Through further reduction and bromination, compound **4** was obtained. Corresponding photoreactive calmodulin-binding peptide was readily prepared via conventional solid-phase peptide synthesis. Hashimoto, M. presented a convenient work to selectively afford $_D$-(Tmd)Phe derivatives **22** and **23**: In the absence of cinchonidine-based asymmetric catalyst and BEMP, the reaction of halogenated TPD and *tert*-butylglycinate benzophenone imine can give a racemate **20** (Scheme 2.5, c). Under the treatment with $_L$-amino acid oxidase, the corresponding $_D$-type can be isolated.[45]

Scheme 2.5 Asymmetric syntheses of (Tmd)Phe.

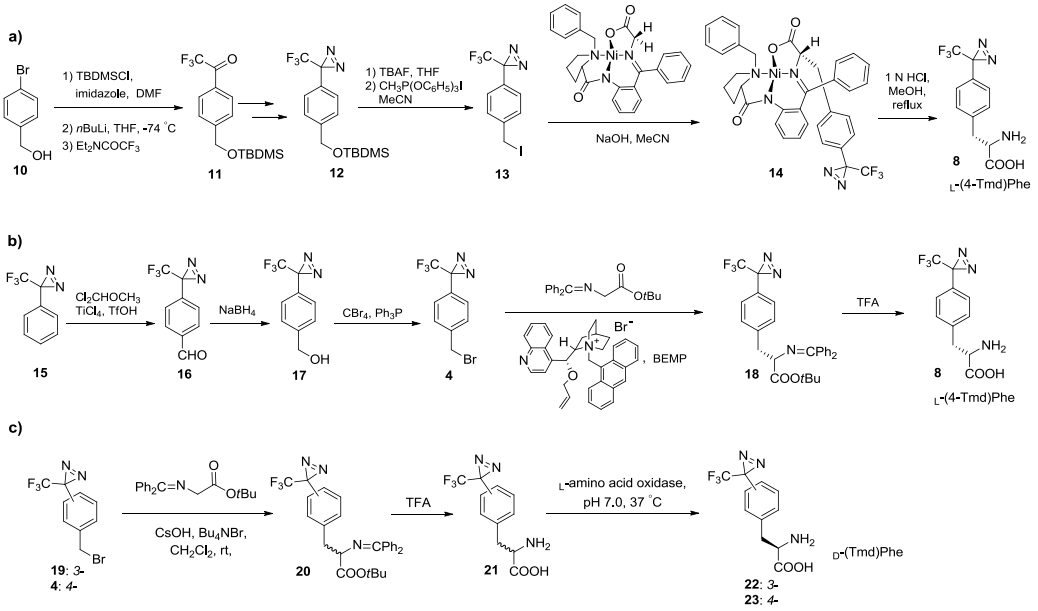

Fillion. D *et al* presented a stereospecific synthesis of Fmoc-$_L$-(4-Tmd)Phe **34** with 14% overall yield via ten steps (Scheme 2.6).[46] Firstly, diiodobenzene **24** was converted into ketone **25** by reacting organolithium salt with ethyl α, α, α-trifluoroacetate. The ketone was subjected into previous strategy for synthesis of

diaziridine derivatives **28** and the preparation of chiral moiety was started from compound **29**. Via protection and iodination, iodate chiral moiety **32** was prepared. The crucial step is a palladium-catalyzed coupling reaction between *p*-diaziridinyliodoaryl derivative **28** and diprotected *β*-iodoalanine **32** with activated Zn* and tris(dibenzylideneacetone)dipalladium(0)/tri-*o*-tolylphosphine catalyst to generate diprotected phenylalanine diaziridine **33**. Following the further oxidation and deprotection, $_{L}$-(Tmd)Phe derivative **34** was obtained.

Scheme 2.6 Stereospecific Synthesis of $_{L}$-(Tmd)Phe derivative

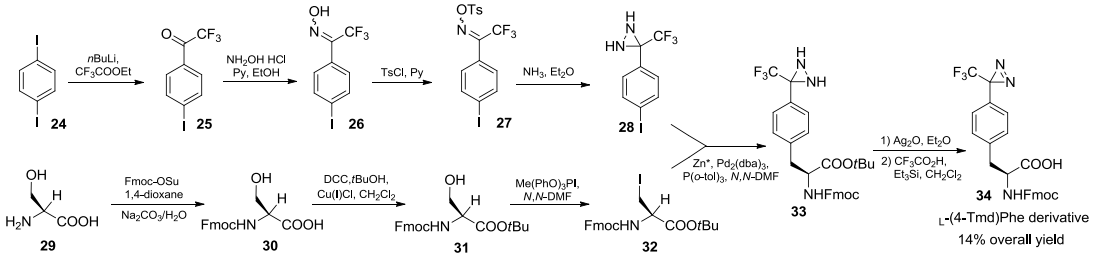

2.2.6.2 Direct construction of trifluoromethyldiazirine on optically pure phenylalanines

Due to the great importance of (Tmd)Phe derivatives, we would like to develop a new method to prepare corresponding (Tmd)Phe derivatives. Initially, commercially available $_{L}$-4-iodophenylalanine derivative **35** was used as the starting material which was protected by *tert*-butyl group to afford compound **36** (Scheme 2.7). Next, compound **36** was treated with MeLi, *t*BuLi and CF_3COOEt to afford trifluoroacetophenone **37**, through the further oximation and tosylation, tosyloxime **38** was prepared. In the presence of NH_3, tosyloxime can readily be converted to diaziridine **39**. Under the further oxidation in the precence of MnO_2, (Tmd)Phe derivative **40** was obtained which was subjected into the following deprotection with TFA to give corresponding (Tmd)Phe slat. Then, the one-pot strategy was tested in

this work and the results indicated that with the addition of $LiNH_2$, the racemization of phenylalanine usually occurred. And the reaction carried out in liquid NH_3 at 80 °C could afford to $_L$-(4-Tmd)Phe in good chiral purity.

Scheme 2.7 Construction of trifluoromethyldiazirine on optically pure $_L$-phenylalanine

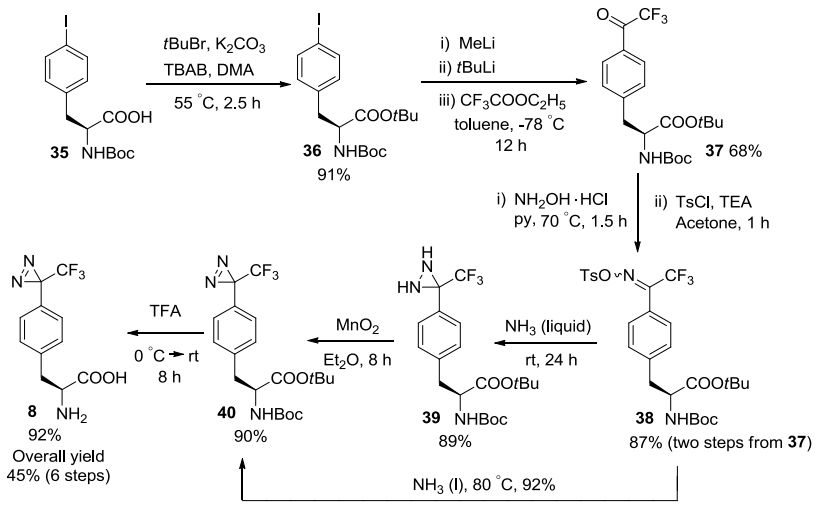

Figure 2.3 UV Spectrum of **8** after different periods of irradiation with CH_3OH

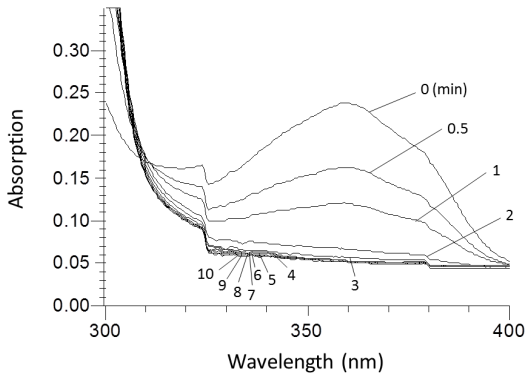

Next, the photoreactivity was tested with CH_3OH under UV irradiation and the half-life was calculated as 1.3 min indicating its good photoreactivity. To confirm the

photoproducts, we carried out the photoreactions of **8** with CH_3OH and CD_3OD, respectively. And the mixtures were directly subjected to MS analysis for the investigation of photoreaction products.

Figure 2.4 Mass analysis of **8** after UV irradiation with CH_3OH

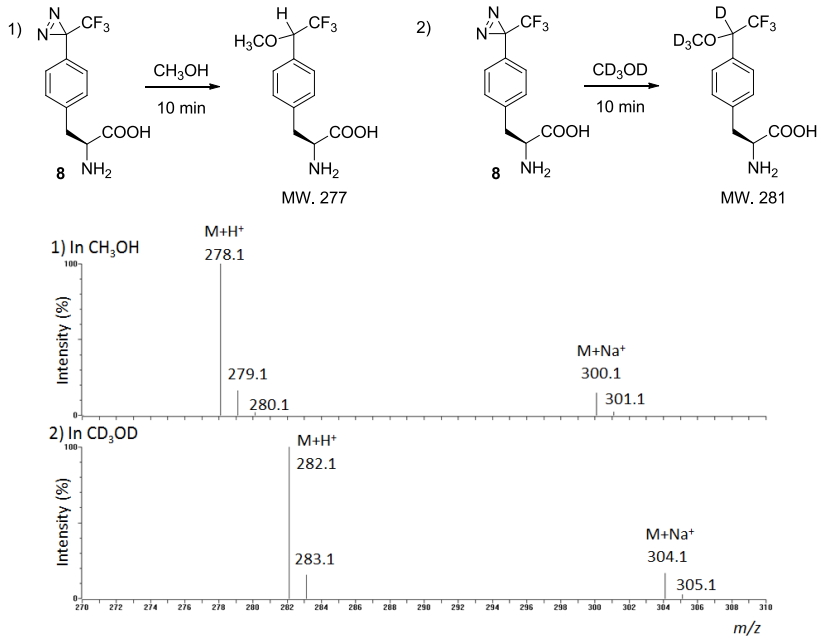

Scheme 2.8 Syntheses of other (Tmd)Phe derivatives

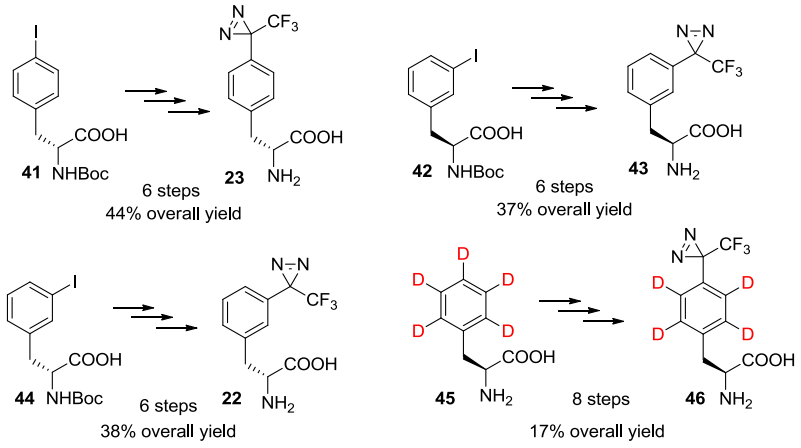

Inspired by these results, preparation of other (Tmd)Phe derivatives were carried

out including $_{D}$-(4-Tmd)Phe **23**, $_{L}$-(3-Tmd)Phe **43**, $_{D}$-(3-Tmd)Phe **22** and deuterated $_{L}$-(4-Tmd)Phe **46**. All the products can be obtained in good overall yields.

2.3 Experimental Section

2.3.1 Synthesis of tosyloximes

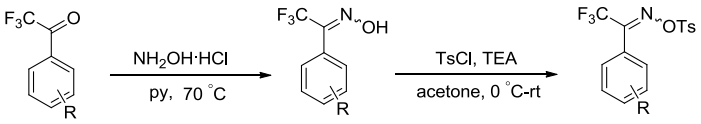

Step 1: synthesis of oximes: 2,2,2-Trifluoro-1-phenylethanone (7 mmol) was dissolved in pyridine (30 mL), then hydroxylamine hydrochloride (1.2 equiv) was added. The mixture was stirred at 70 ℃ for 1 h and was then subjected to rotary evaporation to remove pyridine. The residue was dissolved in ethyl acetate and washed with 1 M HCl, the organic layer was washed with H_2O and brine, dried over $MgSO_4$ and evaporated. The residue was directly used in next step without further purification.

Step 2: synthesis of tosyloximes: To a solution of oxime (5 mmol) in acetone (30 mL) at 0 ℃, triethylamine (3 equiv) was added. Then, *p*-toluenesulfonyl chloride (1.2 equiv) was added to the reaction mixture which was stirred at room temperature for 1 h. After evaporation, the residue was purified by silica gel column chromatography (EtOAc/hexane, 1:3) to afford pure products.

2.3.2 One-pot synthesis of TPD derivatives from corresponding tosyloximes

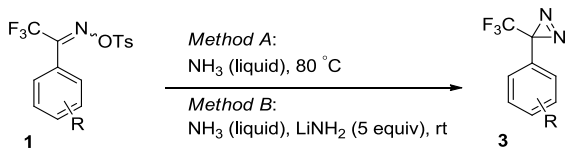

Method A: To liquid NH_3 (10 mL) at -78 ℃ in a sealed tube, tosyloxime (0.3 mmol) in Et_2O (0.5 mL) was added. The reaction was stirred at 80 ℃ until the reaction was

completed. *Method B*: To liquid NH_3 (5 mL) at -78 ℃ in a sealed tube, tosyloxime (0.3 mmol) in Et_2O (0.5 mL) and $LiNH_2$ (5 equiv) was added. The reaction was stirred at room temperature until the reaction was completed.

Post-treatment: *Procedure for* **3a, 3g** and **3h**: After removed the ammonia, the solution was partitioned between Et_2O (30 mL) and H_2O (30 mL). The organic layer was washed by H_2O (three times), brine, dried over $MgSO_4$ and evaporated to afford the desired product. *Procedure for* **3b-3f**: The sealed tube was cooled at -78 ℃ and Et_2O (30 mL) was added. The sealed tube was warmed at room temperature to remove the ammonia gradually. The organic layer was washed by H_2O (three times), brine, dried over $MgSO_4$ and carefully evaporated (0 ℃) to afford the desired product.

2.3.3 Synthesis of deuterated Boc-$_L$-Phe(4-I)-OH

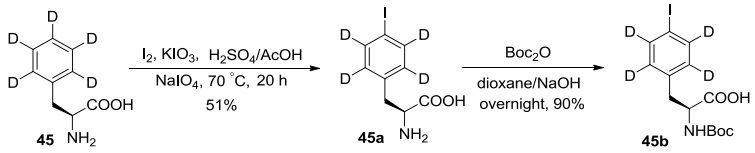

*Step 1: synthesis of **45b***: To a solution of deuterated $_L$-phenylalanine (**45**, 3.00 g, 17.65 mmol) in acetic acid (10 mL) and concentrated sulfuric acid (1.5 mL), iodine (1.79 g, 7.06 mmol) and potassium iodate (0.76 g, 3.52 mmol) were added. The reaction mixture was stirred vigorously at 70 ℃ for 20 h. Sodium periodate (0.12 g, 0.54 mmol) was added until the reaction solution became orange. Acetic acid was removed under rotary evaporation, and the residue was dissolved in water and washed with diethyl ether (20 mL) and dichloromethane (10 mL). The aqueous layer was decolored by activated charcoal (0.55 g). After removel of activated charcoal by filtration, the aqueous layer was adjusted to pH 5 with concentrated NaOH solution. The precipitate was filtered under vacuum and washed with water (30 mL) and ethanol (10 mL) to afford **45a**.

*Step 2: synthesis of **45b***: To a solution of **45a** (2.00 g, 6.78 mmol) in dioxane (5 mL) and 1M NaOH (20 mL) at 0 ℃, a solution of di-*tert*-butyl dicarbonate (1.77 g, 8.14 mmol) in dioxane (5 mL) was added. The reaction mixture was stirred at room temperature overnight. The pH was adjusted to pH 9 by 1M NaOH and stirred for another 3 h. After concentration, the residue was partitioned between water and diethyl ether. The pH of aqueous layer was readjusted to pH 2-3 by 2M HCl and extracted with EtOAc. The EtOAc layer was washed with brine, dried over $MgSO_4$, and concentrated to afford **45b**.

2.3.4 Synthesis of optically pure (Tmd)Phe derivatives

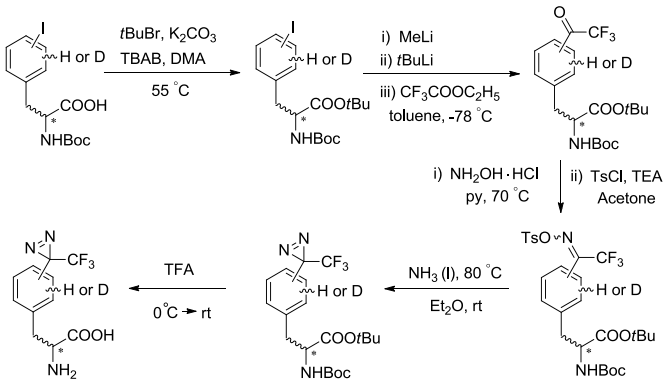

Step 1: synthesis of Boc-Phe(I)-O-tBu. To a solution of Boc-Phe(I)-OH (3 mmol) in *N*,*N*-dimethylacetamide (15 mL) in the presence of anhydrous potassium carbonate (25 equiv) and tetrabutylammonium bromide (1 equiv) at 0 ℃, *tert*-butyl bromide (48 equiv) was added dropwise and the mixture was stirred at 55 ℃ for 2.5 h. After cooling to room temperature, the mixture was added into cold water and extracted with EtOAc. The organic layer was washed with H_2O, brine, dried over $MgSO_4$, and evaporated. The residue was purified by silica gel column chromatography (EtOAc/hexane, 1:4) to afford the desired product.

Step 2: synthesis of Boc-Phe(trifluoroacetyl)-O-tBu. Methyllithium (1.3 equiv, 1.11 mol/L, in diethyl ether) was added dropwise to a solution of Boc-Phe(I)-O-*t*Bu (2.4

mmol) in dry toluene (20 mL) at -78 ℃ under N_2. After 30 minutes, *tert*-BuLi (2.5 equiv, 1.65 mol/L, in *n*-pentane) was added dropwise over a period of 10 minutes. Ethyl trifluoroacetate (7 equiv) was added and the reaction mixture was stirred for another 12 hours at the same temperature. After quenched with saturated ammonium chloride (10 mL), the mixture was extracted by diethyl ether. The organic layer was washed with saturated ammonium chloride, H_2O and brine, dried over $MgSO_4$ and evaporated. The residue was purified by silica gel column chromatography (EtOAc /hexane, 1:9) to afford the desired product.

Step 3: synthesis of Boc-Phe(trifluoro-(hydroxyimino)ethyl)-O-tBu. Boc-Phe(trifluoroacetyl)-O-*t*Bu. (1 mmol) was dissolved in pyridine (20 mL), then hydroxylamine hydrochloride (1.3 equiv) was added. The mixture was stirred at 70 ℃ for 1.5 h and was then subjected to rotary evaporation to remove pyridine. The residue was dissolved in diethyl ether and washed with 1 M HCl, the organic layer was washed with H_2O and brine, dried over $MgSO_4$ and evaporated. The residue was purified by silica gel column chromatography (EtOAc/hexane, 1:4) to afford the desired product.

Step 4: synthesis of Boc-Phe(trifluoro-(tosyloxyimino)ethyl)-O-tBu. To a solution of Boc-Phe(trifluoro- (hydroxyimino)ethyl)-O-*t*Bu (0.8 mmol) in acetone (10 mL) at 0 ℃, triethylamine (3 equiv) was added. *p*-Toluenesulfonyl chloride (1.2 equiv) was added to the reaction mixture which was stirred at room temperature for 1 h. After evaporation, the residue was purified by silica gel column chromatography (EtOAc/hexane, 1:3) to afford the desired product.

Step 5: synthesis of Boc-Phe((trifluoromethyl)-3H-diazirin-3-yl)-O-tBu. To liquid NH_3 (10 mL) at -78 ℃ in a sealed tube, a solution of Boc-Phe(trifluoro-(tosyloxyimino)ethyl)-O-*t*Bu (0.5 mmol) in anhydrous Et_2O was added. The reaction was stirred at 80 ℃ until the reaction was completed. After removed the ammonia, the solution was partitioned between Et_2O (30 mL) and H_2O (30

mL). The organic layer was washed by H_2O (three times), brine, dried over $MgSO_4$ and evaporated to afford the desired product.

Step 6: synthesis of (Tmd)Phe derivatives. Trifluoroacetic acid (3.0 mL) was added to Boc-Phe((trifluoro- methyl)-3*H*-diazirin-3-yl)-O-*t*Bu (0.3 mmol) at 0 ℃. The reaction mixture was stirred at room temperature for 8 h. After evaporation, the residue was purified by silica gel column chromatography (EtOAc/H_2O/MeOH, 8:1:1) to afford the desired product.

2.3.5 Characterization of corresponding products

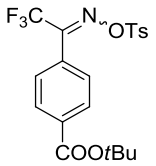

1a. colorless oil (1.99 g, 90%, mixture of *syn*- and *anti*- isomers): ^{1}H-NMR (270 MHz, $CHCl_3$) δ 8.01 – 8.10 (m, 2H), 7.87 – 7.94 (m, 2H), 7.37 – 7.50 (m, 4H), 2.48 (s, 1H), 2.46 (s, 2H), 1.60 (s, 9H); ^{13}C-NMR (68 MHz, $CDCl_3$) δ 164.6 and 164.5, 153.3 (q, $^2J_{CF}$ = 32.7 Hz), 146.4 and 146.3, 135.0 and 134.9, 131.4 and 131.2, 130.3 and 130.0, 129.8 and 129.7, 129.3 and 129.2, 128.8 and 128.4, 127.1, 117.2 (q, $^1J_{CF}$ = 283.9 Hz), 81.9, 28.0, 21.6; ^{19}F-NMR (470 MHz, $CDCl_3$): δ -61.45, -66.82; HRMS-ESI (*m*/*z*) $[M + H]^+$ calcd for $C_{20}H_{21}F_3NO_5S$ 444.1093, found 444.1106.

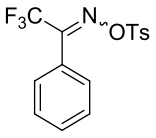

1b. white solid (1.56 g, 91%, mixture of *syn*- and *anti*- isomers): ^{1}H-NMR (270 MHz, $CDCl_3$) δ 7.91 (d, *J* = 7.0 Hz, 2H), 7.50 – 7.57 (m, 1H), 7.43 – 7.45 (m, 4H), 7.38 (d, *J* = 7.0 Hz, 2H), 2.47 (s, 3H); ^{13}C-NMR (68 MHz, $CDCl_3$) δ 154.1 (q, $^2J_{CF}$ = 32.3 Hz), 146.3 and 146.2, 131.9 and 131.7, 131.4 and 131.2, 130.0, 129.2 and 129.1, 128.79

and 128.75, 128.3 and 127.7, 124.6, 117.3 (q, $^{1}J_{CF}$ = 283.8 Hz), 21.5; ^{19}F-NMR (470 MHz, $CDCl_3$): δ -61.53, -66.80. HRMS-ESI (*m/z*) $[M + Na]^+$ calcd for $C_{15}H_{12}F_3NO_3SNa$ 366.0382, found 366.0386.

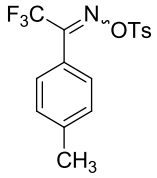

1c. white solid (1.66 g, 93%, mixture of *syn*- and *anti*- isomers): ^{1}H-NMR (270 MHz, $CDCl_3$) δ 7.90 (d, *J* = 8.4 Hz, 2H), 7.28 – 7.40 (m, 4H), 7.22 (d, *J* = 8.4 Hz, 2H), 2.48 (s, 0.6H), 2.46 (s, 2.4H), 2.40 (s, 0.6H), 2.39 (s, 2.4H); ^{13}C-NMR (68 MHz, $CDCl_3$) δ 154.1 (q, $^{2}J_{CF}$ = 32.1 Hz), 146.2 and 146.1, 142.6 and 142.4, 131.5 and 131.3, 129.9, 129.5, 129.2 and 129.1, 128.8 and 128.4, 124.8, 117.5 (q, $^{1}J_{CF}$ = 283.9 Hz), 21.5, 21.3, 21.2; ^{19}F-NMR (470 MHz, $CDCl_3$): δ -61.47, -66.52; HRMS-ESI (*m/z*) $[M + H]^+$ calcd for $C_{16}H_{15}F_3NO_3S$ 358.0725, found 358.0745.

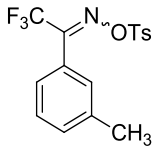

1d. white solid (1.64 g, 92%, mixture of *syn*- and *anti*- isomers): ^{1}H-NMR (270 MHz, $CDCl_3$) δ 7.87 – 7.92 (m, 2H), 7.30 – 7.40 (m, 4H), 7.16 – 7.23 (m, 2H), 2.48 (s, 0.7H), 2.46 (s, 2.3H), 2.39 (s, 0.7H), 2.37 (s, 2.3H); ^{13}C-NMR (68 MHz, $CDCl_3$) δ 154.3 (q, $^{2}J_{CF}$ = 32.3 Hz), 146.3 and 146.1, 138.8 and 138.7, 132.6 and 132.5, 131.6 and 131.3, 129.9 and 129.4, 129.3 and 129.1, 128.7 and 128.6, 127.7, 126.0, 125.5, 117.4 (q, $^{1}J_{CF}$ = 283.8 Hz), 21.5, 21.2 and 21.1; ^{19}F-NMR (470 MHz, $CDCl_3$): δ -61.49, -66.85; HRMS-ESI (*m/z*) $[M + H]^+$ calcd for $C_{16}H_{15}F_3NO_3S$ 358.0725, found 358.0710.

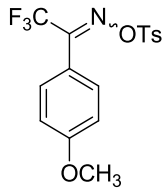

1e. white solid (1.75 g, 94%, mixture of *syn*- and *anti*- isomers): ^{1}H-NMR (270 MHz, $CDCl_3$) δ 7.90 (d, *J* = 8.3 Hz, 2H), 7.36 – 7.47 (m, 4H), 6.90 – 6.98 (m, 2H), 3.86 (s, 1.7H), 3.84 (s, 1.3H), 2.47 (s, 1.7H), 2.46 (s, 1.3H); ^{13}C-NMR (68 MHz, $CDCl_3$) δ 162.7 and 162.2, 153.4 (q, $^{2}J_{CF}$ = 32.9 Hz), 146.2 and 146.0, 131.7 and 131.4, 130.8, 129.9, 129.3 and 129.2, 119.9 (q, $^{1}J_{CF}$ = 278.0 Hz), 116.5, 114.3, 55.3, 21.6; ^{19}F-NMR (470 MHz, $CDCl_3$): δ -61.44, -66.05; HRMS-ESI (*m/z*) $[M + H]^+$ calcd for $C_{16}H_{15}F_3NO_4S$ 374.0674, found 374.0690.

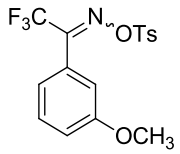

1f. white solid (1.75 g, 94%, mixture of *syn*- and *anti*- isomers): ^{1}H-NMR (270 MHz, $CDCl_3$) δ 7.87 – 7.92 (m, 2H), 7.30 – 7.41 (m, 3H), 6.88 – 7.07 (m, 3H), 3.82 (s, 1.3H), 3.81 (s, 1.7H), 2.48 (s, 1.3H), 2.46 (s, 1.7H); ^{13}C-NMR (68 MHz, $CDCl_3$) δ 159.7, 153.9 (q, $^{2}J_{CF}$ = 32.4 Hz), 146.3 and 146.1, 131.6 and 131.3, 130.1 and 129.9, 130.0, 129.3 and 129.2, 125.7, 121.2 and 120.6, 117.5 and 117.3, 117.4 (q, $^{1}J_{CF}$ = 284.1 Hz), 114.4 and 114.0, 55.3, 21.6; ^{19}F-NMR (470 MHz, $CDCl_3$): δ -61.47, -66.88; HRMS-ESI (*m/z*) $[M + H]^+$ calcd for $C_{16}H_{15}F_3NO_4S$ 374.0674, found 374.0687.

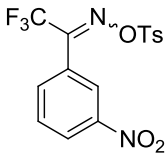

1g. yellow solid (1.69 g, 87%, mixture of *syn*- and *anti*- isomers): ^{1}H-NMR (270 MHz, $CDCl_3$) δ 8.38 – 8.44 (m, 1H), 8.21 (s, 1 H), 7.88 – 7.94 (m, 2H), 7.70 – 7.75 (m, 2H), 7.40 – 7.44 (m, 2H), 2.50 (s, 2.3H), 2.49 (s, 0.7H); ^{13}C-NMR (68 MHz, $CDCl_3$) δ 151.9

(q, $^{2}J_{CF}$ = 34.5 Hz), 148.3, 146.8 and 146.7, 134.5 and 134.4, 130.8, 130.4, 130.2, 129.4 and 129.3, 126.4, 126.1, 124.1 and 123.6, 119.3 (q, $^{1}J_{CF}$ = 277.4 Hz), 21.6; ^{19}F-NMR (470 MHz, $CDCl_3$): δ -61.55, -66.88; HRMS-ESI (*m/z*) $[M + Na]^+$ calcd for $C_{15}H_{11}F_3N_2O_5SNa$ 411.0233, found 411.0238.

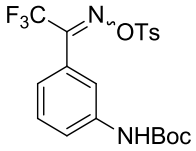

1h. yellow oil (2.27 g, 99%, mixture of *syn*- and *anti*- isomers): ^{1}H-NMR (270 MHz, $CDCl_3$) δ 7.78 – 7.92 (m, 2H), 7.30 – 7.56 (m, 5H), 6.99 – 7.08 (m, 1H), 6.79 (s, 0.3H), 6.77 (s, 0.7H), 2.46 (s, 0.9H), 2.45 (s, 2.1H), 1.52 (s, 2.7H), 1.51 (s, 6.3H); ^{13}C-NMR (68 MHz, $CDCl_3$) δ 153.9 (q, $^{2}J_{CF}$ = 32.4 Hz), 152.6, 146.3 and 146.1, 139.2 and 139.1, 131.4 and 131.2, 130.04 and 129.96, 129.5 and 129.3, 129.3 and 129.2, 125.2, 123.2 and 122.6, 121.6 and 121.4, 118.5 and 117.8, 117.3 (q, $^{1}J_{CF}$ = 283.9 Hz), 81.0, 28.1, 21.6; ^{19}F-NMR (470 MHz, $CDCl_3$): δ -61.50, -66.88; HRMS-ESI (*m/z*) $[M + Na]^+$ calcd for $C_{20}H_{21}F_3N_2O_5SNa$ 481.1016, found 481.1013.

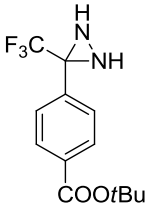

2. colorless oil (86 mg, 99%)[2]: ^{1}H-NMR (270 MHz, $CDCl_3$) δ 8.03 (d, *J* = 8.3 Hz, 2H), 7.68 (d, *J* = 8.3 Hz, 2H), 2.86 (d, *J* = 8.7 Hz, 1H), 2.28 (d, *J* = 8.7 Hz, 1H), 1.60 (s, 9H); ^{13}C-NMR (68 MHz, $CDCl_3$) δ 165.0, 135.7, 133.8, 129.9, 128.1, 123.4 (q, $^{1}J_{CF}$ = 278.3 Hz), 81.6, 57.8 (q, $^{2}J_{CF}$ = 36.3 Hz), 28.0; ^{19}F-NMR (470 MHz, $CDCl_3$): δ -75.24; HRMS-ESI (*m/z*) $[M + H]^+$ calcd for $C_{13}H_{16}F_3N_2O_2$ 289.1164, found 289.1145.

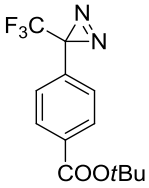

3a. pale yellow oil (*Method A*: 83 mg, 97%; *Method B*: 82 mg, 96%): ^{1}H-NMR (270 MHz, $CDCl_3$) δ 8.00 (d, *J* = 8.6 Hz, 2H), 7.23 (d, *J* = 8.6 Hz, 2H), 1.59 (s, 9H); ^{13}C-NMR (68 MHz, $CDCl_3$) δ 164.8, 133.3, 129.9, 126.3, 122.0 (q, $^{1}J_{CF}$ = 274.8 Hz), 81.7, 28.4 (q, $^{2}J_{CF}$ = 40.2 Hz), 28.0; ^{19}F-NMR (470 MHz, $CDCl_3$): δ -64.97; HRMS-ESI (*m/z*) $[M + Na]^+$ calcd for $C_{13}H_{13}F_3N_2O_2Na$ 309.0827, found 309.0811.

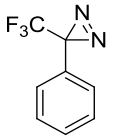

3b. pale yellow oil (*Method A*: 54 mg, 97%; *Method B*: 55 mg, 99%): ^{1}H-NMR (270 MHz, $CDCl_3$) δ 7.34 – 7.43 (m, 3H), 7.18 – 7.22 (m, 2H); ^{13}C-NMR (68 MHz, $CDCl_3$) δ 129.7, 129.3, 128.9, 126.6, 122.3 (q, $^{1}J_{CF}$ = 274.7 Hz), 28.4 (q, $^{2}J_{CF}$ = 40.4 Hz); ^{19}F-NMR (470 MHz, $CDCl_3$): δ -65.26; HRMS-ESI (*m/z*) $[M + H]^+$ calcd for $C_8H_6F_3N_2$ 187.0483, found 187.0461.

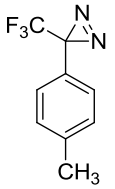

3c. colorless oil (*Method A*: 59 mg, 98%; *Method B*: 58 mg, 97%): ^{1}H-NMR (270 MHz, $CDCl_3$) δ 7.20 (d, *J* = 8.2 Hz, 2H), 7.08 (d, *J* = 8.2 Hz, 2H), 2.36 (s, 3H); ^{13}C-NMR (68 MHz, $CDCl_3$) δ 140.0, 129.6, 127.8, 126.5, 122.4 (q, $^{1}J_{CF}$ = 274.5 Hz), 28.3 (q, $^{2}J_{CF}$ = 40.4 Hz), 21.0; ^{19}F-NMR (470 MHz, $CDCl_3$): δ -65.35; HRMS-ESI (*m/z*) $[M + H]^+$ calcd for $C_9H_8F_3N_2$ 201.0640, found 201.0632.

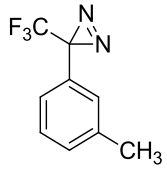

3d. colorless oil (*Method A*: 59 mg, 99%; *Method B*: 60 mg, 100%): ^{1}H-NMR (270 MHz, $CDCl_3$) δ 7.28 (t, *J* = 7.6 Hz, 1H), 7.22 (d, *J* = 7.6 Hz, 1H), 7.01 (d, *J* = 7.6 Hz,

1H), 6.97 (s, 1H), 2.35 (s, 3H); ^{13}C-NMR (68 MHz, $CDCl_3$) δ 138.9, 130.5, 129.2, 128.8, 127.1, 123.7, 122.4 (q, $^1J_{CF}$ = 274.5 Hz), 28.3 (q, $^2J_{CF}$ = 40.4 Hz), 21.2; ^{19}F-NMR (470 MHz, $CDCl_3$): δ -65.16; HRMS-ESI (*m/z*) $[M + H]^+$ calcd for $C_9H_8F_3N_2$ 201.0640, found 201.0644.

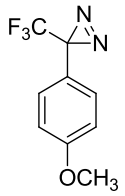

3e. pale yellow oil (*Method A*: 61 mg, 94%; *Method B*: 59 mg, 92%): ^{1}H-NMR (270 MHz, $CDCl_3$) δ 7.15 (d, *J* = 8.7 Hz, 2H), 6.90 (d, *J* = 8.7 Hz, 2H), 3.80 (s, 3H); ^{13}C-NMR (68 MHz, $CDCl_3$) δ 160.8, 128.2, 122.4 (q, $^1J_{CF}$ = 274.6 Hz), 121.0, 114.4, 55.3, 28.1 (q, $^2J_{CF}$ = 40.4 Hz); ^{19}F-NMR (470 MHz, $CDCl_3$): δ -65.63; HRMS-ESI (*m/z*) $[M + H]^+$ calcd for $C_9H_8F_3N_2O$ 217.0589, found 217.0596.

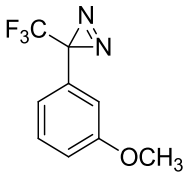

3f. pale yellow oil (*Method A*: 62 mg, 96%; *Method B*: 64 mg, 99%): ^{1}H-NMR (270 MHz, $CDCl_3$) δ 7.28 (t, *J* = 8.1 Hz, 1H), 6.92 (dd, *J* = 8.1, 2.5 Hz, 1H), 6.76 (d, *J* = 8.1 Hz, 1H), 6.69 (s, 1H), 3.77 (s, 3H); ^{13}C-NMR (68 MHz, $CDCl_3$) δ 160.0, 130.7, 130.1, 122.2 (q, $^1J_{CF}$ = 274.5 Hz), 118.8, 115.2, 112.3, 55.2, 28.3 (q, $^2J_{CF}$ = 40.4 Hz); ^{19}F-NMR (470 MHz, $CDCl_3$): δ -65.14; HRMS-ESI (*m/z*) $[M + H]^+$ calcd for $C_9H_8F_3N_2O$ 217.0589, found 217.0590.

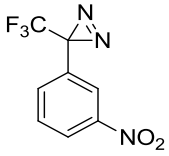

3g. yellow oil (*Method A*: 69 mg, 99%; *Method B*: 68 mg, 98%): ^{1}H-NMR (270 MHz, $CDCl_3$) δ 8.28 – 8.32 (m, 1H), 8.06 (s, 1H), 7.64 (t, *J* = 8.1 Hz, 1H), 7.59 (d, *J* = 8.1 Hz,

1H); ^{13}C-NMR (68 MHz, $CDCl_3$) δ 148.6, 132.4, 131.2, 130.3, 124.7, 121.7, 121.7 (q, $^1J_{CF}$ = 274.9 Hz), 28.0 (q, $^2J_{CF}$ = 41.1 Hz); ^{19}F-NMR (470 MHz, $CDCl_3$): δ -65.16.

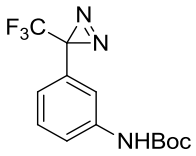

3h. yellow oil (*Method A*: 84 mg, 93%; *Method B*: 82 mg, 91%): ^{1}H-NMR (270 MHz, $CDCl_3$) δ 7.41 (d, *J* = 8.0 Hz, 1H), 7.31 (t, *J* = 8.0 Hz, 1H), 7.20 (s, 1H), 6.87 (d, *J* = 8.0 Hz, 1H), 6.55 (s, 1H), 1.52 (s, 9H); ^{13}C-NMR (68 MHz, $CDCl_3$) δ 152.6, 139.2, 130.1, 129.6, 121.0, 119.6, 122.2 (q, $^1J_{CF}$ = 274.7 Hz), 116.3, 81.1, 28.3 (q, $^2J_{CF}$ = 39.9 Hz), 28.2; ^{19}F-NMR (470 MHz, $CDCl_3$): δ -65.14; HRMS-ESI (*m/z*) $[M - H]^-$ calcd for $C_{13}H_{13}F_3N_3O_2$ 300.0965, found 300.0971.

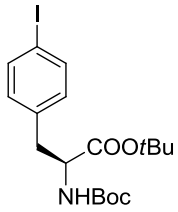

36. colorless oil (1.22 g, 91%): $[\alpha]_D$ +40 (*c* 0.2 $CHCl_3$) (lit.[1]: +33.4, *c* 1.0, $CHCl_3$); ^{1}H-NMR (270 MHz, $CHCl_3$) δ 7.61 (d, *J* = 8.3 Hz, 2H), 6.92 (d, *J* = 8.3 Hz, 2H), 4.98 (d, *J* = 7.8 Hz, 1H), 4.42 (dd, *J* = 12.8, 5.9 Hz, 1H), 2.92 – 3.06 (m, 2H), 1.42 (s, 9H), 1.41 (s, 9H); ^{13}C-NMR (68 MHz, $CDCl_3$) δ 170.7, 155.1, 137.4, 136.2, 131.6, 92.2, 82.2, 79.7, 54.5, 37.9, 28.1, 27.8; HRMS-ESI (*m/z*) $[M + H]^+$ calcd for $C_{18}H_{27}INO_4$ 448.0985, found 448.0986.

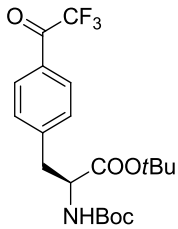

37. pale yellow oil (0.68 g, 68%): $[\alpha]_D$ +26 (*c* 1.0 $CHCl_3$); ^{1}H-NMR (270 MHz, $CDCl_3$) δ 8.00 (d, *J* = 8.1 Hz, 2H), 7.37 (d, *J* = 8.1 Hz, 2H), 5.07 (d, *J* = 8.1 Hz, 1H), 4.50 (dd, *J*

= 10.9, 5.5 Hz, 1H), 3.20 (dd, *J* = 14.0, 5.7 Hz, 1H), 3.10 (dd, *J* = 14.0, 5.7 Hz, 1H), 1.41 (s, 18H); ^{13}C-NMR (68 MHz, $CDCl_3$) δ 180.3 (q, $^2J_{CF}$ = 34.8 Hz), 170.4, 155.0, 145.6, 130.3, 130.0, 128.5, 116.6 (q, $^1J_{CF}$ = 291.3 Hz), 82.4, 79.7, 54.4, 38.6, 28.0, 27.6; ^{19}F-NMR (470 MHz, $CDCl_3$): δ -71.40; HRMS-ESI (*m*/*z*) $[M + H]^+$ calcd for $C_{20}H_{27}F_3NO_5$ 418.1841, found 418.1862.

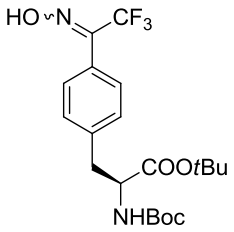

37a. colorless oil (0.40 g, 91%, mixture of *syn*- and *anti*- isomers): $[\alpha]_D$ +30 (*c* 1.0 $CHCl_3$); ^{1}H-NMR (270 MHz, $CDCl_3$) δ 10.73 (s, 0.46H), 10.34 (s, 0.43H), 7.43 (d, *J* = 8.0 Hz, 1H), 7.36 (d, *J* = 8.0 Hz, 1H), 7.24 – 7.27 (m, 1H), 7.17 (d, *J* = 8.0 Hz, 1H), 5.26 – 5.32 (m, 1H), 4.52 (brs, 1H), 3.04 – 3.06 (m, 2H), 1.40 (s, 9H), 1.36 (s, 9H); ^{13}C-NMR (68 MHz, $CDCl_3$) δ 171.6 and 171.4, 155.7 and 155.5, 146.7 (q, $^2J_{CF}$ = 30.1 Hz), 139.0 and 138.6, 129.64 and 129.59, 128.8 and 128.4, 125.1, 120.9 (q, $^1J_{CF}$ = 274.6 Hz), 118.6 (q, $^1J_{CF}$ = 283.0 Hz), 82.7 and 82.6, 80.4 and 80.3, 54.6, 38.6 and 38.3, 28.1, 27.7; ^{19}F-NMR (470 MHz, $CDCl_3$) δ -62.33, -66.15; HRMS-ESI (*m*/*z*) $[M + H]^+$ calcd for $C_{20}H_{28}F_3N_2O_5$ 433.1950, found 433.1962.

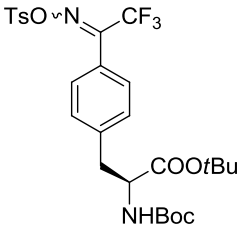

38. colorless oil (0.45 g, 96%, mixture of *syn*- and *anti*- isomers): $[\alpha]_D$ +39 (*c* 1.0 $CHCl_3$); ^{1}H-NMR (270 MHz, $CDCl_3$) δ 7.86 – 7.92 (m, 2H), 7.32 – 7.40 (m, 5H), 7.24 (d, *J* = 8.4 Hz, 1H), 5.01 – 5.11 (m, 1H), 4.44 – 4.51 (m, 1H), 3.00 – 3.13 (m, 2H), 2.48 (s, 1.38H), 2.46 (s, 1.86H), 1.36 – 1.42 (m, 18H); ^{13}C-NMR (68 MHz, $CDCl_3$) δ 170.6,

155.0, 153.8 (q, $^{2}J_{CF}$ =32.9 Hz), 146.2 and 146.0, 141.1 and 141.0, 131.4 and 131.2, 129.98 and 129.94, 129.88, 129.2 and 129.1, 128.8 and 128.4, 126.2 and 123.0, 119.6 (q, $^{1}J_{CF}$ = 277.3 Hz), 117.3 (q, $^{1}J_{CF}$ = 283.5 Hz), 82.4 and 82.3, 79.7, 54.5, 38.6 and 38.3, 28.0, 27.7 and 27.6, 21.5; ^{19}F-NMR (470 MHz, $CDCl_3$) δ -61.49, -66.56; HRMS-ESI (*m*/*z*) $[M + H]^+$ calcd for $C_{27}H_{34}F_3N_2O_7S$ 587.2039, found 587.2065.

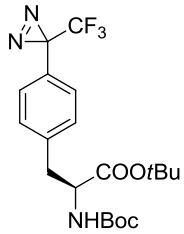

40. colorless oil (0.19 g, 90%, 9 h): $[\alpha]_D$ +35 (*c* 1.0 $CHCl_3$); ^{1}H-NMR (270 MHz, $CDCl_3$) δ 7.22 (d, *J* = 8.4 Hz, 2H), 7.12 (d, *J* = 8.4 Hz, 2H), 5.02 (d, *J* = 7.3 Hz, 1H), 4.44 (dd, *J* = 13.2, 6.1 Hz, 1H), 2.98 – 3.13 (m, 2H), 1.41 (s, 9H), 1.39 (s, 9H); ^{13}C-NMR (68 MHz, $CDCl_3$) δ 170.7, 155.1, 138.6, 130.1, 127.6, 126.4, 122.2 (q, $^{1}J_{CF}$ = 277.7 Hz), 82.3, 79.7, 54.5, 38.2, 28.1 (q, $^{2}J_{CF}$ = 40.6 Hz), 28.1, 27.7; ^{19}F-NMR (470 MHz, $CDCl_3$) δ -65.28; HRMS-ESI (*m*/*z*) $[M + H]^+$ calcd for $C_{20}H_{27}F_3N_3O_4$ 430.1954, found 430.1976.

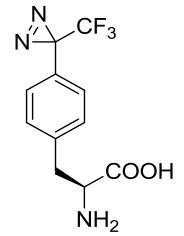

8. white solid as TFA salt (107 mg, 92%): $[\alpha]_D$ -15 (*c* 0.2 CH_3OH); ^{1}H-NMR (270 MHz, D_2O) δ 7.41 (d, *J* = 8.2 Hz, 2H), 7.33 (d, *J* = 8.2 Hz, 2H), 4.00 (t, *J* = 7.9 Hz, 1H), 3.32 (dd, *J* = 14.6, 5.6 Hz, 1H), 3.17 (dd, *J* = 14.6, 5.6 Hz, 1H); ^{13}C-NMR (68 MHz, CD_3OD) δ 173.4, 139.6, 131.5, 128.3, 123.8 (q, $^{1}J_{CF}$ = 273.7 Hz), 56.7, 37.5, 29.4 (q, $^{2}J_{CF}$ = 40.6 Hz); ^{19}F-NMR (470 MHz, CD_3OD) δ -67.06, -76.90; HRMS-ESI (*m*/*z*) $[M + H]^+$ calcd for $C_{11}H_{11}F_3N_3O_2$ 274.0803, found 274.0815; Chiral HPLC (Astec Chirobiotic T, 10%

EtOH) t_R= 7.70 min.

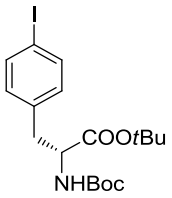

41a. colorless oil (1.24 g, 92%): $[\alpha]_D$ -40 (*c* 0.2 $CHCl_3$); The ^{1}H-, ^{13}C-, ^{19}F-NMR and MS data were identical to compound **5**.

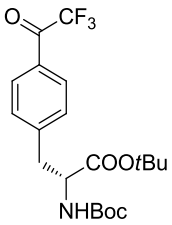

41b. pale yellow oil (0.60 g, 60%): $[\alpha]_D$ -26 (*c* 1.0 $CHCl_3$); The ^{1}H-, ^{13}C-, ^{19}F-NMR and MS data were identical to compound **6**.

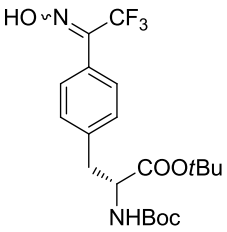

41c. colorless oil (0.43 g, 99%, mixture of *syn*- and *anti*- isomers): $[\alpha]_D$ -30 (*c* 1.0 $CHCl_3$); The ^{1}H-, ^{13}C-, ^{19}F- NMR and MS data were identical to compound **s7**.

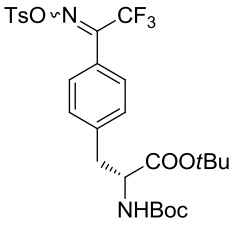

41d. colorless oil (0.44 g, 94%, mixture of *syn*- and *anti*- isomers): $[\alpha]_D$ -39 (*c* 1.0 $CHCl_3$); The ^{1}H-, ^{13}C-, ^{19}F- NMR and MS data were identical to compound **7**.

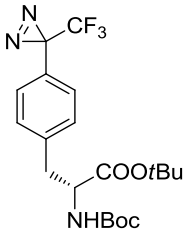

41e. colorless oil (0.20 g, 91%, 10 h): $[\alpha]_D$ -35 (*c* 1.0 $CHCl_3$); The ^{1}H-, ^{13}C-, ^{19}F- NMR and MS data were identical to compound **8**.

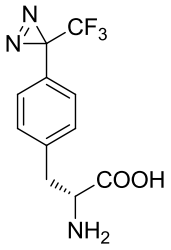

23. white solid as TFA salt (109 mg, 94%): $[\alpha]_D$ +15 (*c* 0.2 CH_3OH); The ^{1}H-, ^{13}C-, ^{19}F-NMR and MS data were identical to compound **9**. Chiral HPLC (Astec Chirobiotic T, 10% EtOH) t_R= 8.45 min.

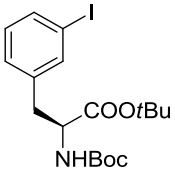

42a. colorless oil (1.28 g, 95%): $[\alpha]_D$ +55 (*c* 0.2 $CHCl_3$); ^{1}H-NMR (270 MHz, $CDCl_3$) δ 7.57 (d, *J* = 7.8 Hz, 1H), 7.52 (s, 1H), 7.15 (d, *J* = 7.8 Hz, 1H), 7.02 (t, *J* = 7.8 Hz, 1H), 5.02 (d, *J* = 6.3 Hz, 1H), 4.42 (dd, *J* = 12.7, 5.9 Hz, 1H), 3.00 (d, *J* = 5.2 Hz, 2H), 1.43 (s, 9H), 1.41 (s, 9H); ^{13}C-NMR (68 MHz, $CDCl_3$) δ 170.7, 155.1, 139.0, 138.6, 136.0, 130.1, 128.9, 94.3, 82.4, 79.8, 54.6, 37.9, 28.2, 27.9; HRMS-ESI (*m*/*z*) $[M + H]^+$ calcd for $C_{18}H_{27}INO_4$ 448.0985, found 448.0968.

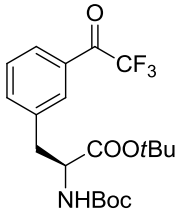

42b. pale yellow oil (0.55 g, 55%): $[\alpha]_D$ +40 (*c* 0.2 $CHCl_3$); ^{1}H-NMR (270 MHz,

$CDCl_3$) δ 7.96 (d, *J* = 7.7 Hz, 1H), 7.88 (s, 1H), 7.56 (d, *J* = 7.7 Hz, 1H), 7.48 (t, *J* = 7.7 Hz, 1H), 5.08 (d, *J* = 6.6 Hz, 1H), 4.49 (dd, *J* = 13.5, 5.7 Hz, 1H), 3.22 (dd, *J* = 13.7, 5.7 Hz, 1H), 3.11 (dd, *J* = 13.7, 5.7 Hz, 1H), 1.42 (s, 9H), 1.41 (s, 9H); ^{13}C-NMR (68 MHz, $CDCl_3$) δ 180.6 (q, $^2J_{CF}$ = 35.4 Hz), 170.5, 155.1, 138.2, 136.9, 131.2, 130.0, 129.1, 128.8, 116.7 (q, $^1J_{CF}$ = 291.6 Hz), 82.6, 79.9, 54.5, 38.2, 28.1, 27.8; ^{19}F-NMR (470 MHz, $CDCl_3$): δ -71.27; HRMS-ESI (*m*/*z*) $[M + H]^+$ calcd for $C_{20}H_{27}F_3NO_5$ 418.1841, found 418.1834.

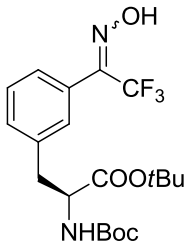

42c. colorless oil (0.37 g, 86%, mixture of *syn*- and *anti*- isomers): $[\alpha]_D$ +45 (*c* 0.2 $CHCl_3$); ^{1}H-NMR (270 MHz, $CDCl_3$) δ 7.28 – 7.37 (m, 4H), 5.14 (d, *J* = 7.1 Hz, 1H), 4.49 (dd, *J* = 12.2, 6.0 Hz, 1H), 3.09 (d, *J* = 5.6 Hz, 2H), 1.42 (s, 9H), 1.38 (s, 9H); ^{13}C-NMR (68 MHz, $CDCl_3$) δ 171.3, 155.5, 147.1 (q, $^2J_{CF}$ = 29.9 Hz), 136.9 and 136.8, 131.6 and 131.3, 130.6, 129.9 and 129.6, 128.5, 127.0 and 126.7, 120.9 (q, $^1J_{CF}$ = 274.4 Hz), 118.5 (q, $^1J_{CF}$ = 282.9 Hz), 82.6, 80.2, 54.6, 38.2, 28.1, 27.7; ^{19}F-NMR (470 MHz, $CDCl_3$): δ -62.25, -66.35; HRMS-ESI (*m*/*z*) $[M + H]^+$ calcd for $C_{20}H_{28}F_3N_2O_5$ 433.1950, found 433.1958.

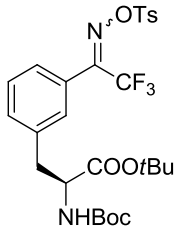

42d. colorless oil (0.44 g, 94%, mixture of *syn*- and *anti*- isomers): $[\alpha]_D$ +30 (*c* 0.2 $CHCl_3$); ^{1}H-NMR (270 MHz, $CDCl_3$) δ 7.87 – 7.92 (m, 2H), 7.29 – 7.40 (m, 5H), 7.17 – 7.24 (m, 1H), 4.97 – 5.06 (m, 1H), 4.41 – 4.47 (m, 1H), 3.07 (d, *J* = 4.0 Hz, 2H), 2.49

(s, 1H), 2.47 (s, 2H), 1.41 (s, 9H), 1.36 (s, 9H); ^{13}C-NMR (68 MHz, $CDCl_3$) δ 170.6, 155.1, 154.0 (q, $^2J_{CF}$ = 31.7 Hz), 146.2 and 146.1, 137.7 and 137.5, 133.0 and 132.9, 131.5 and 131.2, 130.0 and 129.9, 129.3 and 129.2, 129.0, 128.84 and 128.78, 127.76 and 124.7, 127.4 and 127.1, 119.6 (q, $^1J_{CF}$ = 277.7 Hz), 117.3 (q, $^1J_{CF}$ = 283.7 Hz), 82.4, 79.8, 54.5, 38.3 and 38.2, 28.1, 27.7, 21.6; ^{19}F-NMR (470 MHz, $CDCl_3$): δ -61.47, -66.68; HRMS-ESI (*m*/*z*) $[M + H]^+$ calcd for $C_{27}H_{34}F_3N_2O_7S$ 587.2039, found 587.2050.

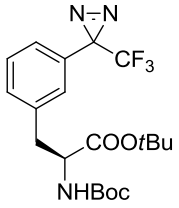

42e. colorless oil (0.19 g, 89%, 11 h): $[\alpha]_D$ +45 (*c* 0.2 $CHCl_3$); ^{1}H-NMR (270 MHz, $CDCl_3$) δ 7.33 (t, *J* = 7.7 Hz, 1H), 7.25 (d, *J* = 7.7 Hz, 1H), 7.12 (d, *J* = 7.7 Hz, 1H), 6.92 (s, 1H), 5.01 (d, *J* = 7.4 Hz, 1H), 4.44 (dd, *J* = 13.4, 6.3 Hz, 1H), 2.99 – 3.14 (m, 2H), 1.43 (s, 9H), 1.40 (s, 9H); ^{13}C-NMR (68 MHz, $CDCl_3$) δ 170.6, 155.1, 137.7, 131.0, 129.2, 128.9, 127.6, 125.2, 122.2 (q, $^1J_{CF}$ = 274.5 Hz), 82.4, 79.8, 54.5, 38.2, 28.2 (q, $^2J_{CF}$ = 40.5 Hz), 28.1, 27.8; ^{19}F-NMR (470 MHz, $CDCl_3$): δ -65.10; HRMS-ESI (*m*/*z*) $[M + H]^+$ calcd for $C_{20}H_{27}F_3N_3O_4$ 430.1954, found 430.1949.

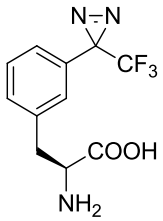

43. white solid as TFA salt (114 mg, 98%). $[\alpha]_D$ -10 (*c* 0.2 CH_3OH); ^{1}H-NMR (270 MHz, D_2O) δ 7.37 (t, *J* = 7.6 Hz, 1H), 7.29 (d, *J* = 7.6 Hz, 1H), 7.16 (d, *J* = 7.6 Hz, 1H), 7.07 (s, 1H), 3.87 (t, *J* = 6.6 Hz, 1H), 3.17 (dd, *J* = 14.5, 5.5 Hz, 1H), 3.02 (dd, *J* = 14.5, 5.5 Hz, 1H); ^{13}C-NMR (68 MHz, CD_3OD) δ 173.7, 138.6, 132.4, 130.9, 130.8, 128.7, 126.9, 123.7 (q, $^1J_{CF}$ = 274.4 Hz), 56.6, 37.7, 29.4 (q, $^2J_{CF}$ = 40.5 Hz); ^{19}F-NMR (470

MHz, CD_3OD): δ -66.91, -76.87; HRMS-ESI (*m*/*z*) $[M + H]^+$ calcd for $C_{11}H_{11}F_3N_3O_2$ 274.0803, found 274.0775; Chiral HPLC (Astec Chirobiotic T, 10% EtOH) t_R= 7.60 min.

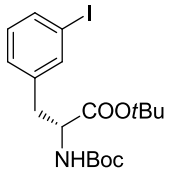

44a. colorless oil (1.32 g, 98%): $[\alpha]_D$ -55 (*c* 0.2 $CHCl_3$); The ^1H-, ^{13}C-, ^{19}F- NMR and MS data were identical to compound **s12a**.

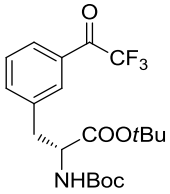

44b. pale yellow oil (0.52 g, 52%): $[\alpha]_D$ -40 (*c* 0.2 $CHCl_3$); The ^1H-, ^{13}C-, ^{19}F- NMR and MS data were identical to compound **s12b**.

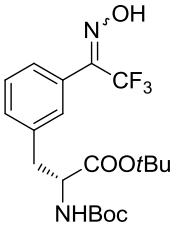

44c. colorless oil (0.39 g, 89%, mixture of *syn*- and *anti*- isomers): $[\alpha]_D$ -45 (*c* 0.2 $CHCl_3$); The ^1H-, ^{13}C-, ^{19}F- NMR and MS data were identical to compound **s12c**.

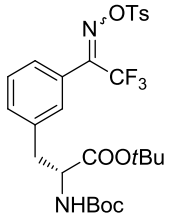

44d. colorless oil (0.46 g, 98%, mixture of *syn*- and *anti*- isomers): $[\alpha]_D$ -30 (*c* 0.2 $CHCl_3$); The ^1H-, ^{13}C-, ^{19}F- NMR and MS data were identical to compound **s12d**.

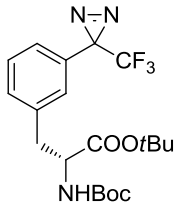

44e. colorless oil (0.19 g, 90%, 10 h): $[\alpha]_D$ -45 (*c* 0.2 $CHCl_3$); The ^1H-, ^{13}C-, ^{19}F- NMR and MS data were identical to compound **s12e**.

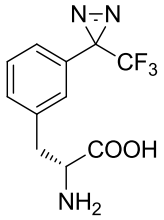

22. white solid as TFA salt (109 mg, 94%): $[\alpha]_D$ +10 (*c* 0.2 CH_3OH); The ^1H-, ^{13}C-, ^{19}F-NMR and MS data were identical to compound **13**. Chiral HPLC (Astec Chirobiotic T, 10% EtOH) t_R= 8.08 min.

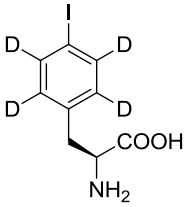

45a. white solid (2.66 g, 51%): $[\alpha]_D$ +20 (*c* 1.0, 0.5 M HCl); ^1H-NMR (270 MHz, NaOD/D_2O) δ 3.37 (t, *J* = 6.8 Hz, 1H), 2.84 (dd, *J* = 13.5, 5.4 Hz, 1H), 2.67 (dd, *J* = 13.5, 5.4 Hz, 1H); ^{13}C-NMR (68 MHz, NaOD/D_2O) δ 182.8, 138.6, 137.7 (t, *J* = 23.3 Hz), 131.8 (t, *J* = 23.1 Hz), 91.6, 57.8, 40.8; HRMS-ESI (*m*/*z*) $[M + H]^+$ calcd for $C_9H_7D_4INO_2$ 296.0086, found 296.0088.

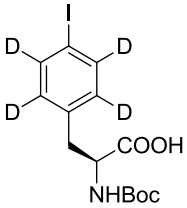

45b. white solid (2.41 g, 90%): $[\alpha]_D$ +15 (*c* 0.2 CH_3OH); ^1H NMR (270 MHz, CD_3OD) δ 4.33 (dd, *J* = 8.7, 4.9 Hz, 1H), 3.12 (dd, *J* = 13.8, 4.8 Hz, 1H), 2.85 (dd, *J* = 13.8, 4.8

Hz, 1H), 1.37 (s, 9H); ^{13}C-NMR (68 MHz, CD_3OD) δ 175.2, 157.8, 138.5, 138.2 (t, *J* = 24.0 Hz), 132.2 (t, *J* = 23.9 Hz), 92.3, 80.6, 55.9, 38.1, 28.6; HRMS-ESI (*m*/*z*) $[M + H]^+$ calcd for $C_{14}H_{15}D_4INO_4$ 396.0610, found 396.0602.

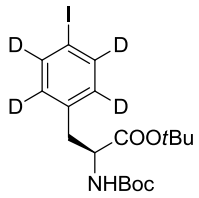

45c. colorless oil (1.22 g, 90%): $[\alpha]_D$ +45 (*c* 0.2 $CHCl_3$); ^{1}H NMR (270 MHz, $CDCl_3$) δ 4.99 (d, *J* = 7.8 Hz, 1H), 4.42 (dd, *J* = 13.2, 6.2 Hz, 1H), 2.92 – 3.07 (m, 2H), 1.42 (s, 9H), 1.41 (s, 9H); ^{13}C-NMR (68 MHz, $CDCl_3$) δ 170.8, 155.1, 137.0 (t, *J* = 26.7 Hz), 136.0, 131.2 (t, *J* = 24.4 Hz), 91.9, 82.2, 79.7, 54.5, 37.8, 28.2, 27.8; HRMS-ESI (*m*/*z*) $[M + H]^+$ calcd for $C_{18}H_{23}D_4INO_4$ 452.1236, found 452.1236.

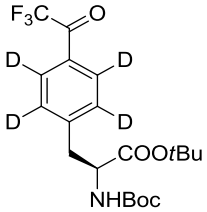

45d. pale yellow oil (0.58 g, 57%): $[\alpha]_D$ +30 (*c* 0.2 $CHCl_3$); ^{1}H-NMR (270 MHz, $CDCl_3$) δ 5.07 (d, *J* = 6.9 Hz, 1H), 4.50 (dd, *J* = 11.6, 5.0 Hz, 1H), 3.21 (dd, *J* = 13.6, 6.2 Hz, 1H), 3.11 (dd, *J* = 13.6, 6.2 Hz, 1H), 1.41 (s, 18H); ^{13}C-NMR (68 MHz, $CDCl_3$) δ 180.3 (q, $^2J_{CF}$ = 34.7 Hz), 170.5, 155.1, 145.4, 130.0 (t, *J* = 25.9 Hz), 129.8 (t, *J* = 24.8 Hz), 128.4, 116.7 (q, $^1J_{CF}$ = 291.5 Hz), 82.6, 79.9, 54.4, 38.6, 28.1, 27.8; ^{19}F-NMR (470 MHz, $CDCl_3$): δ -71.49; HRMS-ESI (*m*/*z*) $[M + H]^+$ calcd for $C_{20}H_{23}D_4F_3NO_5$ 422.2092, found 422.2108.

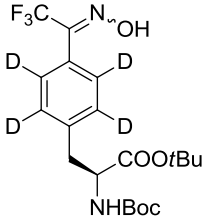

45e. colorless oil (0.39 g, 89%, mixture of *syn*- and *anti*- isomers): $[\alpha]_D$ +25 (*c* 0.2 $CHCl_3$); ^{1}H-NMR (270 MHz, $CDCl_3$) δ 10.11 (s, 0.47 H), 9.49 (s, 0.36 H), 5.17 – 5.27 (m, 1H), 4.47 – 4.54 (m, 1H), 3.05 – 3.08 (m, 2H), 1.41 (s, 9H), 1.37 (s, 9H); ^{13}C-NMR (68 MHz, $CDCl_3$) δ 171.6 and 171.4, 155.7 and 155.6, 146.7 (q, $^2J_{CF}$ = 30.3 Hz), 138.9 and 138.4, 129.2 (t, *J* = 22.8 Hz) and 129.0, 128.0 (t, *J* = 21.0 Hz), 120.9 (q, $^1J_{CF}$ = 274.7 Hz), 118.6 (q, $^1J_{CF}$ = 283.1 Hz), 82.74 and 82.65, 80.4 and 80.3, 54.6, 38.5 and 38.2, 28.1, 27.7; ^{19}F-NMR (470 MHz, $CDCl_3$) δ -62.31, -66.38; HRMS-ESI (*m*/*z*) $[M + H]^+$ calcd for $C_{20}H_{24}D_4F_3N_2O_5$ 437.2201, found 437.2194.

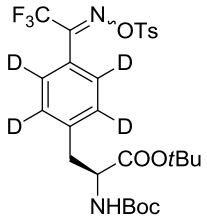

45f. colorless oil (0.45 g, 95%, mixture of *syn*- and *anti*- isomers). $[\alpha]_D$ +45 (*c* 0.2 $CHCl_3$); ^{1}H-NMR (270 MHz, $CDCl_3$) δ 7.86 – 7.92 (m, 2H), 7.36 – 7.40 (m, 2H), 5.04 – 5.13 (m, 1H), 4.42 – 4.49 (m, 1H), 3.01 – 3.16 (m, 2H), 2.47 (s, 1.01), 2.46 (s, 1.91), 1.36 – 1.45 (m, 18H); ^{13}C-NMR (68 MHz, $CDCl_3$) δ 170.6, 155.1, 153.8 (q, $^2J_{CF}$ = 32.7 Hz), 146.2 and 146.1, 141.1 and 141.0, 131.5 and 131.3, 129.9, 129.6, 129.3 and 129.2, 128.4 (t, *J* = 22.2 Hz), 126.1, 117.4 (q, $^1J_{CF}$ = 283.9 Hz), 82.4, 79.8, 54.5, 38.6 and 38.3, 28.1, 27.7, 21.6; ^{19}F-NMR (470 MHz, $CDCl_3$) δ -61.43, -66.48; HRMS-ESI (*m*/*z*) $[M + H]^+$ calcd for $C_{27}H_{30}D_4F_3N_2O_7S$ 591.2290, found 591.2284.

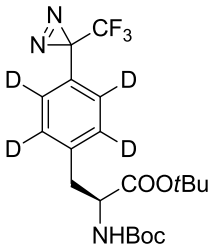

45g. colorless oil (0.20 g, 93%, 10 h): $[\alpha]_D$ +45 (*c* 0.2 $CHCl_3$); ^{1}H-NMR (270 MHz, $CDCl_3$) δ 5.01 (d, *J* = 6.3 Hz, 1H), 4.44 (d, *J* = 6.2 Hz, 1H), 2.98 – 3.13 (m, 2H), 1.40 (s,

9H), 1.39 (s, 9H); ^{13}C-NMR (68 MHz, $CDCl_3$) δ 170.8, 155.1, 138.4, 129.7 (t, *J* = 22.4 Hz), 127.6, 126.1 (t, *J* = 24.8 Hz), 122.2 (q, $^1J_{CF}$ =274.6 Hz), 82.4, 79.8, 54.6, 38.1, 28.2 (q, $^2J_{CF}$ = 40.4 Hz), 28.1, 27.8; ^{19}F-NMR (470 MHz, $CDCl_3$) δ -65.34; HRMS-ESI (*m*/*z*) $[M + H]^+$ calcd for $C_{20}H_{23}D_4F_3N_3O_4$ 434.2205, found 434.2180.

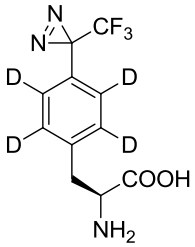

46. white solid as TFA salt (108 mg, 92%): $[\alpha]_D$ -15 (*c* 0.2 CH_3OH); ^{1}H-NMR (270 MHz, D_2O) δ 4.00 (t, *J* = 7.4 Hz, 1H), 3.32 (dd, *J* = 14.6, 7.8 Hz, 1H), 3.17 (dd, *J* = 14.6, 7.8 Hz, 1H); ^{13}C-NMR (68 MHz, CD_3OD) δ 174.1, 139.6, 131.1 (t, *J* = 23.7 Hz), 129.0, 127.8 (t, *J* = 24.3 Hz), 123.8 (q, $^1J_{CF}$ =273.9 Hz), 56.9, 37.5, 29.3 (q, $^2J_{CF}$ = 40.4 Hz); ^{19}F-NMR (470 MHz, CD_3OD) δ -67.13, -77.05; HRMS-ESI (*m*/*z*) $[M + H]^+$ calcd for $C_{11}H_7D_4F_3N_3O_2$ 278.1054, found 278.1053; Chiral HPLC (Astec Chirobiotic T, 10% EtOH) t_R= 7.79 min.

2.4 Conclusions

In this work, we developed a novel strategy to prepare TPD derivatives from the corresponding tosyloximes in a one-pot reaction. It was found that the NH_2^- generated from liquid NH_3 or lithium amide is a new species to prepare TPD derivatives. Many TPD derivatives are tolerable in these conditions. The one-pot strategy can significantly shorten the synthetic rout of TPD or TPD-based components in PAL field. By using this strategy, many (Tmd)Phe derivatives were prepared in good purity and yield.

3 TfOD-Mediated H/D Exchange of Cross-Linkable Aromatic α-Amino Acids

3.1 Introduction

Scheme 3.1 Syntheses of deuterated aromatic α-amino acids.

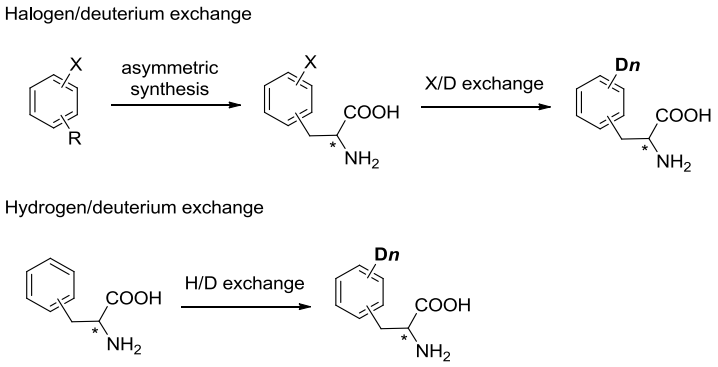

The combination of deuterated compounds and Mass analysis is a good strategy to quantitatively measure the bioactive peptides and proteins.[47] For this purpose, deuterated α-amino acids have emerged as the important starting components. Conventionally, two methods are widely used to prepare deuterated α-amino acids: halogen/deuterium exchange and hydrogen/deuterium (H/D) exchange (Scheme 3.1). For halogen/deuterium exchange strategy[48], halogen-substituted aromatics were used as the precursor which can convert to α-amino acids via asymmetric synthesis. Then, the halogenated α-amino acids were incorporated into peptides followed with the further halogen/deuterium exchange to afford deuterated α-amino acids. H/D Exchange[49] is the other widely used method used for the preparation of deuterated α-amino acids. With the deuterated reagents (D_2O, *etc.*) in certain condition (high temperature *etc.*), the protons in aromatic ring of α-amino acids can be exchanged by deuterium to afford deuterated α-amino acids. However, for previous methods, long

reaction times, high temperature and the use of additives are required.

Trifluoromethanesulfonic acid (TfOH) has been used as an effective catalyst for the Friedel–Crafts acylation[50, 51]. Its derivative, deuterated trifluoromethanesulfonic acid (TfOD), is widely used as the reagent to investigate the reaction mechanism such as the effect of the stereochemistry of the α- and β-position of amino acids. When TfOD was used as the reagent to investigate the intermediate of the reaction of compounds **47** and **48**, we found that an effective H/D exchange occurred on the aromatic ring (Scheme 3.2). Inspired by these results, our group reported an effective TfOD-mediated H/D exchange strategy to prepare the corresponding deuterated α-amino acids (Scheme 3.3).[30] In the presence of TfOD, a rapid and controllable H/D exchange was achieved. The deuteration proceeded well at room temperature and the α-amino acids are highly soluble in the reaction mixture which is a great advantage to prepare deuterated α-amino acids.

Scheme 3.2 Friedel–Crafts reaction and hydrogen/deuterium exchange on aromatic protons in TfOD.

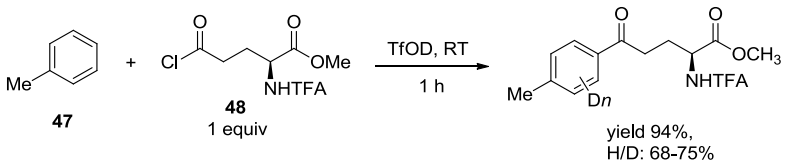

Scheme 3.3 TfOD-mediated H/D exchange

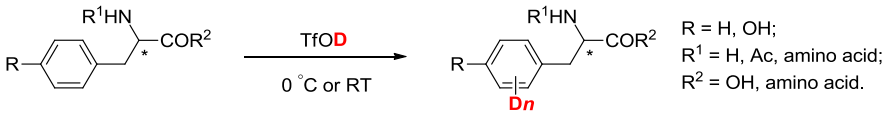

Cross-linking α-amino acids have been widely used for the investigation of ligand-biomolecules interactions.[52] Deuterated cross-linking α-amino acids will be

useful tools for the further identification of the labeled components with the combination of Mass analysis. Based on these backgrounds, we would like to prepare deuterated cross-linking α-amino acids with the TfOD-based H/D exchange strategy in this work.

3.2 Results and Discussion

3.2.1 Cross-linkable α-amino acid derivatives used in this work

Table 3.1 Cross-linkable α-amino acid derivatives.

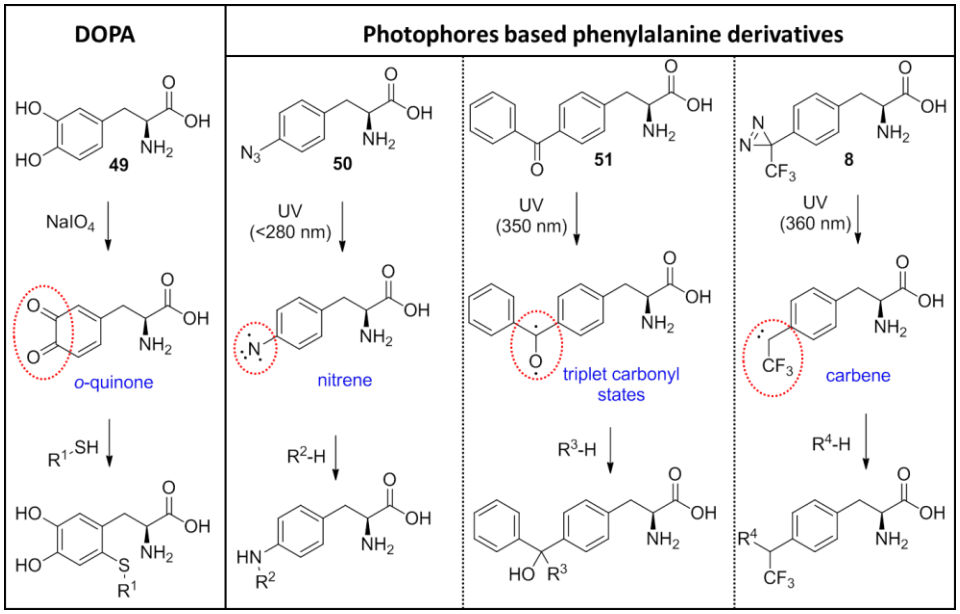

3,4-Dihydroxy-$_L$-phanylalanine ($_L$-DOPA, **49**) that has been used as a cross-linkable reagents for many years.[53] In the presence of periodate, it can be converted to quinone derivative that can be further attacked by the other compounds to form the cross-linking structures. Photophore-based components are kinds of important structures to investigate the corresponding interaction between ligands and receptors.[54] Photophore-based $_L$-phanylalanines are important to investigate peptides

or protein in PAL field. Under the UV irradiation, they can convert to cross-linkable intermediates that can insert into the other compounds. In this work, we examined four different cross-linkable α-amino acids. $_L$-DOPA **49** and three photophores-based $_L$-phenylalanines including 4-azido-$_L$-phenylalanine **50**, 4-benzoyl-$_L$-phenylalanine **51** and 4-[3-(trifluoromethyl)-3*H*-diazirin-3-yl]-$_L$-phenylalanine ($_L$-(4-Tmd)Phe) **8** as shown in Table 3.1.

3.2.2 TfOD-mediated H/D exchange for $_L$-DOPA

Table 3.2 H/D exchange for $_L$-DOPA.

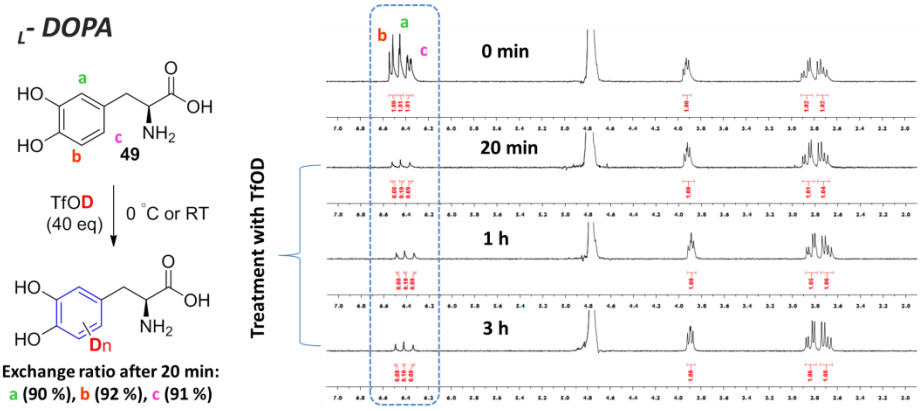

Due to the effect of hydroxyls to the aromatic ring, we speculated that the $_L$-DOPA **49** will show high reactivity during the H/D exchange process. Initially, $_L$-DOPA was treated with 40 equiv of TfOD at room temperature. The exchange ratios were calculated by ^{1}H NMR of the reaction mixtures. As can be seen in Table 3.2, H/D exchange proceeded rapidly and the exchange ratios were higher than 90% for three positions within 20 min. To test the feasibility of this strategy at low temperature, we carried out the standard reaction at 0 °C. Satisfactorily, high efficiency (>90%

exchange ratio) can be also obtained within 20 min that indicating its good thermal adaptability. To further identify the deuteration degree, we subjected the reaction mixture to ESI-TOF-MS and the results also indicated the all deuterated $_{L}$-DOPA (*m/z* 201 and 198 for deuterated $_{L}$-DOPA and undeuterated one, respectively).

3.2.3 TfOD-mediated H/D exchange for photophores-based $_{L}$-phenylalanines

3.2.3.1 H/D exchange for 4-azido-$_{L}$-phenylalanine

Scheme 3.4 H/D exchange for 4-azido-$_{L}$-phenylalanine.

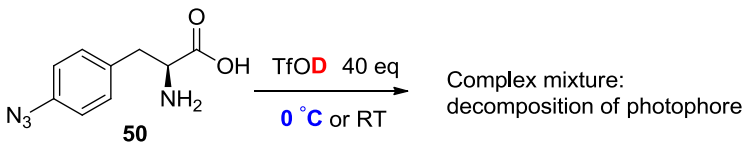

4-Azido-$_{L}$-phenylalanine **50** was treated with TfOD at room temperature, but a complex mixture was obtained (Scheme 3.4). Although the reaction was carried out at 0 °C, similar result was found. Detail investigation indicated that the azide group could react with TfOD which indicating that the azide group is not suitable for this strategy.[55]

3.2.3.2 H/D exchange for 4-benzoyl-$_{L}$-phenylalanine

Scheme 3.5 H/D exchange for 4-benzoyl-$_{L}$-phenylalanine

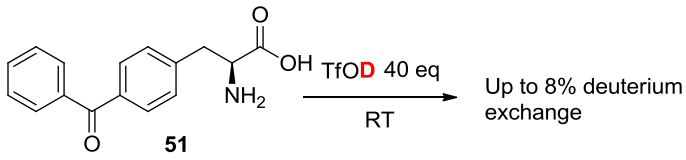

4-Benzoyl-$_{L}$-phenylalanine **51** as another widely used photophore-based

phenylalanine was examined in this work (Scheme 3.5). However, although the treatment was proceed for one day, the total H/D exchange was less than 8% which was detected by ^{1}H NMR. Analysis of the reaction mixture by mass spectrum showed no difference between the 4-benzoyl-$_{L}$-phenylalanine before and after treatment with TfOD. These results indicated that the carbonyl group, a strong electron-withdrawing group, significantly inhibited the H/D exchange mediated by TfOD.

3.2.3.3 H/D exchange for $_{L}$-(4-Tmd)Phe

Table 3.3 H/D exchange for $_{L}$-(4-Tmd)Phe.

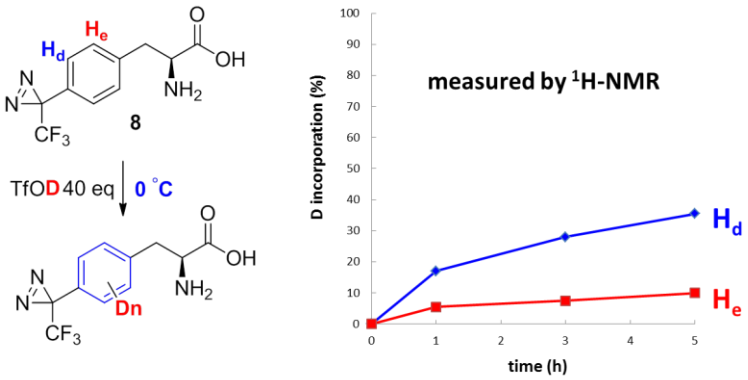

$_{L}$-(4-Tmd)Phe was subjected into the deuteration strategy (Table 3.3). It was found that the diazirine ring decomposed within 1 h at room temperature. This result matched well with that the diazirine ring is unstable in strong acidic conditions.[56,57] When the reaction was carried out at 0 °C for 5 h, no decomposion can be detected which indicating the low temperature (0 °C) should be required for the H/D exchange for $_{L}$-(4-Tmd)Phe. ^{1}H NMR spectrum indicated that 35 and 10% exchange occurred at the 2- and 3-positions, respectively. Notably, long incubation (>5 h) will lead to the decomposition of diazirine.

3.2.4 *N*-acetyl protection as a strategy to improve H/D exchange

Even though the TfOD-mediated H/D exchange is suitable for $_{L}$-DOPA and $_{L}$-(4-Tmd)Phe, the relative low exchange ratio for the latter one should be further improved. Further this purpose, we tested the *N*-acetyl protection strategy. In this work, the amino groups of α-amino acids were protected by acetyl group and were then subjected into the TfOD-mediated H/D exchange system (Table 3.4). Initially

Table 3.4 *N*-Acetyl protection to improve H/D exchange of tyrosine and tryptophan

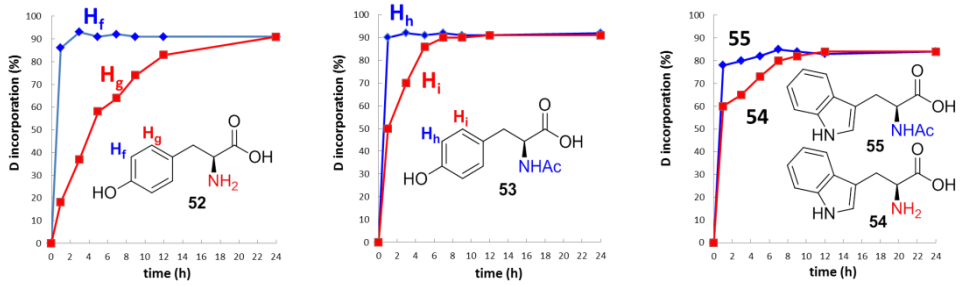

tyrosine and tryptophan were used as the model substrates. For tyrosine, its protected derivative showed higher exchange ratio than that of unprotected one especially for the proton at 2-position. The consistent result was obtained when tryptophan was tested which indicating that the *N*-acetyl protection work well for the improvement of H/D exchange. The possible reason should be that *N*-acetyl protection can prevent the neutralization of TfOD with amino group.

Figure 3.1 H/D exchange of *N*-acetyl protected **46** and **48**.

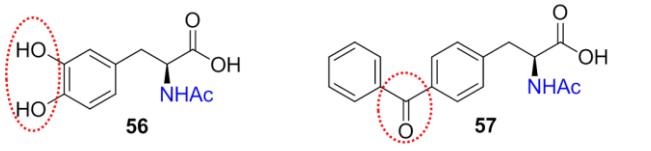

H/D exchange > 90%
(for each position)

H/D exchange : around 8%
(for all of positions)

Table 3.5 H/D exchange of *N*-acetyl protected **8**.

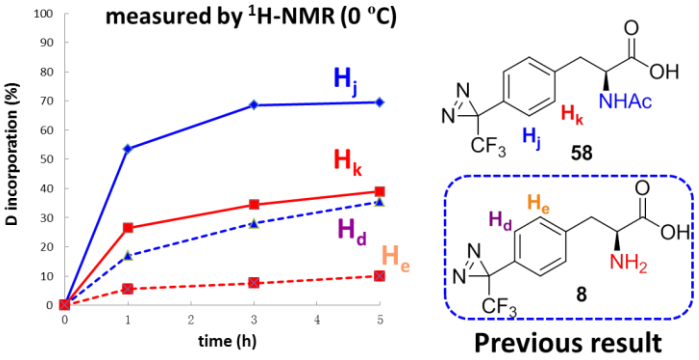

Next, cross-linkable α-amino acids were subjected to the above strategy. For $_{L}$-DOPA and 4-benzoyl-$_{L}$-phenylalanine, *N*-acetyl protection can not improve the exchange ratio indicating the crucial electronic effect for the reaction (Figure 3.1). Then, deuteration for *N*-acetyl protected $_{L}$-(4-Tmd)Phe was carried out (Table 3.5). Interestingly, the exchange ratio was significantly improved which reached to 70 and 30% for 2- and 3-positions, respectively. Compared with unprotected one, *N*-acetyl protected $_{L}$-(4-Tmd)Phe showed higher reactivity under the standard conditions.

3.3 Experimental Section

3.3.1 General procedures for hydrogen-deuterium exchange with TfOD.

Cross-linkable aromatic α-amino acid derivatives (0.25 mmol) were dissolved in TfOD (0.9 mL, 10 mmol) at a specific temperature. The reaction mixture was diluted with H_2O (0.6 mL) followed by ^{1}H-NMR and ESI-TOF mass analysis.

3.3.2 General procedures for acetylation of aromatic α-amino acid derivatives

Aromatic α-amino acid derivatives (0.4 mmol) were dissolved in methanol (2 mL) and acetic anhydride (0.8 mmol) was added dropwise at 40 ℃. The reaction mixture was stirred at same temperature for overnight and concentrated. The residue was subjected to silica-column chromatography (CH_2Cl_2:CH_3OH= 4:1, then ethyl acetate:CH_3OH= 1:1) to afford pure *N*-acetyl compounds in 60-75% yield.

3.4 Conclusions

In this work, we presented a strategy for cross-linkable α-amino acids such as $_L$-DOPA and photophore-based $_L$-phenylalanine derivatives. The findings indicated that the substituents have significant effect on the exchange ratios. As for diazirine-based $_L$-(4-Tmd)Phe, moderate exchange could be obtained. To further improve the deuteration efficiency, an *N*-acetyl protection was introduced, which is able to increase the exchange ratio especially for diazirine-based $_L$-(4-Tmd)Phe. The corresponding work will be of great importance for the elucidation of ligand-receptor interaction with the combination of Mass analysis.

4 Metabolic Studies of Photoreactive Aromatic α-Amino Acid Derivatives with *Klebsiella* sp. CK6

4.1 Introduction

Klebsiella sp. CK6, a rhizobacterium isolated from a dipterocarp sapling in Central Kalimantan, Indonesia, is able to grow with $_{L}$-tryptophan in a nitrogen-limited condition (Figure 4.1).[58] It has been reported that some bacteria can use transaminase for the oxidative deamination reaction of $_{L}$-tryptophan to afford indol-3-acetic acid via intermediary indole-3-pyruvic acid (IAA).[59] Under the treatment by *Klebsiella* sp. CK6, $_{L}$-tryptophan can be converted to IAA and tryptophol (TOL), and indole-3-lactic acid (ILA). However, corresponding work focused on other aromatic α-amino acids are rarely reported. Furthermore, regardless of the great importance of photoaffinity labeling (PAL) in the investigation of peptides and proteins, there are no reported about the metabolism of photophore or photophore-based components in the presence of microorganism such as *Klebsiella* sp. CK6.

Figure 4.1 *Klebsiella* sp.

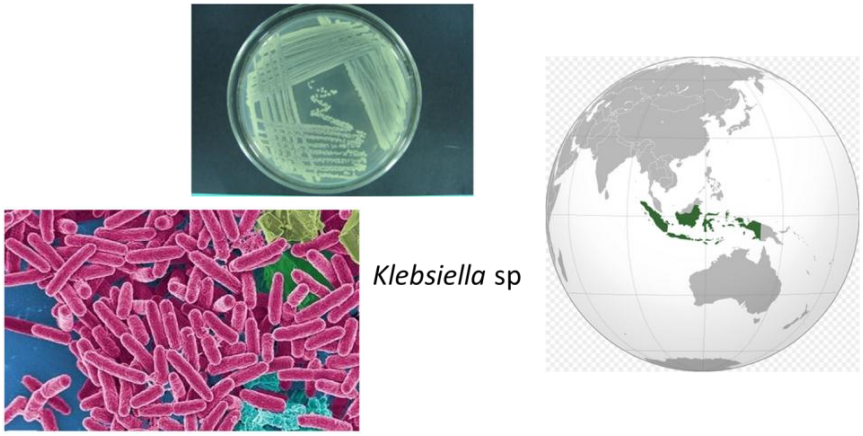

Phenylalanine, a kind of essential amino acid, is of great importance for physiological activity of human beings. Photophore-based phenylalanines have been widely used for the investigation of corresponding peptides and proteins in the field of PAL. To further broaden the application scope of PAL and to investigate the metabolism of photophore-based amino acids in the presence of *Klebsiella* sp. CK6. In this work, for the first time, we investigate the metabolites of photophore-based phenylalanines under the treatment of *Klebsiella* sp. CK6. The effect factors for the different of metabolic pathway were also considered and discussed in this study. This work is of great importance for the application of PAL in the microbial field.

4.2 Results and Discussion

4.2.1 Inoculation of $_L$-phenylalanine with *Klebsiella* sp. CK6

Scheme 4.1 Inoculation of $_L$-phenylalanine with *Klebsiella* sp. CK6.

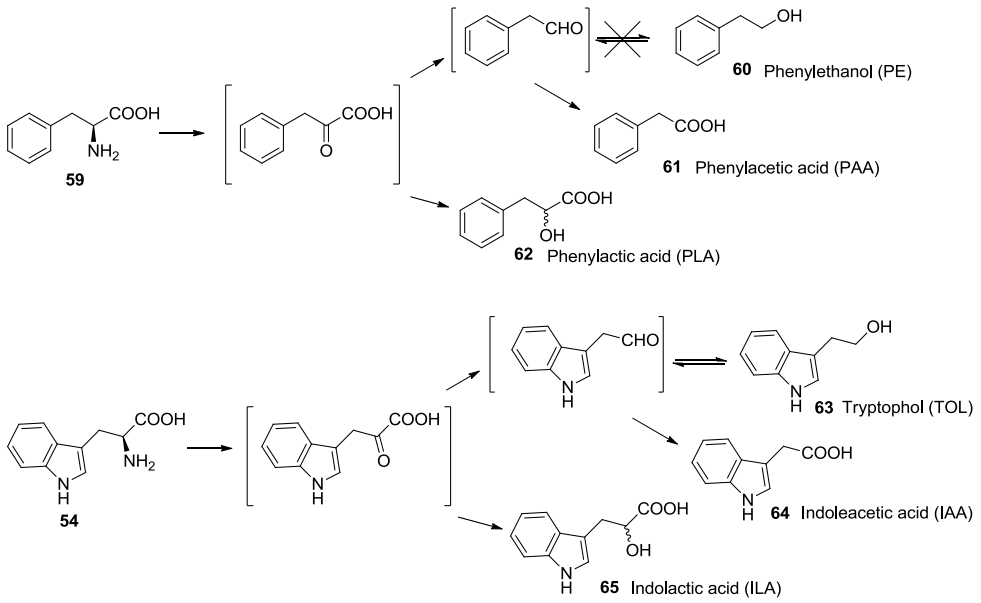

$_L$-Phenylalanine **59** was inoculated with *Klebsiella* sp. CK6 at 28 ℃ for one

week under nitrogen-limiting conditions, and cell growth did not change compared to when the L-tryptophan was used as nitrogen source. It was found that phenylacetic acid **61** (PAA) and phenyllactic acid **62** (PLA) were detected as the major metabolites from L-phenylalanine that was supplemented at pH 6. However, phenylethanol **60** (PE) was not detected in this condition. As for tryptophan **54**, the tryptophol **63** (TOL) type of metabolite are easily detected as shown in the Scheme 4.1. The possible reason should be that the reduction of aldehyde toalcohol recognized the indole ring. Further investigation indicated that D-Phenylalanine was metabolized to less PLA and PAA as compared with the L-Phenylalanine. The above-mentioned results indicated that the metabolic pathways of L-tryptophan and L-phenylalanine were slightly different due to their structures speciality.

4.2.2 Inoculation of photoreactive L-phenylalanine with *Klebsiella* sp. CK6

Table 4.1 Inoculation of photoreactive L-phenylalanine with *Klebsiella* sp. CK6.

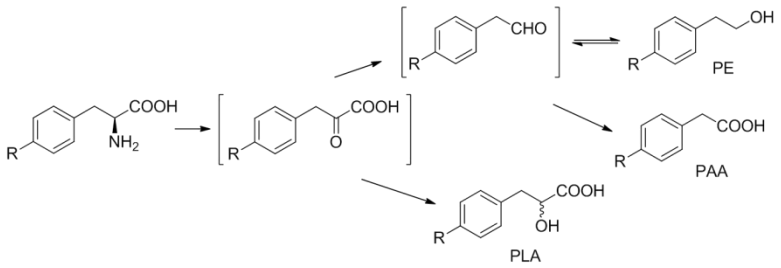

L-Phe derivatives	PLA derivatives	PE derivative	PAA derivatives
50 N_3	✗	✗	**50c** ○
51 	✗	**51b** ○	**51c** ○
8 F_3C N=N	**8a** ○	✗	✗
66 NO_2	**66a** ○	✗	✗

The photoreactive $_{L}$-phenylalanine (**50**, **51** and **8**) and 4-nitro-$_{L}$-phenylalanine **66** were subjected into the same experimental procedure as compared with $_{L}$-phenylalanine (Table 4.1). It was found that inoculation of the 4-azido-$_{L}$-phenylalanine with *Klebsiella* sp. CK6 in the standing condition afforded an azide-substituted PAA derivative as the main metabolite. IR measurements indicated that the azide group (2,140 cm^{-1}) retained after inoculation. As for 4-benzoyl-$_{L}$-phenylalanine, both of benzoyl-substituted PAA and phenylethanol (PE) derivatives can be detected after the incubation. While, no PLA derivative can be found in the mixture. The inoculation of $_{L}$-(4-Tmd)Phe into *Klebsiella* sp. CK6 afforded trifluormethyldiazirinyl-substituted PLA as the sole product. The UV spectrum around 350 nm indicated the diazirine ring. To make a comparison with $_{L}$-(4-Tmd)Phe, 4-nitro-$_{L}$-phenylalanine was also examined in the standard conditions.

On the basis of above results, we would like to summarize the effect factors for the formation of different metabolites. For 4-benzoyl-$_{L}$-phenylalanine a PE type derivative was detected after the incubation of *Klebsiella* sp. CK6 which is consistent with that of $_{L}$-tryptophan. Viewed from their structures, we predicted that the bicyclic moiety should be responsible for the formation of PE type derivatives. Furthermore, for 4-benzoyl-$_{L}$-phenylalanine and 4-azido-$_{L}$-phenylalanine, both of them can afford to PAA type derivatives after the incubation. Thus, we speculated that the formation should be resulted from the resonance between substituent and aromatic ring. For 4-(3-trifluoromethyldiazirinyl)-$_{L}$-phenylalanine and 4-nitro-$_{L}$-phenylalanine, the electron-withdrawing group could promote the reduction of α-keto group that was preferred to further decarboxylation giving phenyllactic acid as the product.

4.3 Experimental Section

4.3.1 Synthesis of 4-azido-$_L$-phenylalanine

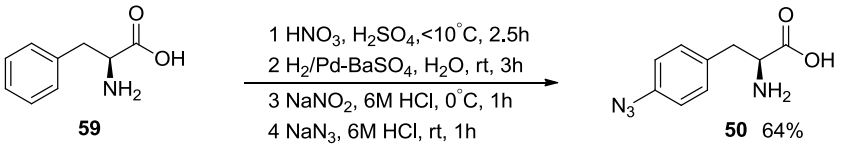

A solution of HNO_3(60%) and concentrated H_2SO_4 (1.4:1.1 v/v) was prepared and chilled to 10 ℃. Then, a portion of the solution (3.5 mL) was added dropwise to a solution of $_L$-phenylalanine **59** (4.139 g, 25.1 mmol) in H_2SO_4 (98%, 12.5 mL). The reaction mixture was stirred at 10 ℃ for 2.5 h. The reaction solution was then adjusted to pH 5 with NH_4OH. The formed pale yellow precipitate was collected by filtration, washed with water and MeCN, and then dried to afford 4-nitro-$_L$-phenylalanine as a yellow powder (4.748 g, 90%). 4-Nitro-$_L$-phenylalanine (2.006 g, 9.54 mmol) was suspended in water (35 mL) and subjected to hydrogenation at RT for 3 h with 0.2 g of 5% palladium-barium sulfate. The catalyst was filtered through a Celite pad, and the pale brown filtrate was concentrated. The residue was washed with MeCN to afford a pale brown mass (1.460 g, 85%). Without further purification, the 4-amino-$_L$-phenylalanine derivative (0.060 g, 0.33 mmol) was dissolved in 6N HCl (4 mL). Sodium nitrate in water (0.030 g/0.5 mL) was added at 0 ℃. The reaction mixture was stirred for further 40 min and diluted with 6N HCl (0.25 mL). Subsequently, sodium azide in water (0.033 g/0.75 mL) was added at 0 ℃. The reaction mixture was stirred for 5 min, and then warmed to room temperature and concentrated. The residue was reprecipitated from MeCN to give a pure colorless amorphous mass (0.0435 g, 64%).

4.3.2 Synthesis of 4-benzoyl-$_L$-phenylalanine

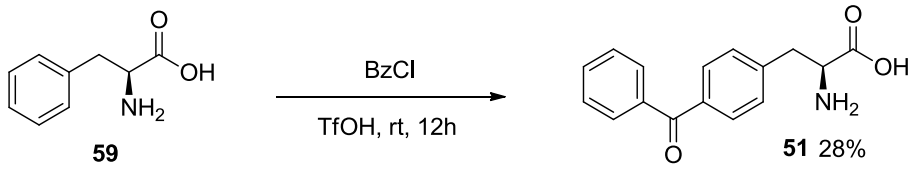

Trifluoromethanesulfonic acid (0.5 mL) was added to $_L$-phenylalanine **59** (16.5 mg, 0.1 mmol) in a tube fitted with a screw cap and PTFE-faced rubber liner. After the solution became homogeneous, benzoyl chloride (8 equiv) was added at 0 ℃. The reaction mixture was stirred at RT for further 12 h, and then poured into ice water and extracted with EtOAc. The organic layer was washed with saturated NaCl, dried over $MgSO_4$ and filtrated. The filtrate was concentrated and the corresponding residue was subjected to silica column chromatography (EtOAc/MeOH/H_2O = 8:1:1) to afford colorless amorphous mass (7.5 mg, 28%, 98% ee).

4.3.3 Synthesis of $_L$-(4-Tmd)Phe

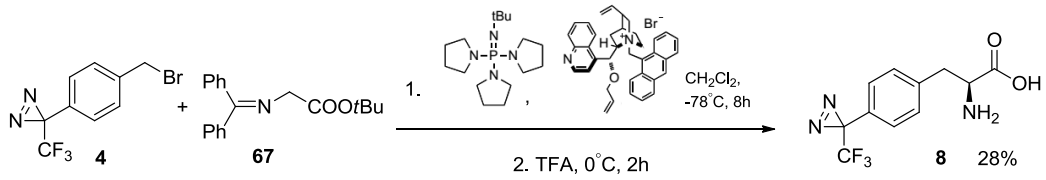

The diazirinyl benzyl bromide **4** (5, 30.0 mg, 0.10 mmol) was reacted with diphenyliminoglycine *t*-butyl ester **67** (6, 40.8 mg, 0,14 mmol) in the presence of catalytic cinchonidium salt and phosphazene base BTPP at -78 ℃. The reaction mixture was further treated with TFA without any treatment. The reaction mixture was concentrated and subjected to silica column chromatography (EtOAc/ MeOH/H_2O = 8:1:1) to afford colorless solid (7.7 mg, 28%, 98% ee). As our recent report, through the direct introduction of TPD into phenylalanine, we can also obtain the corresponding product in good yield.[29]

4.3.4 Culture medium and growth conditions

Phenylalanine derivatives in DMSO/H_2O (1:1; 75 mg/L) were filtered using a filter unit and then supplemented. The inoculated mixture formed the standing culture under conditions of 28 ℃ for 7 days in the dark. After incubation, cultured media were centrifuged at 3,500 $\times g$ for 10 min. The supernatant was adjusted to pH 2.5 with aqueous HCl and was then extracted with EtOAc for three times. The organic layer was dried over $MgSO_4$, filtered, and concentrated to afford a residue. The crude residue was subjected to silica column chromatography to afford pure metabolites.

4.3.5 Characterization of corresponding products

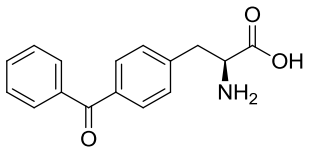

51. ^{1}H-NMR (CD_3OD): δ 7.76 (d, 2H, *J* = 8.6 Hz, Ar), 7.75 (d, 2H, *J* = 8.6 Hz, Ar), 7.64 (t, 1H, *J* = 7.4 Hz, Ar), 7.52 (t, 2H, *J* = 7.4 Hz, Ar), 7.47 (d, 2H, *J* = 8.0 Hz, Ar), 3.83 (m, 1H, H_α), 3.35 (m, 1H, H_β), 3.09 (m, 1H, H_β).

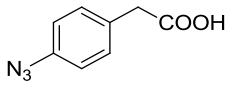

50c. δ 7.28 (d, 2H, *J* = 7.8 Hz, Ar), 7.01 (d, 2H, *J* = 7.8 Hz, Ar), 3.65 (m, 2H, 2-H), IR (film): 2150 cm^{-1}, ESI-MS (negative): *m/z* 176 $[M-H]^-$.

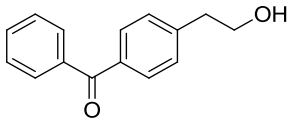

51b. 1H-NMR ($CDCl_3$): δ 7.77 (m, 4H, Ar), 7.60 (d, 1H, *J* = 7.8 Hz, Ar), 7.48 (d, 2H, *J* 7.8 Hz, Ar), 7.36 (d, 2H, *J* = 7.8 Hz, Ar), 3.93 (t, 2H, *J* = 7.8 Hz, CH_2), 2.97 (m, 2H, *J* = 7.8 Hz, CH_2), FD-MS: *m/z* 226 $[M]^-$.

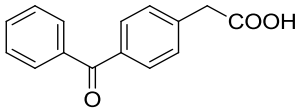

51c. 1H-NMR (CDCl3): δ 7.80 (m, 4H, Ar), 7.58 (d, 1H, *J* = 7.8 Hz, Ar), 7.49 (d, 2H, *J* = 7.8 Hz, Ar), 7.42 (d, 2H, *J* = 7.8 Hz, Ar), 3.68 (m, 2H, 2-H), FD-MS: *m/z* 240 $[M]^-$.

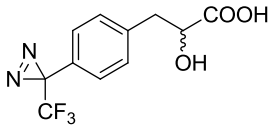

8a. ^{1}H-NMR (CD_3OD): δ 7.38 (d, 2H, *J* 7.8 Hz, Ar), 7.12 (d, 2H, *J* 7.8 Hz, Ar), 4.20 (m, 1H, 2-H), 3.46 (m, 1H, 3-Ha), 3.15 (m, 1H, 3-Hb), ESI-MS (negative): *m/z* 273 $[M-H]^-$, 246 $[M-N_2-H]^-$. λ_{max} (ε) (CH_3OH) 355 (380).

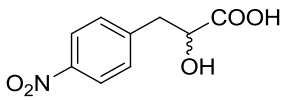

66a. ^{1}H-NMR (CD_3OD): δ 8.15 (d, 2H, *J* = 7.8 Hz, Ar), 7.51 (d, 2H, *J* = 7.8 Hz, Ar), 4.37 (m, 1H, 2-H), 3.56 (m, 1H, 3-Ha), 3.03 (m, 1H, 3-Hb), ESI-MS (negative): *m/z* 210 $[M-H]^-$.

4.4 Conclusions

In conclusion, the metabolic study for incubation of photoreactive $_L$-phenylalanine with *Klebsiella* sp CK6 was presented in this work. The results indicated that the photoreactive $_L$-phenylalanine proceed in a similar pathway compared with nomal $_L$-phenylalanine under the incubation of *Klebsiella* sp CK6. The effect factors especially the substituent effect was described. It is the first report about the metabolite analysis of various photoreactive $_L$-phenylalanines incubated by *Klebsiella* sp CK6, which can be used for the further photoaffinity labeling of metabolic enzymes,

5 TPD-Based Photoreactive Saccharins for Photoaffinity Labeling of Gustatory Receptors

5.1 Introduction

Sweetness is one of the important tastes that humans can distinguish. Numerous sweeteners are used in our daily life, industrial manufacture and scientific research such as sucrose, xylose, saccharin, glucose, sucralose, *etc*. Among of them, saccharin (Figure 5.1) is one of the widely used sweeteners that is several hundred times sweeter that sucrose. Interestingly, it presents bitter taste at high concentrations. It was well known that the sweet and bitter taster receptors are G protein-coupled receptors and human heterodimeric sweet taste receptor (hT1R2-hT1R3) can responds to a lot of chemical substances.[60] To investigate the interaction between saccharin derivatives with their receptors, many methods are utilized including X-ray crystallography, NMR spectroscopy and molecular modeling. However, due to the limited structural information of the ligands and receptor, the receptor bound conformation of the sweeteners remains ambiguous.

Figure 5.1 Saccharin.

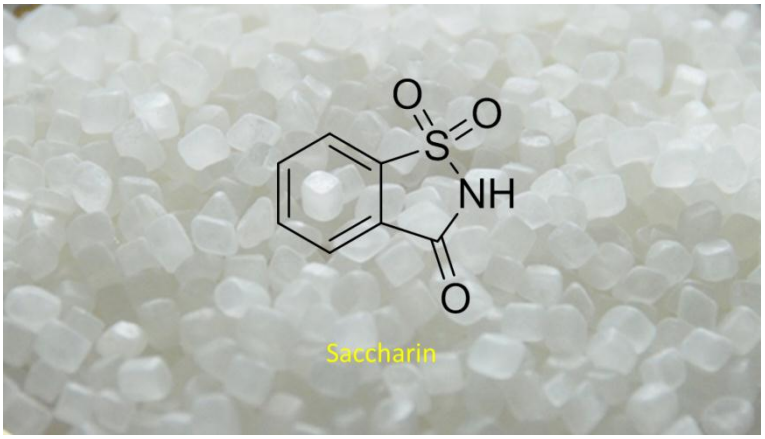

PAL is an excellent strategy to investigate the structural and functional relationships between bioactive compounds and receptors. To construct photophore-based saccharins will be a useful strategy to investigate the interaction between saccharin and its receptor. Previously, arylazide-based saccharins as a kind of photoreactive component had been reported for the click reaction,[61] but no work focused on the photoaffinity labeling can be found. Among of the photophores used in PAL, 3-trifluoromethyl-3-phenyl-diazirine (TPD) has been used as the most promising one due to its many advantages. In this work, we would like to prepare TPD-based saccharin derivatives that can be used as promising reagents to investigate the binding information of saccharin and its receptor.

5.2 Results and Discussion

5.2.1 Synthesis of TPD-based saccharin derivatives

To introduce photophore to a substrate, how to minimize the effect of photophore against their natural biological activities is one of the important factors that we should consider. Previously, Suamin et al reported that substitutions at the 5- and 6-positions in saccharin were tolerated with regards to its biological activities.[62] Inspired by this work, we would like to introduce diazirine to 5- and 6-positions of saccharin, respectively. 2,2,2-Trifluoro-1-(*p*-tolyl)ethanones **68** were used as the starting material which were initially treated with hydroxylamine hydrochloride in the presence of NaOH and EtOH to afford oximes **69** (Scheme 5.1). An alternative strategy with pyridine as the solvent at 70 °C can afford the desired product in slight higher yield.[63] The oximes were then subjected to tosylation in the presence of tosylchloride in pyridine to afford compounds **1c** and **1d**. Next, tosyloximes were converted to corresponding TPD via two method: one is the conventional strategy to construct TPD

through the intermediate diaziridine. Tosyloxime was stirred in the liquid ammonia for 18 h and the corresponding diaziridine **70** was obtained which was further oxidized to TPD in the presence of I_2 and triethylamine. The other strategy is our reported one-pot method. Tosyloximes were directly treated with liquid ammonia at 80 °C or with the addition of $LiNH_2$ at room temperature. Both of these methods can readily afford to TPD in good yield. Furthermore, there is no necessary for the isolation of intermediated diaziridine that significantly benefited the synthetic procedure.

Scheme 5.1 Synthesis of TPD derivatives.

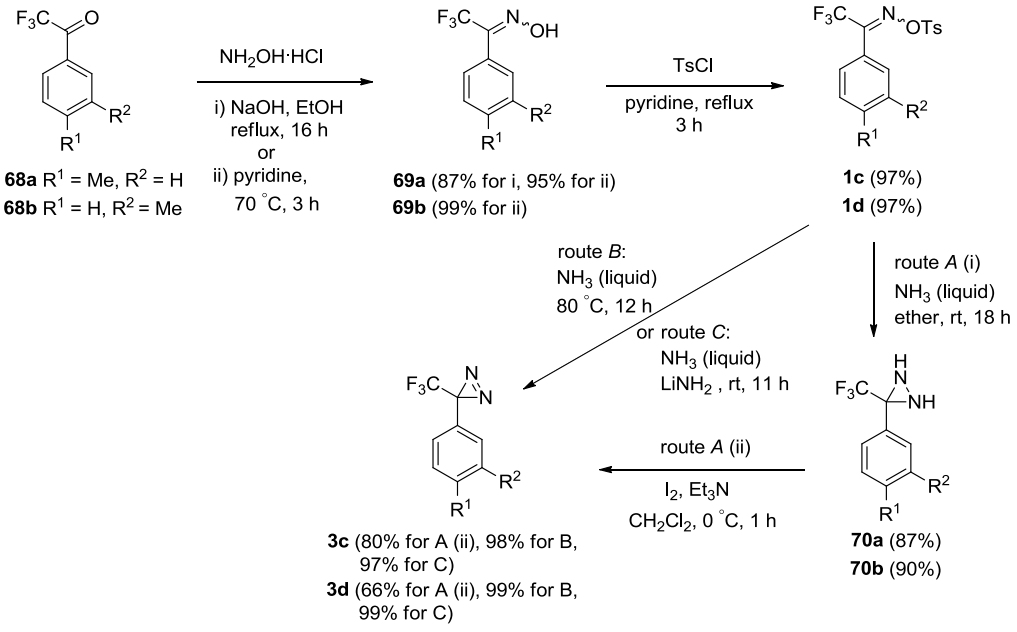

With 3-(*p*-or *m*-tolyl)-3-(trifluoromethyl)-3*H*-diazirines in hand (**3c** and **3d**), we started to synthesize corresponding photoreactive saccharins (Scheme 5.2). TPD derivatives were initially treated with chlorosulfonic acid at -20 °C to afford the aromatic chlorosulfonation at adjacent position of methyl group. Then, the sulfonyl chloride was converted to corresponding *N*-alkylated sulfonamide with *t*$BuNH_2$ at RT. The oxidative cyclization was carried out in the presence of H_5IO_6 and CrO_3. To

improve the reaction yield, we performed these three reactions as one-pot without the isolation of corresponding intermediates. Finally, the desired product was obtained in a yield of 30%. Next, compound **71a** and **71b** were treated with trifluoroacetic acid (TFA) under reflux to give photoreactive saccharin derivatives **72a** and **72b**. Due to the low solubility of compound **72a** and **72b** in water, we converted them to corresponding sodium salts with aqueous sodium hydroxide to improve their solubility.

Scheme 5.2 Synthesis of photoreactive saccharin derivatives.

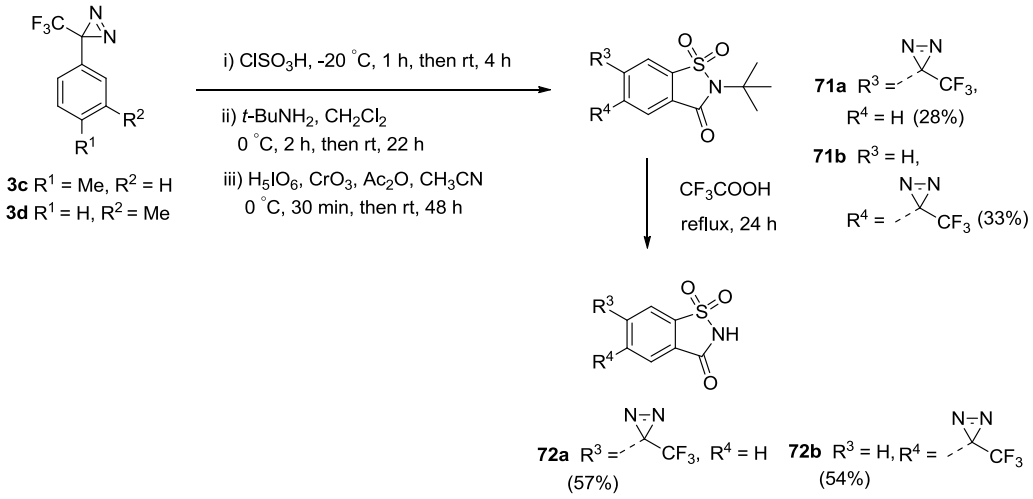

5.2.2 HPLC, photolysis and gustator receptor assay of photoreactive saccharin

5.2.2.1 HPLC and photolysis of photoreactive saccharins

HPLC analysis was conducted with a ODS column with elution of 30% MeOH (Figure 5.2). The absorption was detected under 215 nm or 350 nm (for diazirine ring). ^{19}F NMR spectra at -65 ppm well indicated that the diazirine ring are tolerate under the synthetic procedure.[56]

Figure 5.2 HPLC analysis of saccharin **72a** and **72b.**

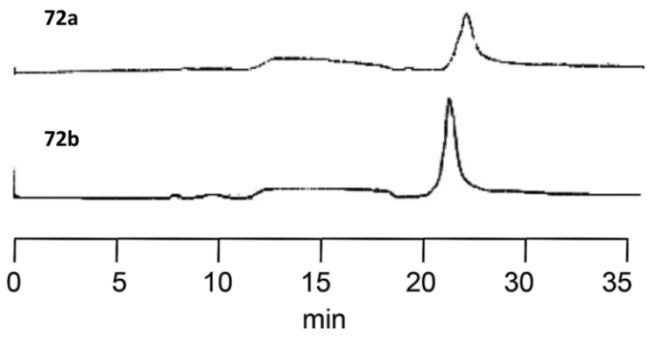

Figure 5.3 Photoreactions of **72a** and **72b** with MeOH.

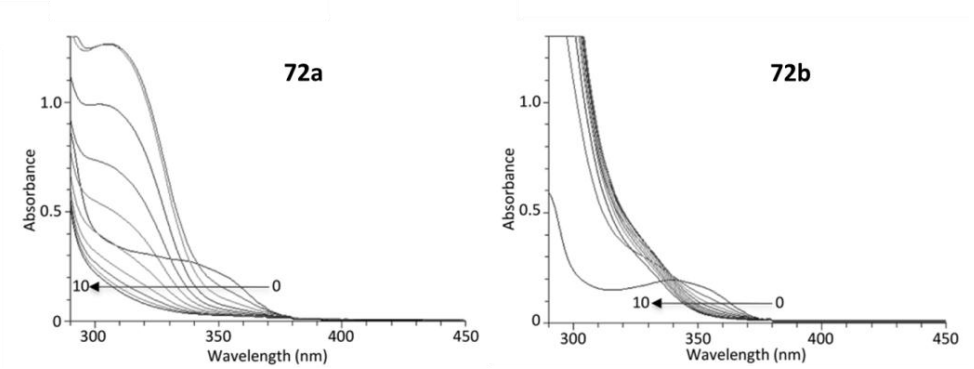

Photoreactions of **72a** and **72b** with MeOH were also carried out to identify their photoreactive property (Figure 5.3). Previously, it has been reported that the diazo derivatives, the major byproducts can not afford carbenes under UV irradiation with a concentration over 10 Mm.[64] While, with a concentration lower than 1 mM, diazo derivative can readily afford to carbene under the irradiation at 350 nm. Thus, methanolic solutions of **72a** and **72b** (1 mm) were irradiated with a black light (15 W) at a distance of 3 cm. The absorbance around 350 nm were measured at each minute. The half-life of photoreactive saccharin derivatives **72a** and **72b** were calculated as 77 and 107 s respectively. Compared with the half-life of diazirinyl α-amino acid derivatives, compound **72a** and **72b** showed shorter half-life.[65] The ^{19}F NMR

spectrum showed that the chemical peaks was changed from -65 to -78 ppm after irradiation, which are consistent with previous report. Furthermore, the signal of diazo (-58 ppm) can not be found in the mixture.[64]

5.2.2.2 Gustator receptor assay of photoreactive saccharins

Figure 5.4 Gustatory receptor assay of **72a** and **72b**.

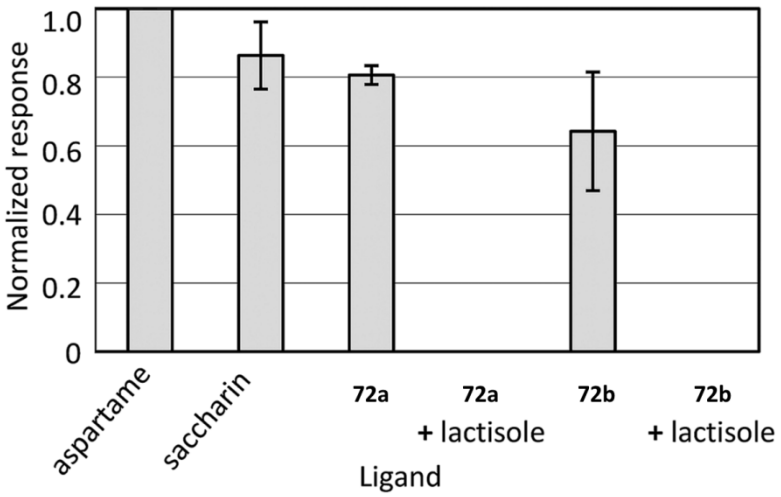

The photoreactive saccharin derivatives **72a** and **72b** were subjected to preliminary gustatory receptor assay to identify their affinity (Figure 5.4). The HEK293 T cells[66] were transfected with G_{16}/gust25 and hT1R2-hT1R3 (sweet), hT2R31 and hT2R43 (bitter) constructs. Corresponding interaction were detected by Ca^{2+} imaging analysis on cultured cells. The cells were defined as responding positively when the fluorescence ratio F340/F380 of the calcium sensor increased above 0.15 after the addition of reagents. It was found that saccharin, compound **69a** and **69b** have 90, 80 and 65% relative sweetness activity against the aspartame for the hT1R2-hT1R3 expressed on HEK-293 T cell. With the addition of lactisole, one of the specific inhibitors in the sweet taste assay, the responses were completely inhibited.

Furthermore, the response of **72a** and **72b** toward bitter receptor hT2R31 were calculated as 60 and 80%, respectively. The other bitter receptors such as hT2R43[67] has no response to **72a** and **72b** at a concentration of 10 mM.

5.3 Experimental Section

5.3.1 Synthetic section

*Synthesis of 2,2,2-trifluoro-1-(p-tolyl)ethanone oxime (**69a**):* i) in EtOH: 2,2,2-trifluoro-1-(*p*-tolyl)ethanone **68a** (0.104 g, 0.55 mmol) in EtOH (5 mL) was added to hydroxylamine hydrochloride (0.0459 g, 0.66 mmol) and NaOH (0.064 g, 1.6 mmol) in EtOH (5 mL). The reaction mixture was refluxed for 16 h, and then concentrated. The residue was partitioned between ether and water. The organic layer was washed with 0.01 M HCl and water, dried over $MgSO_4$, filtrated and concentrated to afford colorless amorphous mass (0.0974 g, 87%). ii) in pyridine: 2,2,2-trifluoro-1-(*p*-tolyl)ethanone **68a** (1.13 g, 6.0 mmol) was dissolved in pyridine (30 mL), then hydroxylamine hydrochloride (0.500 g, 7.2 mmol) was added. The mixture was stirred at 70 ℃ for 1 h and was then subjected to rotary evaporation to remove pyridine. The residue was dissolved in ethyl acetate and washed with 1 M HCl, the organic layer was washed with H_2O and brine, dried over $MgSO_4$ and concentrated to afford colorless amorphous mass (1.17 g, 96%). The product was mixture of *syn*- and *anti*- isomers:

*Synthesis of 2,2,2-trifluoro-1-(m-tolyl)ethanone oxime (**69b**)***:*** The same treatment of 2,2,2-trifluoro-1-(*m*-tolyl)ethanone **68b** (1.13 g, 6.0 mmol) in pyridine was carried out as that just described above to afford **69b** (1.21 g, 99%) as a colorless amorphous mass.

*Synthesis of 2,2,2-trifluoro-1-(p-tolyl)ethanone O-tosyl oxime (**1c**):* To a solution of oxime **69a** (0.910 g, 4.5 mmol) in acetone (30 mL) at 0 ℃, triethylamine (1.87 mL, 13.4 mmol) was added. Then, *p*-toluenesulfonyl chloride (0.945 g, 5.0 mmol) was added to the reaction mixture that was stirred at room temperature for 1 h. After evaporation, the residue was purified by silica gel column chromatography (EtOAc/hexane, 1:3) to afford colorless amorphous mass (1.50 g, 93%, mixture of *syn*- and *anti*- isomers). *2,2,2-trifluoro-1-(m-tolyl)ethanone O-tosyl oxime (**1d**):* The same treatment of **69b** (1.04 g, 5.1 mmol) was carried out as that just described above to afford **1d** as colorless amorphous mass (1.68 g, 92%, mixture of *syn*- and *anti*- isomers). *3-(p-tolyl)-3-(trifluoromethyl)diaziridine (**70a**)*: To liquid NH_3 (20 mL) at -78 ℃ in a sealed tube, tosyloxime **1c** (1.02 g, 2.9 mmol) in ether (5 mL) was added. The reaction mixture was stirred at room temperature for 8 h. After evaporation of NH_3 gas, the reaction mixture was partitioned between ether and water. The organic layer was washed with brine, dried over $MgSO_4$ and evaporated. The residue was subjected to silica-column chromatography (AcOEt/hexane 1:5) to afford 3-(*p*-tolyl)-3-(trifluoromethyl)diaziridine **70a** as colorless amorphous mass (0.502 g, 87%).

*Synthesis of 3-(m-tolyl)-3-(trifluoromethyl)diaziridine (**70b**):* The same treatment of **1d** (1.030 g, 2.9 mmol) was carried out as that just described above to afford **70b** as colorless amorphous mass (0.524 g, 90%).

*Synthesis of 3-(p-tolyl)-3-(trifluoromethyl)-3H-diazirine (**3c**):* Route A (stepwise conversions via diaziridine); The diaziridine **70a** (0.143 g, 0.71 mmol) was dissolved in CH_2Cl_2 (5 mL) and triethylamine (0.29 mL), and cooled at 0 ℃. Iodine (0.199 g, 0.78 mmol) was added dropwisely. The reaction mixture was stirred for 1 h and was washed with 1 M NaOH, H_2O and brine. The organic layer was dried over $MgSO_4$, filtrated and concentrated. The residue was subjected to silica-column

chromatography ($CHCl_3$/EtOAc, 19:1) to afford **3c** colorless oil (0.114 g, 80%). Route B (one-pot synthesis); To liquid NH_3 (10 mL) at -78 ℃ in a sealed tube, tosyloxime **1c** (0.711 g, 2.0 mmol) was added. The reaction was stirred at 80 ℃ for 11 h. The sealed tube was cooled at -78 ℃ and the reaction mixture was diluted with Et_2O (50 mL). The sealed tube was warmed at room temperature to remove the ammonia gradually. The organic layer was washed by H_2O, brine, dried over $MgSO_4$ and carefully evaporated (0 ℃) to afford colorless oil (0.392 g, 98%). Route C (one-pot with $LiNH_2$); To liquid NH_3 (5 mL) at -78 ℃ in a sealed tube, tosyloxime **1c** (0.711 g, 2.0 mmol) and $LiNH_2$ (0.230 g, 10 mmol) was added. The reaction was stirred at room temperature for 12 h. The sealed tube was cooled at -78 ℃ and the reaction mixture was diluted with Et_2O (50 mL). The sealed tube was warmed at room temperature to remove the ammonia gradually. The organic layer was washed by H_2O (three times), brine, dried over $MgSO_4$ and carefully evaporated (0 ℃) to afford colorless oil (0.388 g, 97%).

*Synthesis of 3-(m-tolyl)-3-(trifluoromethyl)-3H-diazirine (**3d**):* Route A (stepwise conversions via diaziridine); The same treatment of **70b** (0.143 g, 0.71 mmol) was carried out as that just described above to afford **3d** (0.094 g, 66%) as colorless oil with identical manner described above. Route B (one-pot synthesis); The same treatment of **1d** (0.715 g, 2.0 mmol) was carried out as that just described above to afford **3d** (0.3960 g, 99%) as colorless oil. Route C (one-pot with $LiNH_2$); The same treatment of **1d** (0.722 g, 2.0 mmol) as that just described to afford **3d** (0.400 g, 99%) as colorless oil.

*Synthesis of N-tert-butyl-6-(3-(trifluoromethyl)-3H-diazirin-3-yl)-1,2-benzisothiazole-3-one-1,1-dioxide (**71a**):* Chlorosulfonic acid (0.380 mL, 5.7 mmol) was cooled at -20 ℃. Compound **3c** (0.115 g, 0.57 mmol) was added dropwise and the reaction mixture was stirred at same temperature for 1 h, warmed to room temperature, and

stirred for 4 h, then poured into ether and ice water. The organic layer was washed with saturated $NaHCO_3$, dried over $MgSO_4$ and filtrated. The filtrate was concentrated to afford crude 2-methyl-5-(3-(trifluoromethyl)-3*H*-diazirin-3-yl)benzene-1-sulfonyl chloride as pale yellow oil. The crude residue in CH_2Cl_2 (1 mL) was added to *t*$BuNH_2$ (0.130 mL, 1.2 mmol) in CH_2Cl_2 (1 mL) at 0 ℃. The reaction mixture was stirred at same temperature for 2 h, and then warmed to room temperature for 3 h. The reaction mixture was washed with 0.1 M HCl and saturated $NaHCO_3$, dried over $MgSO_4$ and filtrated. The filtrate was concentrated to afford *N-tert*-butyl-2-methyl-5-(3-(trifluoromethyl)-3*H*-diazirin-3-yl) benzenesulfonamide as pale yellow oil. CrO_3 (6.0 mg, 0.06 mmol) and acetic anhydride (0.430 mL, 4.5 mmol) were added to ortho-periodic acid (1.06 g, 4.6 mmol) in CH_3CN (10 mL). The crude material in minimum volume in CH_3CN was added at 0 ℃. The reaction mixture was stirred at room temperature for 2 d and concentrated. The residue was redissolved in EtOAc and washed with saturated $NaHCO_3$, saturated $Na_2S_2O_3$ and brine. The organic layer was dried over $MgSO_4$, filtrated and concentrated. The crude oil was subjected to silica gel column chromatography (hexane/CH_2Cl_2, 3:1) to afford **71a** as pale yellow amorphous mass (0.056 g, 28%).

*Synthesis of N-tert-butyl-5-(3-(trifluoromethyl)-3H-diazirin-3-yl)-1,2-benzisothiazole-3-one-1,1-dioxide (**71b**):* The same treatment of **3d** (0.136 g, 0.68 mmol) was carried out as that just described above to afford 2-methyl-4-(3-(trifluoromethyl)-3*H*-diazirin-3-yl)benzene-1-sulfonyl chloride. The same treatment of the residue was carried out as that just described above to afford *N-tert*-butyl-2-methyl-4-(3-(trifluoromethyl)-3*H*-diazirin-3-yl) benzenesulfonamide. The same treatment of the residue with H_5IO_6, CrO_3 and acetic anhydride as that just described for **71b** (0.0781 g, 33%).

*Synthesis of 6-(3-(trifluoromethyl)-3H-diazirin-3-yl)-1,2-benzisothiazole-3-one-1,1-dioxide (**72a**):* Compound **71a** (13.5 mg, 39 mmol) was dissolved in TFA (2 mL). The reaction mixture was refluxed for 24 h, and then concentrated. The residue was dissolved in EtOAc and washed with saturated $NaHCO_3$, 1 M HCl, then brine. The organic layer was dried over $MgSO_4$ and filtrated. The filtrate was concentrated, then the residue was recrystallized from EtOAc and hexane at -20 ℃ to afford **72a** (6.5 mg, 57%) as colorless amorphous mass.

*Synthesis of 5-(3-(trifluoromethyl)-3H-diazirin-3-yl)-1,2-benzisothiazole-3-one-1,1-dioxide (**72b**):* Compound **71b** (13.2 mg, 38 mmol) in TFA (2 mL) was treated same manner described for **71a**. The residue was recrystallized from EtOAc and hexane at -20 ℃ to afford **72b** as afford colorless amorphous mass (6.0 mg, 54%). l_{max} (*e*) (CH_3OH) 280 (1005), 340 (280).

5.3.2 HPLC purification for TPD-based saccharin derivatives

The suspension of **72a** and **72b** in aqueous solution were made alkaline with 1M NaOH. The sodium salts were subjected to HPLC (Tosoh TSKgel ODS-80Ts (4.6 x 250 mm), 30% MeOH, 1 mL / min, detection at 215 nm or 350 nm).

5.3.3 Photolysis of TPD-based saccharin derivatives with MeOH

Methanolic solutions of **72a** and **72b** (1 mM) were irradiated with black light (15 W) at a distance 3 cm. The spectrum of each minute was measured. The decrease in absorbance at around 350 nm was plotted and used to calculate half-life. ^{19}F NMR (470 MHz, CD_3OD): d = -78.0 ppm (from **72a** and **72b**). HRMS (ESI): calcd. for $C_{10}H_9F_3NO_4S$ 296.0199; found 296.0191 (from **72a**), 296.0194 (from **72b**)

5.3.4 Gustatory-tasting effect assay

Synthetic compounds **72a** and **72b** were tested in a gustatory-tasting effect assay. This utilized Ca^{2+} imaging analysis on cultured cells using similar conditions to those previously described. Briefly, HEK293T cells were transfected with G_{16}/gust25 and hT1R2-hT1R3 (sweet), hT2R31 and hT2R43 (bitter) constructs. Ca^{2+} imaging analysis was performed essentially as described by Ueda et al.[23] Cells were defined as responding positively when the fluorescence ratio F340/F380 of the calcium sensor increased above 0.15 after the addition of a reagent.

5.3.5 Characterization of corresponding products

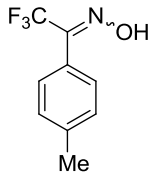

69a. The product was mixture of *syn*- and *anti*- isomers: ^{1}H NMR (270 MHz, $CDCl_3$): *d* = 9.01 (brs, 1H), 7.37–7.44 (m, 2H), 7.21–7.29 (m, 2H), 2.39 (s, 0.8H), 2.38 (s, 2.2H) ppm. ^{13}C NMR (68 MHz, $CDCl_3$): *d* = 148.2 (q, $^{2}J_{C,F}$ = 30.6 Hz), 141.2 and 141.0, 129.42 and 129.36, 128.7 and 128.3, 123.0, 118.5 (q, $^{1}J_{C,F}$ = 283.0 Hz), 21.3 and 21.2 ppm. ^{19}F NMR (470 MHz, $CDCl_3$): *d* = -62.4, -66.6 ppm. HRMS (ESI): calcd. for $C_9H_9F_3NO$ 204.0636; found 204.0632.

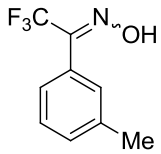

69b. ^{1}H NMR (270 MHz, $CDCl_3$): *d* = 8.76 (brs, 0.6H), 8.59 (brs, 0.4H), 7.29–7.40 (m, 4H), 2.40 (s, 1.8H), 2.39 (s, 1.2H) ppm. ^{13}C NMR (68 MHz, $CDCl_3$): *d* = 148.4 (q, $^{2}J_{CF}$ = 30.7 Hz), 148.1 (q, $^{2}J_{C,F}$ = 32.4 Hz), 138.6, 131.6 and 131.4, 129.8 and

129.1, 129.0 and 128.6, 125.9 and 125.7, 125.5, 120.7 (q, $^{1}J_{C,F}$ = 274.8 Hz), 118.4 (q, $^{1}J_{C,F}$ = 282.9 Hz), 21.2 and 21.1 ppm. ^{19}F NMR (470 MHz, $CDCl_3$): *d* = -62.4, -66.8 ppm. HRMS (ESI): calcd. for $C_9H_9F_3NO$ 204.0636; found 204.0628.

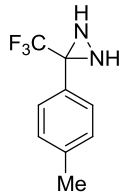

70a. ^{1}H NMR (270 MHz, $CDCl_3$): *d* = 7.50 (d, *J* = 8.0 Hz, 2H), 7.22 (d, *J* = 8.0 Hz, 2H), 2.76 (d, *J* = 8.0 Hz, 1H), 2.38 (s, 3H), 2.19 (d, *J* = 8.0 Hz, 1H) ppm. ^{13}C NMR (68 MHz, $CDCl_3$): *d* = 140.3, 129.5, 128.9, 128.1, 123.7 (q, $^{1}J_{C,F}$ = 278.1 Hz), 57.8 (q, $^{2}J_{C,F}$ = 35.9 Hz), 21.1 ppm. ^{19}F NMR (470 MHz, $CDCl_3$): *d* = -75.7 ppm. HRMS (ESI): calcd. for $C_9H_{10}F_3N_2$ 203.0796, found 203.0785.

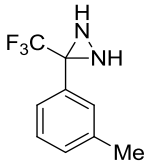

70b. ^{1}H NMR (270 MHz, $CDCl_3$): *d* = 7.40 – 7.42 (m, 2H), 7.31 (t, *J* = 7.8 Hz, 1H), 7.25 (d, *J* = 7.8 Hz, 1H), 2.77 (d, *J* = 8.0 Hz, 1H), 2.38 (s, 3H), 2.21 (d, *J* = 8.0 Hz, 1H) ppm. ^{13}C NMR (68 MHz, $CDCl_3$): *d* = 138.7, 131.7, 131.0, 128.73, 128.69, 125.3, 123.6 (q, $^{1}J_{C,F}$ = 278.2 Hz), 58.0 (q, $^{2}J_{C,F}$ = 35.9 Hz), 21.2 ppm. ^{19}F NMR (470 MHz, $CDCl_3$): *d* = -76.0 ppm. HRMS (ESI): calcd. for $C_9H_{10}F_3N_2$ 203.0796, found 203.0796.

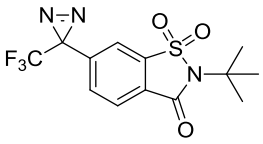

71a. l_{max} (*e*) (CH_3OH) 290 (850), 340 (300). ^{1}H NMR (270 MHz, $CDCl_3$): *d* = 8.03 (d, *J* = 8.0 Hz, 1 H), 7.64 (s, 1 H), 7.59 (d, *J* = 8.0 Hz, 1 H), 1.77 (s, 9 H) ppm. ^{13}C NMR (68 MHz, $CDCl_3$): *d* = 158.8, 138.7, 136.2, 131.9, 128.2, 125.2, 121.4 (q, $^{1}J_{C,F}$ =

275.5 Hz), 118.4, 61.8, 28.4 (q, $^{2}J_{C,F}$ = 41.6 Hz), 27.8 ppm. ^{19}F NMR (470 MHz, $CDCl_3$): *d* = -64.7 ppm. HRMS (ESI): calcd. for $C_{13}H_{13}F_3N_3O_2S$ 348.0630; found 348.0646.

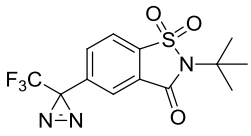

71b. l_{max} (*e*) (CH_3OH) 280 (900), 340 (300). ^{1}H NMR (270 MHz, $CDCl_3$): *d* = 7.89 (d, *J* = 8.0 Hz, 1 H), 7.82 (s, 1 H), 7.63 (d, *J* = 8.0 Hz, 1 H), 1.77 (s, 9 H) ppm. ^{13}C NMR (68 MHz, $CDCl_3$): *d* = 158.7, 138.5, 135.8, 132.2, 128.3, 122.7, 121.4 (q, $^{1}J_{C,F}$ = 281.1 Hz), 120.9, 61.8, 28.3(q, $^{2}J_{C,F}$ = 38.8 Hz), 27.7 ppm. ^{19}F NMR (470 MHz, $CDCl_3$): *d* = -64.7 ppm. HRMS (ESI): calcd. for $C_{13}H_{13}F_3N_3O_3S$: 348.0630; found 348.0626.

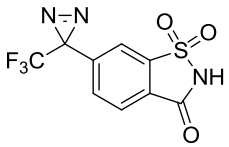

72a. l_{max} (*e*) (CH_3OH) 290 (920), 337 (303). ^{1}H NMR (270 MHz, CD_3OD): *d* = 8.11 (1H, d, *J* = 8.0 Hz), 7.90 (1H, s), 7.84 (1H, d, *J* = 8.0 Hz) ppm. ^{13}C NMR (68 MHz, CD_3OD): *d* = 161.3, 142.3, 137.3, 133.8, 130.6, 126.8, 123.1 (q, $^{1}J_{C,F}$ = 275.1 Hz), 120.4 29.7 (q, $^{2}J_{C,F}$ = 41.2 Hz) ppm. ^{19}F NMR (470 MHz, CD_3OD): *d* = -66.7 ppm. HRMS (ESI): calcd. for $C_9H_5F_3N_3O_3S$: 292.0004; found 292.0020.

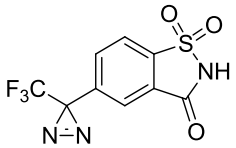

72b. l_{max} (*e*) (CH_3OH) 280 (1005), 340 (280). ^{1}H NMR (270 MHz, CD_3OD): *d* = 8.11 (d, *J* = 8.0 Hz, 1 H), 7.86 (s, 1 H), 7.83 (d, *J* = 8.0 Hz, 1 H) ppm. ^{13}C NMR (68 MHz, CD_3OD): *d* = 161.2, 142.3, 136.5, 134.3, 130.5, 123.9, 123.1, 123.0 (q, $^{1}J_{C,F}$ = 275.1

Hz), 29.5 (q, $^{2}J_{C,F}$ = 41.2 Hz) ppm. ^{19}F NMR (470 MHz, CD_3OD): *d* = -62.7 ppm. HRMS (ESI): calcd. for $C_9H_5F_3N_3O_3S$: 292.0004; found 292.0014.

5.4 Conclusions

In this work, we presented an effective method to introduce diazirine to saccharin for construction of photoreactive saccharin derivatives. Further study indicated both of the photoreactive saccharin derivatives have enough affinity for the sweet and bitter taste receptors. These works will be able to elucidate the binding information of their ligands and receptors.

6 Preparation of Photoreactive 1'-Sucrose: A Cosolvent-Promoted O-Benzylation Strategy with Silver(I) Oxide

6.1 Introduction

Figure 6.1 Sucrose and the 1'-position

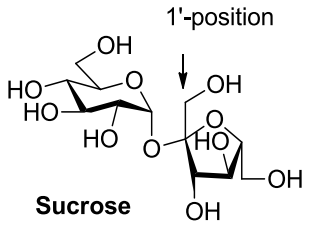

Sucrose, or saccharose, serves as a crucial component for the preparation of surfactants, macrocyclic derivatives, functional materials, food additives, and pharmaceutical compounds (Figure 6.1).[68-71] Furthermore, it is the major form of transported carbon in many plant species and is transported through cell membranes in many tissue types.[72] Viewed for its structure, it consists of three primary hydroxyls and five secondary hydroxyls. As an important sweetener, it was widely used and investigated. While, it was found that not all of the sucrose derivatives are sweet even if one hydroxyl was substituted with other group. To investigate sucrose carrier protein and the physiology of sucrose transport, modification of the 1'-position to prepare nonnatural sucrose is the widely used strategy.[73-75] Furthermore, sucralose, fructooligosaccharides (1-kestose, nystose, and 1-*β*-fructofuranosylnystose) and the *Achyranthes bidentata* B1 polysaccharides, isolated from a traditional Chinese herbal medicine *Ac*. *Bidentata* Blume, could all be regarded as the 1'-substituted sucroses

that indicating the tolerance for modification of the 1'-position. However, among the primary hydroxyls of sucrose, 1'-hydroxyl presents the lowest reactivity in many reactions,[76-78] which brings many challenges for the further modification of 1'-position of sucrose.

Scheme 6.1 Benzylation of hydroxyl with NaH or Ag_2O.

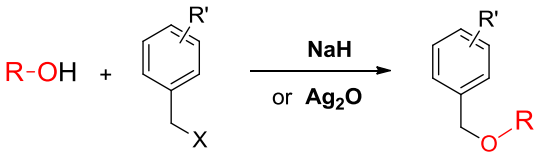

Benzylation of hydroxyl groups are crucial research topic in synthetic chemistry and carbohydrate field. The benzyl ether and it variant are kinds of widely used protecting groups for hydroxyl due to their inherent stability, easy installation, compatibility with many reaction conditions, and numerous deprotection methods.[79] To mediate the O-benzylation of carbohydrates and corresponding hydroxyl groups, sodium hydride (NaH)[80-83] and silver(I) oxide (Ag_2O)[84-88] are the major regents (Scheme 6.1). For many years, NaH-mediated O-benzylation show higher efficiency to prepare corresponding protection, but its strong alkaline condition, substrate limitation and tedious postprocessing are major barriers for its wide application. Ag_2O-mediated O-benzylation has been used for many years and show great advantages due to its mild conditions, easy postprocessing, and low environmental impact. However, in many reports, the benzylation meet some problem such as the preparation of fresh Ag_2O, poor solubility of the substrate, excess use of reagents, low reaction yields, or long reaction times. With the same time, the benzylation mechanisms are still ambiguous. A great effort should be eagerly carried out to further improve it.

To achieve an effective method to modify the 1'-position of sucrose and to improve the Ag_2O-mediated O-benzylation, we developed a cosolvent-promoted O-benzylation strategy that can not only improve the reaction solubility but also increase the benzylation efficiency for 1'-position of sucrose. The method is simple, mild and highly effective. Involved this strategy, a photoreactive 1'-sucrose derivative was prepared in good yield which can be used as a promising regent to investigate sucrose and its receptor in the field of PAL. The reaction mechanisms of benzylation with primary and secondary benzyl bromides were also elaborated. Furthermore, application scope with alcohols, glucose, and ribose derivatives was also carried out.

6.2 Results and Discussion

6.2.1 Benzylation of 1'-hydroxyl of sucrose with Ag_2O in CH_2Cl_2

Scheme 6.2 Enzymatic hydrolysis of octaacetylsucrose to afford compound **74**.

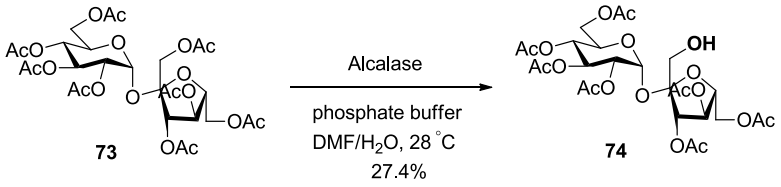

To benzylate 1'-hydroxyl of sucrose, we would like to prepare 1'-OH-heptaacetylsucrose **74** as the precursor. Previously, two major methods are widely used to afford 1'-OH-heptaacetylsucrose: one is the chemical strategy via multiple protection and deprotection,[89, 90] the other involves enzymatic strategy through the treatment of octaacetylsucrose with enzymes.[91, 92] To conveniently construct compound **74**, we select the enzymatic strategy of which octaacetylsucrose **73** was treated with alcalase in a phosphate buffer containing a mixture of DMF and

H_2O to afford 1'-OH-heptaacetylsucrose **74** in a 27.4% yield (Scheme 6.2). During the measurement by ^1H NMR to confirm its structure, we found two types of ^1H NMR for compound **74** (Figure 6.2). For type 1, the signal of 1'-protons divided into double, but a double-double type of signal was found for one proton of type 2. In our work, type 2 was easily obtained during the measurement. With the addition of one drop of D_2O, type 2 can be converted to type 1. Thus, we predicted that this kind of difference should be derived from the deuterium exchange occurred at 1'-hydroxyl in the presence of some active proton containing reagents (D_2O, *etc*) existed in $CDCl_3$ or introduced during the measurement.

Figure 6.2 Two types of ^1H NMR for 1'-hydrogens of compound **74**.

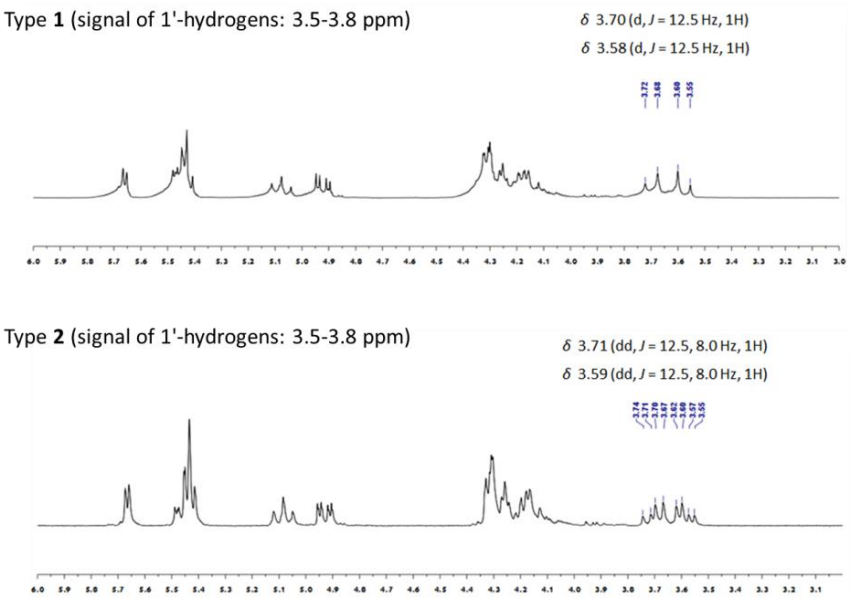

Next, sucrose **74** was reacted with *p*-(trifluoromethyl)benzyl bromide **75a** with in the presence of Ag_2O (Table 6.1). Dichloromethane was selected as the reaction solvent which is the commonly used solvent in carbohydrate field. However, the reaction carried out at room temperature afford to desired product **76a** in 8% of yield after 144 h. Further temperature optimization indicated that 60 °C is ideal for the

benzylation of sucrose **74**. Through the investigation of reagents amount, we found that 2 equiv of **75a** and 3 equiv of Ag_2O should be retained to afford high efficiency. To further improve the reaction, we carried out some control experiments in the presence of additives, but these failed to improve the reaction yield. Interestingly, the

Table 6.1 O-Benzylation of 1'-sucrose with **75a** in the presence of Ag_2O.[a]

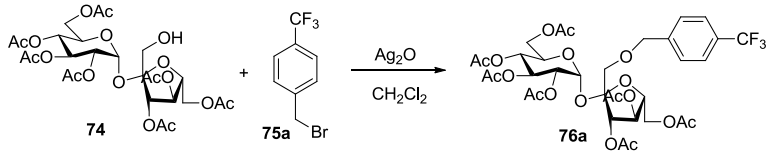

entry	**75a** (equiv)	Ag_2O (equiv)	temp (℃)	time (h)	yield **76a** (%)[b]
1	2	2	rt	144	8
2	2	2	40	70	14
3	2	2	60	24	17
4	2	2	80	16	15
5	2	3	60	24	21
6	2	4	60	18	17
7[c]	2	3	60	24	trace
8[d]	2	3	60	24	0
9[e]	2	3	60	24	23
10[e]	4	6	60	24	38
11[e]	6	9	60	24	53
12[e]	8	12	60	24	69
13[e]	10	15	60	24	82

[a]Reaction conditions: **74** (0.1 mmol), 7**5a**, Ag_2O, CH_2Cl_2 (1 mL), MS 4 Å (200 mg) in a sealed tube under dark. [b]Isolated yield. [c]KI (0.01 equiv) was added. [d]*n*-Bu_4NI (0.01 equiv) was added. [e]Under N_2.

N_2 protection made a contribution to the reaction although only 23% of yield was obtained in this case. Unquestionably, increasing the amount of benzyl bromide and Ag_2O can lead to higher reaction yield, but this strategy is not suitable for wide application especially for the benzylation with precious benzyl bromides.

6.2.2 Solvent optimization and investigation of the derivation for benzyl bromide

In the consideration of the crucial solvent effect on nucleophilic substitution, we conducted a comprehensive solvent optimization for benzylation (Table 6.2). To make a comparison of the solvents, we selected the dipole moment (μ) and dielectric constant (ε) as general indicators of solvent polarity[93]. As can be seen in Table 6.2, the benzylation of **74** was evidently sensitive to the reaction solvents. When the reactions were performed in high-polarity solvents such as MeCN, DMF and acetone, no desired product can be found in the reaction mixture. While, low polarity solvent such as EtOAc and $CHCl_3$ can afford to desired product in 19% and 39% yield, respectively. THF or 1,4-dioxane also failed to give effective benzylation of sucrose **74**. The desired products were obtained in moderate yield in other solvents. To our delight, when the reactions were carried out in cylcohexane, *n*-hexane, and *n*-pentane, desired product **76a** can be obtained in excellent yield, even though the above-mentioned solvents are really used in carbohydrate due to their relatively low solubility. The corresponding results indicated that the benzylation of **74** correlated more closely with the solvent's dielectric constant (ε) than dipole moment (μ).

Table 6.2 Solvent Optimization.[a]

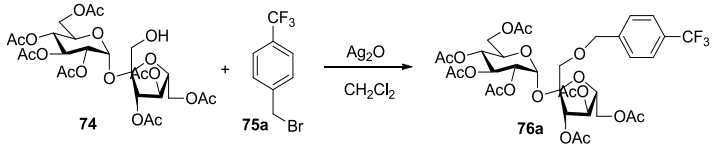

entry	solvent	μ^b	ε^c	time (h)	yield **76a** (%)[d]
1	MeCN	3.2	37.5	24	0
2	DMF	3.8	36.7	24	0
3	acetone	2.9	20.6	24	0
4	CH_2Cl_2	1.8	9.1	24	23
5	THF	1.8	7.6	24	0
6	EtOAc	1.7	6.0	24	19
7	$CHCl_3$	1.1	4.8	24	39
8	Et_2O	1.3	4.3	12	56
9	isopropyl ether	1.2	3.9	12	59
10	toluene	0.4	2.4	20	47
11	benzene	0	2.3	16	50
12	1,4-dioxane	0.4	2.2	24	0
13	CCl_4	0	2.2	16	62
14	cyclohexane	0.3	2.0	16	76
15	*n*-hexane	0	1.9	16	79
16	*n*-pentane	0	1.8	16	78

[a]Reaction conditions:**74** (0.1 mmol), **75a** (2.0 equiv), Ag_2O (3.0 equiv), solvent (1 mL), MS 4Å (200 mg), in a sealed tube at 60 °C under N_2. [b]Dipole moment (debye). [c]Dielectric constant (F/m). [d]Isolated yield.

For the solvents that can not afford to desired product, we found that sucrose **74** remained but benzyl bromide **75a** was consumed completely. For the reaction carried

out in DMF, a complex mixture was found which should be due to the ester migration

Table 6.3 Derivation of **75a** in the presence of Ag_2O.[a]

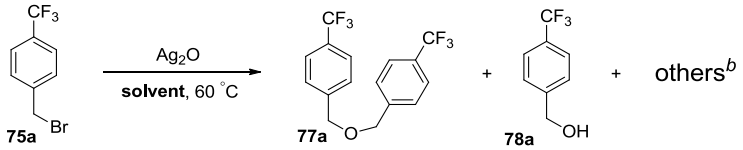

entry	solvent	time (h)	**77a**/**78a**/others (%)[c]	**77a**/**78a**/others (%)[d]
1	MeCN	15	10/62/28	10/57/33
2	DMF	4	-[e]	-[e]
3	acetone	6	4/22/74	4/24/72
4	THF	8	2/20/78	2/12/86
5	1,4-dioxane	18	27/60/13	24/57/19
6	CH_2Cl_2	13	86/4/10	84/4/12
7	EtOAc	20	63/8/29	58/12/30
8	$CHCl_3$	20	40/4/56	47/6/47
9	Et_2O	16	83/7/10	76/8/16
10	isopropyl ether	18	83/3/14	78/5/17
11	toluene	24	61/2/37	60/3/37
12	benzene	24	71/1/28	79/2/19
13	CCl_4	32	90/1/9	82/2/16
14	cyclohexane	30	99/0/1	95/0/5
15	*n*-hexane	32	98/0/2	93/0/7
16	*n*-pentane	32	98/0/2	96/0/4

[a]Reaction conditions: **75a** (0.2 mmol), Ag_2O (1.0 equiv), solvent (0.5 mL), MS 4Å (100 mg), in a sealed tube at 60 ℃ under N_2. [b]Others: unidentified products. [c]Ratios were determined by ^{1}H-NMR for reaction mixtures. [d]Ratios were determined by ^{19}F-NMR for reaction mixtures. [e]Complicated mixtures, ratios were not successfully determined.

of **74**. To get a well understanding about the effect factors for benzylating of **74** as well as the derivation of benzyl bromide **75a**, a series of control experiments of which benzyl bromide was directly treated with Ag_2O in the absence of sucrose were carried out (Table 6.3). In the solvent that failed to benzylate sucrose, we found the benzyl alcohol or other product was generate in the control experiments. Interestingly, for cyclohexane, *n*-hexane and *n*-pentane, the solvents that can give desired products in excellent yields, diether was detected as the major product. These results indicated that the formation of dibenzyl ether and benzyl alcohol was greatly inhibited, and the inertness of n-hexane also made contribution to the benzylation of sucrose **74**. Notably, when DMSO was used as the solvent, an oxirane derivative was formed from benzyl bromide in the presence of Ag_2O.[94] Involved this strategy, we successfully prepared a double-diazirine containing oxirane which should be used as a promising reagent in the field of PAL.[95]

6.2.3 Cosolvent-promoted O-benzylation of 1'-sucrose by *p*-(trifluoromethyl)benzyl bromide

Previous results indicated that *n*-hexane is the optimal solvent for the benzylation of sucrose, but the low solubility of *n*-hexane for the substrates especially carbohydrates severely limit its application. To solve this problem and to further improve the reaction yield, we would like to invite a cosolvent strategy that is widely in organic synthesis. The solvents tested were dived based on their miscibility with *n*-hexane. The results showed that hexane-immiscible solvents such as MeCN and DMF failed to afford **76a**. When the hexane-miscible solvent were used as the solvent, the reaction can give desired product and the highest yield was obtained for the reaction carried out in *n*-hexane/CH_2Cl_2 as a volumn ratio of 4/1. It should be noted that the combination of cyclohexane and CH_2Cl_2 also afford to desired product in

excellent yield.

Table 6.4 Cosolvent-promoted O-benzylation of **74** with Ag_2O.[a]

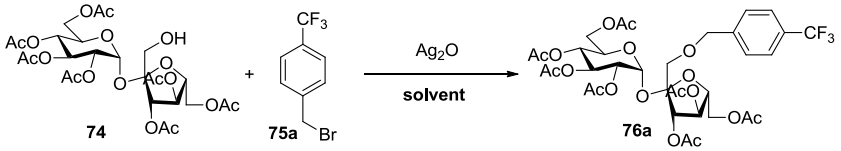

entry	solvent (volume ratio)	time (h)	yield **76a** (%)[b]
1	*n*-hexane/MeCN (4/1)	24	0
2	*n*-hexane/DMF (4/1)	24	0
3	*n*-hexane/THF (4/1)	24	trace
4	*n*-hexane/acetone (4/1)	24	35
5	*n*-hexane/EtOAc (4/1)	20	79
6	*n*-hexane/$CHCl_3$ (4/1)	20	76
7	***n*-hexane/CH_2Cl_2 (4/1)**	**15**	**91**
8	cyclohexane/CH_2Cl_2 (4/1)	15	90
9	*n*-hexane/CH_2Cl_2 (2/1)	15	79

[a]Reaction conditions:**74** (0.1 mmol), **75a** (2.0 equiv), Ag_2O (3.0 equiv), solvent (1 mL), MS 4Å (200 mg), in a sealed tube at 60 °C under N_2. [b]Isolated yield.

To emphasize the efficiency of cosolvent for the benzylation of sucrose **74**, a kinetic investigation of the benzylation of sucrose **74** in CD_2Cl_2 (Figure 6.3, a) and deuterated cosolvent (Figure 6.3, b) were performed. Due to the similar efficiency and commercial availability, cyclohexane-d_{12} was used to displace *n*-hexane to construct the cosolvent with CD_2Cl_2 for kinetic investigation. The ratios for all substances were calculated by ^{1}H NMR of the reaction mixture. As for the reaction carried out in CH_2Cl_2, benzyl bromide **75a** was consumed rapidly with the formation of desired product **76a** as well as the byproduct **77a**. Obviously, the formation of **77a** was prior

to the desired product **76a**. Benzyl bromide **75a** was completely consumed within 15 h. When the reaction was performed in deuterated cosolvent, the formation of desired product was greatly improved. In addition, byproduct **77a** was significantly inhibited in this case. To our delight, benzyl bromide **75a** still remained in the reaction after 15 h. These results indicated that the cosolvent system is able to improve the reaction yield by inhibiting the formation of byproduct.

Figure 6.3 Kinetic investigation of the benzylation of sucrose **74** in different solvents.

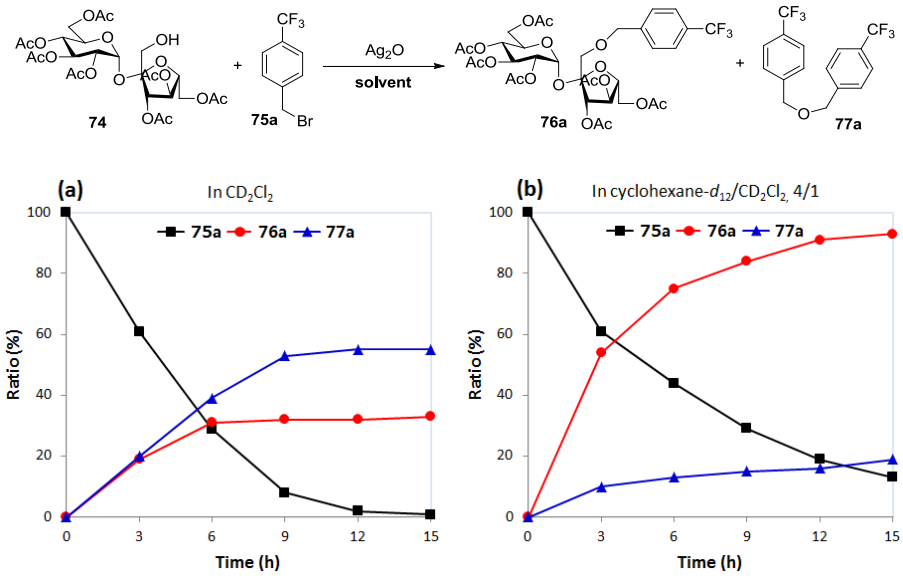

6.2.4 Cosolvent-promoted O-benzylation of 1'-sucrose with other benzyl bromides

With the optimal conditions in hand, we performed cosolvent-promoted O-benzylation of sucrose **74** with other benzyl bromides. As can been seen in Table 6.5, primary benzyl bromides bearing an electron-deficient group is able to give good yields compared with that substituted with an electron-rich group, which indicating that the significant role of electronic nature of the aryl ring for the reaction. Benzyl

bromides that were substituted with electron-deficient groups such as -CF_3 and -NO_2, which are types of meta-directors in electrophilic aromatic substitution, the meta-substituted benzyl bromides (**76b** and **76d**) showed slight priority to benzylate

Table 6.5 Cosolvent-promoted O-benzylation of **74** with other benzyl halides.

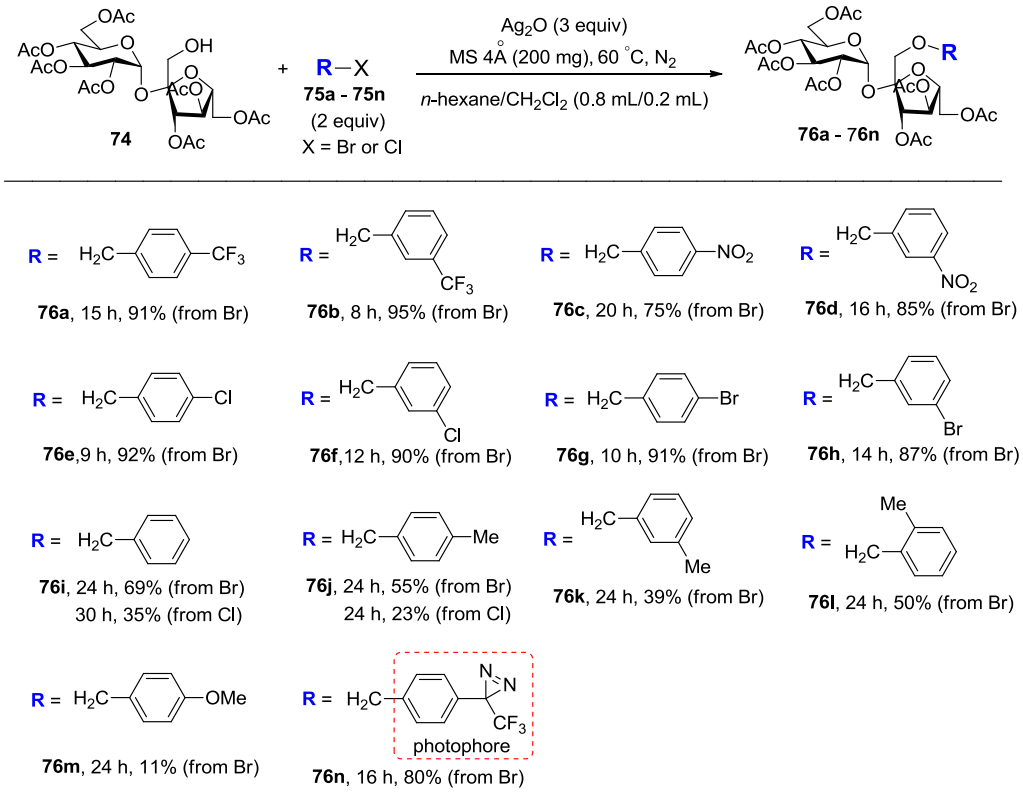

sucrose **74** compared with para-substituted benzyl bromides (**76a** and **76c**). While, when the substituents were changed to -Cl and –Br that are kinds of ortho/para-directors in electrophilic aromatic substitution, an opposite was obtained. For the benzylation with methyl-substituted benzyl bromides, the para- and ortho-substituted benzyl bromides could afford to desired product in higher yield. Benzyl chloride presented lower reactivity compared with benzyl bromides. A strong electron-rich substituent benzyl bromide reacted with sucrose **74** in only 11% yield.

As expected, TPD-based benzyl bromide could react with sucrose **74** to afford photoreactive sucrose derivative in 80% yield.

Benzylation of sucrose **74** with secondary benzyl bromide **75o** was considered to investigate the stereochemistry of the reaction. To our surprised, the reaction readily afford to desired product in good yield within 5 h (Scheme 6.3). The enantioenriched secondary benzyl bromides were tested, and the results indicated that the desired product was obtained in the same enantiomeric ratio. Furthermore, dibenzyl ether, the major byproduct in this reaction, was detected with a *dl*- and *meso*-mixture in a ratio of 1/1. These results proved that the benzylation with secondary benzyl bromide should proceed via a planar benzyl intermediate.

Scheme 6.3 O-Benzylation of **74** with secondary benzyl bromide **75o**.

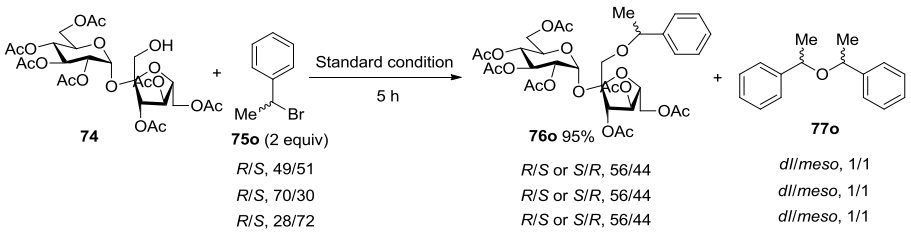

6.2.5 Deacylation of benzylated sucroses and photoreaction of photoreactive 1'-sucroses

Finally, all of the 1'-benzylated sucrose derivatives were treated with methanolic ammonia to remove the acetyl protection (Scheme 6.4 a). And the corresponding products were isolated in good yields. For compound **79n**, a photoreactive 1'-benzylated sucrose, was subjected to the photoreactivity investigation (Scheme 6.4 b). Under UV irradiation, its half-life toward MeOH is 1.1 min indicating its good photoreactivity for the investigation of sucrose in photoaffinity labeling (Scheme 6.4 c). To further investigate its photoreactive product, we performed the reaction in

CH_3OH or CD_3OD, respectively. The product was identified by MS analysis due to the significant difference between deuterium and hydrogen (Figure 6.4). These results showed that the O-C type additive was the major product for the photoreaction of photoreactive sucrose **79n** with CH_3OH.

Scheme 6.4 Deacylation of benzylated sucroses and photoreaction of **79n**.

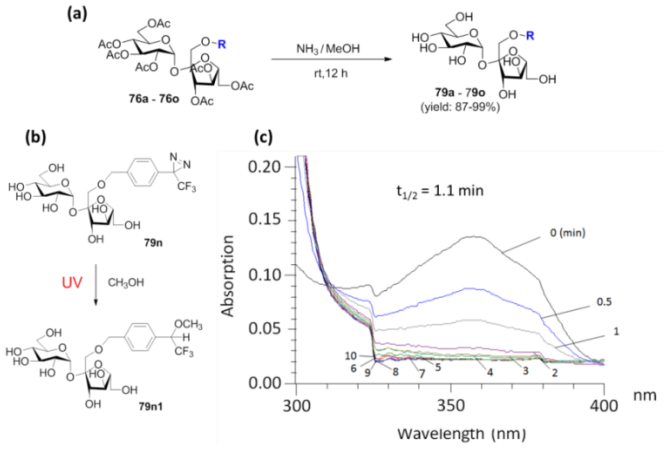

Figure 6.4 MS analysis of the photoreactive products of **79n**.

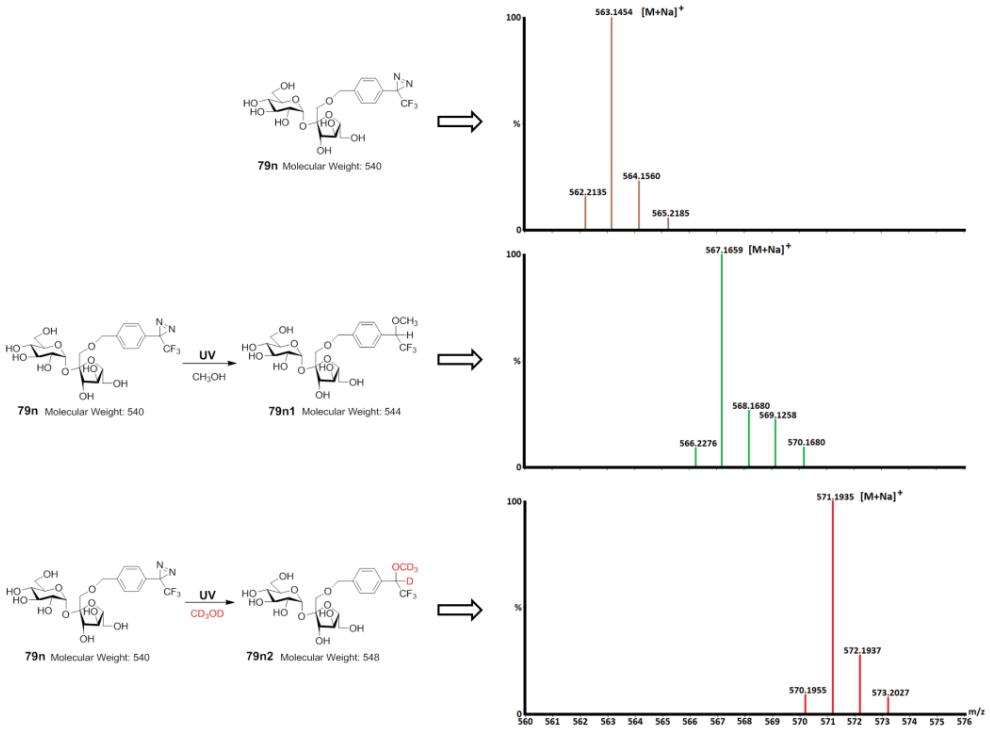

6.2.6 Scope investigation of cosolvent-promoted O-benzylation

To further expand the application scope of cosolvent-promoted strategy and confirm its efficiency, we examined many substrates as shown in Table 6.6 4-Bromobenzyl bromide **75g** was selected as the model benzylating reagent due to its lower price and high efficiency. As expected, the aliphatic alcohols can readily react

Table 6.6 Scope investigation of cosolvent-promoted O-benzylation.

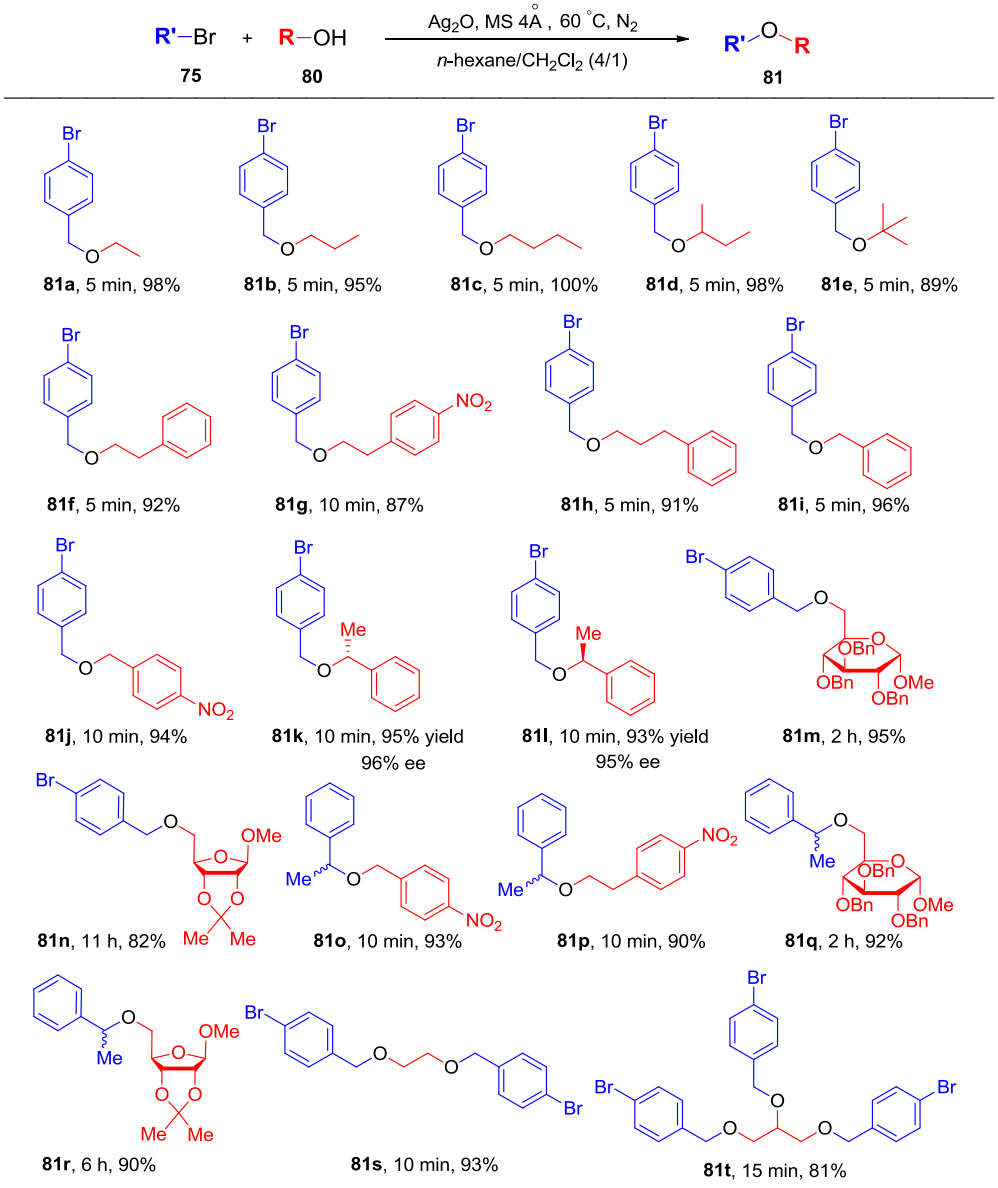

with **75g** to give the desired products in excellent yields. For the benzylation of aromatic alcohols, the cosolvent strategy also worked well. Next, enantioenriched secondary benzyl alcohols were tested in the reaction and the chiral purity of the desired product could be well retained after the reaction. To broaden the application of cosolvent-promoted benzylation strategy in carbohydrate field, other carbohydrates such as gluocose and ribose derivatives were used and the corresponding desired products can be obtained in good isolated yields that indicating the excellent applicability of cosolvent-promoted benzylation strategy in carbohydrate field. Secondary benzyl bromide **75o** also worked well in this work. Finally, the benzylation of polyols such as ethanediol and glycerol was carried out, and the multibenzylated products can be obtained in good isolated yields.

6.2.7 Mechanism investigation for O-benzylation of 1'-sucrose

To elaborate the benzylation mechanism, many control experiments were carried out as shown in Scheme 6.5. Firstly, 2,2,6,6-tetramethylpiperidin-1-oxyl (TEMPO) as a radical scavenger was used to confirm the possibility of radical pathway. In the presence of 2 equiv of TEMPO, the benzylation yield of the standard reaction dropped to 55%. And the corresponding benzyl-TEMPO adduct can be detected by ^{1}H NMR and ESI-HRMS. The formation of benzyl-TEMPO adduct **82a** may indicated a radical process, but 10 equiv of TEMPO can not inhibit the reaction completely. Furthermore, no bibenzyl derivative **83a** was detected in the reaction which is the common product generated in radical pathway[96]. A control experiment of which **75a** was directly reacted with TEMPO and the benzyl-TEMPO product can be obtained in 76% yield. A competition experiment of which sucrose was treated with three different benzyl bromides simultaneously was carried out. The results showed that benzylation of 1with primary benzyl bromide bearing a strong electron-rich substituent (**75m**)

proceeded much more slowly than the other two substrates. Based on the above-mentioned results, a SN_2 pathway should be more reliable for benzylation of **74** with primary benzyl bromides. As for the benzylation of sucrose **74** with secondary benzyl bromide, we found that addition of 2 equiv of TEMPO has no significantly effect on the reaction even though the TEMPO adduct **82o** was detected in the reaction. It indicated that SN_2 pathway should be involved in the benzylation of sucrose **74** with secondary benzyl bromide.

Scheme 6.5 Control experiments.

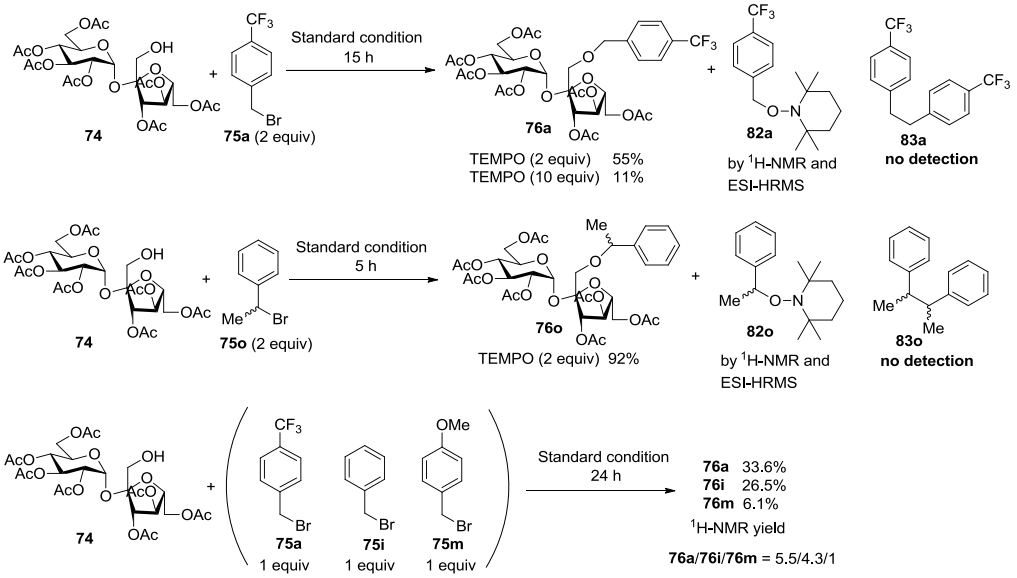

On the basis of these results, a plausible benzylation mechanism was outline (Scheme 6.6). For the benzylation with primary benzyl bromide, the bromine of **75a** is initially abstracted by Ag_2O forming a long-chain intermediate. Then the intermediate is further attacked by the 1'-hydroxyl of sucrose to afford the desired product **76a**. For the pathway of the formation of byproducts, the silver alkosy[97] intermediate B was formed via self-cyclization which was followed with the formation of diether and alcohol derivatives. Furthermore, the benzylation with secondary benzyl bromide

involved a halogenophilic attack by Ag_2O and the removal of bromine forming a planar benzylic carbocation C. Next, the planar benzylic carbocation C was attacked by hydroxyl group toward two sides to afford a racemic products. In addition, dibenzyl ether and alcohol were also constructed in the reaction.

Scheme 6.6 Mechanistic hypothesis.

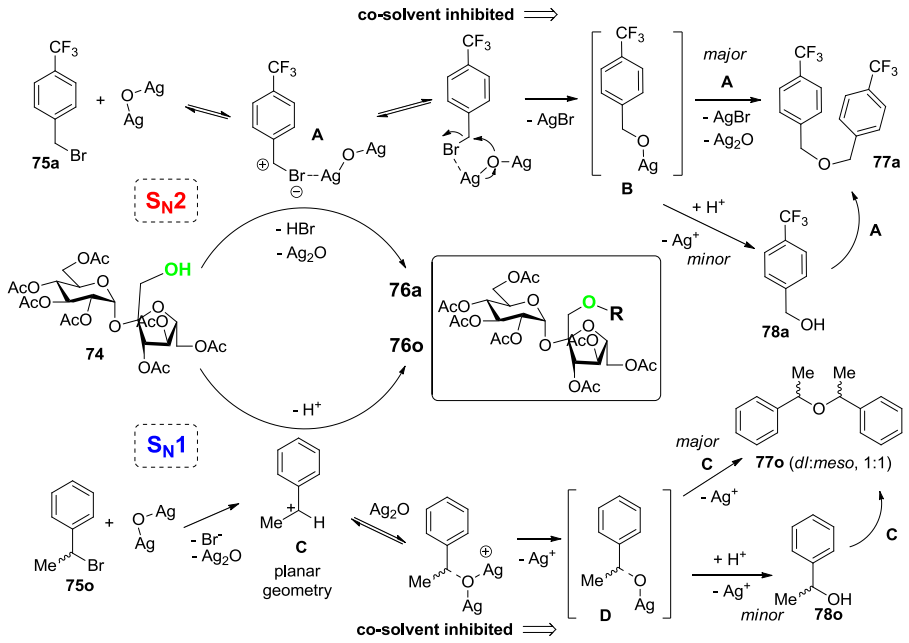

6.3 Experimental Section

6.3.1 Synthesis of 1'-OH-heptaacetylsucrose

To the solution of octaacetyl sucrose (1.00 g, 1.47 mmol) in 0.1 M phosphate buffer (50 mL, pH 7) containing a mixture of DMF and H_2O (10 mL, DMF:H_2O=1:3), Alcalase® 2.4 L (2 mL) was added. The mixture was incubated at 37 ℃ for 24 h. The mixture was extracted with ethyl acetate, concentrated under reduced pressure, then subjected to column chromatography on silica gel (EtOAc:*n*-hexane, 10:1) to afford

1'-OH-heptaacetylsucrose **74** (0.25 g, 27.4%).

6.3.2 Cosolvent-promoted O-benzylation of 1'-sucrose in the present of Ag_2O

To a solution of 1'-OH-heptaacetylsucrose **74** (0.1 mmol, 64 mg) in co-solvent (*n*-hexane/CH_2Cl_2, 0.8 mL/0.2 mL) in a glass sealed tube, benzyl bromide **75** (2.0 equiv), Ag_2O (3.0 equiv) and molecular sieves 4Å (200 mg) were added, respectively. The reaction mixture was stirred at 60 ℃ under dark in the presence of N_2. After the reaction was finished, the mixture was filtered by celite (or centrifugation) and concentrated, and the residue was purified through silica gel column chromatography (EtOAc:Hexane=3:2) to afford corresponding 1'-benzylated sucrose derivative.

6.3.3 Preparation of enantioenriched (*R*)-1-(1-bromoethyl)benzene and (*S*)-1-(1-bromoethyl)benzene

To a stirred solution of (*S*)-1-phenyl ethanol or (*R*)-1-phenyl ethanol (1.0 g, 8.2 mmol) in anhydrous hexane (30 mL) at 0 °C, PBr_3 (0.5 equiv) was added dropwise. The reaction was monorted by TLC analysis. After reaction for 15 min, the reaction mixture was slowly poured into 50 mL ice-water. The organic phase was washed with saturated $NaHCO_3$ solution (30 mL×2), 1 M HCl (30 mL), and brine (30 mL×3), respectively, dried with anhydrous $MgSO_4$, and concentrated by evaporation. A: yield: 93%, $_D$ = +41 (*c* 1, $CHCl_3$); ratio: (*R*)-**75o**/(*S*)-**75o** = 70/30 (by HPLC), Daicel Chiralpak AY-H, *i*-PrOH-hexane 0/100, flow rate 0.2 mL/min, t_R: 23.80 min (*R*)-**75o** and 25.09 min (*S*)-**75o**, 210 nm detection. B: yield: 93%, $_D$ = -41 (*c* 1, $CHCl_3$); ratio: (*S*)-**75o**/(*R*)-**75o** = 72/28 (by HPLC), Daicel Chiralpak AY-H, *i*-PrOH-hexane 0/100, flow rate 0.2 mL/min,

t_R: 23.88 min (*R*)-**75o** and 25.19 min (*S*)-**75o**, 210 nm detection. C: For commercial available (1-bromoethyl)benzene: $_D$ = 0 (*c* 1, $CHCl_3$); ratio: (*R*)-**75o**/(*S*)-**75o** = 49/51 (by HPLC), Daicel Chiralpak AY-H, *i*-PrOH-hexane 0/100, flow rate 0.2 mL/min, t_R: 23.85 min (*R*)-**75o** and 25.16 min (*S*)-**75o**, 210 nm detection.

6.3.4 Deacylation of 1'-benzylated sucrose derivatives

To a solution of 1'-benzylated sucrose derivative **76** (0.2 mmol) in methanol (4 mL), NH_3 gas was bubbled. Then the mixture was stirred at room temperature for 12 h. After removal of the solvent under vacuo, the residue was purified through silica gel column chromatography (EtOAc:MeOH=5:1) to afford 1'-benzylated sucrose.

6.3.5 Cosolvent-promoted O-benzylation of alcohols, glucose and ribose derivatives in the present of Ag_2O

To a solution of **80** (0.3 mmol) in co-solvent (*n*-hexane/CH_2Cl_2, 4/1) in a glass sealed tube, benzyl bromide (2.0 equiv for **81a-81r**, 4.0 equiv for **81s**, 6.0 equiv for **81t**), Ag_2O (3.0 equiv for **81a-81r**, 6.0 equiv for **81s**, 9.0 equiv for **81t**) and molecular sieves 4Å were added, respectively. The reaction mixture was stirred at 60 ℃ under dark in the presence of N_2. After the reaction was finished, the mixture was filtered by celite (or centrifugation) and concentrated, and the residue was purified through silica gel column chromatography (CH_2Cl_2:Hexane=1:1 for **81a-81l**, **81o-81p**; EtOAc:hexane=1:2 for **81m-81n**, **81q-81t**) to afford corresponding products.

6.3.6 UV-vis Analysis of photoreactive 1'-sucrose in CH_3OH and CD_3OD

A methanolic solution (1 mM, 1 mL) of compound **79n** in a quartz cuvette was irradiated under 100 W black-light at a distance 1 cm from the surface of light source.

The half-life ($t_{1/2}$) was calculated from the decrements of the absorbance around 356 nm.

6.3.7 Characterization of corresponding products

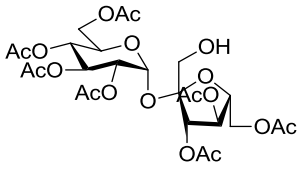

74. Colorless oil (0.25 g, 27.4%):$[\alpha]_D$ +50 (*c* 0.2 $CHCl_3$) (lit.: +43, *c* 2.0 $CHCl_3$); ^{1}H NMR (270 MHz, $CDCl_3$) δ 5.67 (d, *J* = 3.7 Hz, 1H), 5.49 – 5.42 (m, 3H), 5.09 (t, *J* = 9.7 Hz, 1H), 4.93 (dd, *J* = 10.4, 3.7 Hz, 1H), 4.33 – 4.11 (m, 6H), 3.71 (d, *J* = 12.6 Hz, 1H), 3.59 (d, *J* = 12.6 Hz, 1H), 2.19 (s, 3H), 2.12 (s, 3H), 2.09 (s, 6H), 2.08 (s, 3H), 2.04 (s, 3H), 2.02 (s, 3H); ^{13}C NMR (68 MHz, $CDCl_3$) δ 170.82, 170.78, 170.6, 170.3, 170.1(2C), 169.6, 105.2, 89.8, 78.7, 76.4, 74.7, 70.1, 69.7, 68.4, 68.2, 63.6, 63.5, 61.7, 20.5 (7C); HRMS-ESI (m/z) $[M + Na]^+$ calcd for $C_{26}H_{36}O_{18}Na$ 659.1799, found 659.1822.

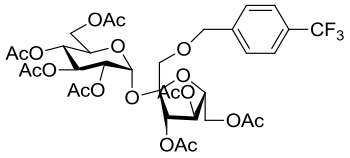

76a. Colorless oil (72.3 mg, 91%): $[\alpha]_D$ +55 (*c* 1 $CHCl_3$); ^{1}H NMR (270 MHz, $CDCl_3$) *δ* 7.62 (d, *J* = 8.1 Hz, 2H), 7.47 (d, *J* = 8.1 Hz, 2H), 5.71 – 5.69 (m, 2H), 5.48 – 5.39 (m, 2H), 5.08 (t, *J* = 9.7 Hz, 1H), 4.86 (dd, *J* = 10.3, 3.8 Hz, 1H), 4.65 (s, 2H), 4.32 – 4.12 (m, 6H), 3.64 (d, *J* = 10.5 Hz, 1H), 3.44 (d, *J* = 10.5 Hz, 1H), 2.13 (s, 3H), 2.12 (s, 3H), 2.08 (s, 3H), 2.04 (s, 6H), 2.01 (s, 3H), 1.94 (s, 3H); ^{13}C NMR (68 MHz, $CDCl_3$) *δ* 170.5, 170.4, 170.0, 169.8, 169.6, 169.4, 141.6, 129.8 (q, *J* = 32.1 Hz), 127.5, 125.2 (d, *J* = 3.5 Hz), 124.0 (q, *J* = 272.5 Hz), 104.1, 89.4, 78.3, 75.4, 74.3, 72.5, 70.1, 70.0, 69.5, 68.1, 68.0, 63.1, 61.4, 20.2 and 20.0 (7C); ^{19}F-NMR (470 MHz, $CDCl_3$): *δ* = -62.53

ppm; HRMS-ESI (m/z) $[M + Na]^+$ calcd for $C_{34}H_{41}F_3O_{18}Na$ 817.2143, found 817.2161.

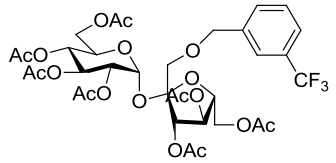

76b. Colorless oil (75.4 mg, 95%): $[\alpha]_D$ +52 (*c* 1 $CHCl_3$); ^{1}H NMR (270 MHz, $CDCl_3$) δ 7.62 – 7.49 (m, 4H), 5.72 – 5.69 (m, 2H), 5.48 – 5.40 (m, 2H), 5.08 (t, *J* = 8.9 Hz, 1H), 4.86 (dd, *J* = 10.3, 3.7 Hz, 1H), 4.65 (s, 2H), 4.31 – 4.11 (m, 6H), 3.66 (d, *J* = 10.5 Hz, 1H), 3.46 (d, *J* = 10.5 Hz, 1H), 2.13 (s, 3H), 2.12 (s, 3H), 2.08 (s, 3H), 2.04 (s, 6H), 2.01 (s, 3H), 1.95 (s, 3H); ^{13}C NMR (68 MHz, $CDCl_3$) δ 170.8, 170.7, 170.3, 170.10, 170.06, 169.9, 169.7, 138.7, 130.91 (q, *J* = 32.5 Hz), 130.86, 129.0, 124.7 (q, *J* = 3.7 Hz), 124.3 (q, *J* = 3.7 Hz), 124.1 (q, *J* = 271.7 Hz), 104.3, 89.6, 78.5, 75.6, 74.4, 72.9, 70.5, 70.2, 69.7, 68.3, 68.2, 63.4, 61.6, 20.5 and 20.4 and 20.3 (7C); ^{19}F-NMR (470 MHz, $CDCl_3$): δ = -62.64 ppm; HRMS-ESI (m/z) $[M + Na]^+$ calcd for $C_{34}H_{41}F_3O_{18}Na$ 817.2143, found 817.2166.

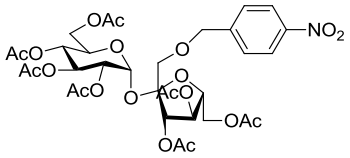

76c. Colorless oil (57.8 mg, 75%): $[\alpha]_D$ +54 (*c* 1 $CHCl_3$); ^{1}H NMR (270 MHz, $CDCl_3$) δ 8.23 (d, *J* = 8.7 Hz, 2H), 7.54 (d, *J* = 8.7 Hz, 2H), 5.72 – 5.69 (m, 2H), 5.49 – 5.41 (m, 2H), 5.09 (t, *J* = 9.7 Hz, 1H), 4.86 (dd, *J* = 10.3, 3.7 Hz, 1H), 4.70 (s, 2H), 4.33 – 4.13 (m, 6H), 3.70 (d, *J* = 10.5 Hz, 1H), 3.49 (d, *J* = 10.5 Hz, 1H), 2.15 (s, 3H), 2.12 (s, 3H), 2.09 (s, 3H), 2.06 (s, 3H), 2.04 (s, 3H), 2.01 (s, 3H), 1.98 (s, 3H); ^{13}C NMR (68 MHz, $CDCl_3$) δ 170.8, 170.7, 170.3, 170.02 (2C), 169.95, 169.6, 147.7, 145.1, 127.9, 123.8, 104.3, 89.6, 78.5, 75.6, 74.4, 72.4, 70.9, 70.3, 69.7, 68.3, 68.2, 63.3, 61.6, 20.51 and 20.46 and 20.39 (7C); HRMS-ESI (m/z) $[M + Na]^+$ calcd for $C_{33}H_{41}NO_{20}Na$ 794.2120, found 794.2119.

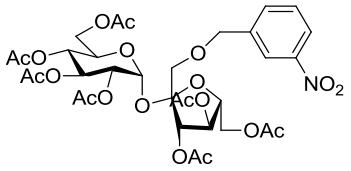

76d. Colorless oil (65.6 mg, 85%): $[\alpha]_D$ +60 (*c* 1 $CHCl_3$); ^1H NMR (270 MHz, $CDCl_3$) δ 8.23 (s, 1H), 8.17 (d, *J* = 8.1 Hz, 1H), 7.70 (d, *J* = 8.1 Hz, 1H), 7.55 (t, *J* = 8.1 Hz, 1H), 5.72 – 5.69 (m, 2H), 5.48 – 5.41 (m, 2H), 5.08 (t, *J* = 9.7 Hz, 1H), 4.86 (dd, *J* = 10.4, 3.7 Hz, 1H), 4.70 (s, 2H), 4.34 – 4.12 (m, 6H), 3.70 (d, *J* = 10.4 Hz, 1H), 3.50 (d, *J* = 10.4 Hz, 1H), 2.14 (s, 3H), 2.13 (s, 3H), 2.09 (s, 3H), 2.06 (s, 3H), 2.04 (s, 3H), 2.01 (s, 3H), 1.99 (s, 3H); ^{13}C NMR (68 MHz, $CDCl_3$) δ 170.8, 170.7, 170.3, 170.08, 170.06, 170.0, 169.7, 148.6, 139.9, 133.4, 129.6, 122.9, 122.3, 104.2, 89.6, 78.5, 75.6, 74.4, 72.4, 70.9, 70.2, 69.7, 68.3, 68.2, 63.3, 61.6, 20.5 and 20.4 (7C); HRMS-ESI (m/z) $[M + Na]^+$ calcd for $C_{33}H_{41}NO_{20}Na$ 794.2120, found 794.2135.

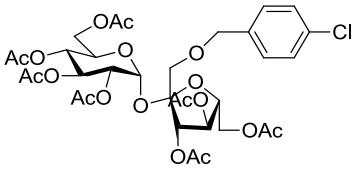

76e. Colorless oil (70.1 mg, 92%): $[\alpha]_D$ +54 (*c* 1 $CHCl_3$); ^1H NMR (270 MHz, $CDCl_3$) δ 7.33 (d, *J* = 8.6 Hz, 2H), 7.28 (d, *J* = 8.6 Hz, 2H), 5.69 – 5.67 (m, 2H), 5.48 – 5.38 (m, 2H), 5.08 (t, *J* = 9.7 Hz, 1H), 4.86 (dd, *J* = 10.4, 3.7 Hz, 1H), 4.55 (s, 2H), 4.32 – 4.11 (m, 6H), 3.60 (d, *J* = 10.5 Hz, 1H), 3.41 (d, *J* = 10.5 Hz, 1H), 2.13 (s, 3H), 2.12 (s, 3H), 2.09 (s, 3H), 2.04 (s, 6H), 2.01 (s, 3H), 1.96 (s, 3H); ^{13}C NMR (68 MHz, $CDCl_3$) δ 170.8, 170.6, 170.2, 170.1 (2C), 169.8, 169.6, 136.0, 133.7, 129.1, 128.7, 104.4, 89.6, 78.4, 75.6, 74.5, 72.8, 70.2, 70.0, 69.7, 68.2 (2C), 63.4, 61.6, 20.5 and 20.4 and 20.3 (7C); HRMS-ESI (m/z) $[M + Na]^+$ calcd for $C_{33}H_{41}Cl^{35}O_{18}Na$ 783.1879, found 783.1882 or calcd for $C_{33}H_{41}Cl^{37}O_{18}Na$ 785.1850, found 785.1863.

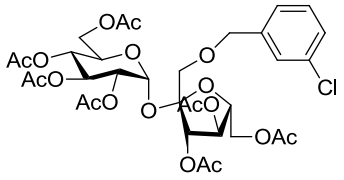

76f. Colorless oil (68.6 mg, 90%): $[\alpha]_D$ +56 (*c* 1 $CHCl_3$); ^1H NMR (270 MHz, $CDCl_3$) δ 7.35 (s, 1H), 7.30 – 7.20 (m, 3H), 5.71 – 5.68 (m, 2H), 5.47 – 5.39 (m, 2H), 5.08 (t, *J* = 9.6 Hz, 1H), 4.86 (dd, *J* = 10.4, 3.8 Hz, 1H), 4.56 (s, 2H), 4.31 – 4.11 (m, 6H), 3.62 (d, *J* = 10.5 Hz, 1H), 3.43 (d, *J* = 10.5 Hz, 1H), 2.14 (s, 3H), 2.12 (s, 3H), 2.09 (s, 3H), 2.05 (s, 3H), 2.03 (s, 3H), 2.01 (s, 3H), 1.97 (s, 3H); ^{13}C NMR (68 MHz, $CDCl_3$) δ 170.8, 170.7, 170.2, 170.1 (2C), 169.9, 169.7, 139.7, 134.5, 129.8, 128.1, 127.7, 125.7, 104.4, 89.6, 78.5, 75.6, 74.5, 72.8, 70.2 (2C), 69.7, 68.2 (2C), 63.4, 61.6, 20.51 and 20.47 and 20.3 (7C); HRMS-ESI (m/z) $[M + Na]^+$ calcd for $C_{33}H_{41}Cl^{35}O_{18}Na$ 783.1879, found 783.1899 or calcd for $C_{33}H_{41}Cl^{37}O_{18}Na$ 785.1850, found 785.1870.

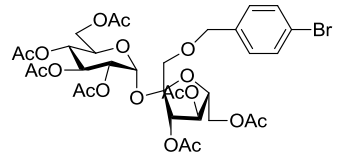

76g. Colorless oil (73.4 mg, 91%): $[\alpha]_D$ +56 (*c* 1 $CHCl_3$); ^1H NMR (270 MHz, $CDCl_3$) δ 7.48 (d, *J* = 8.2 Hz, 2H), 7.23 (d, *J* = 8.2 Hz, 2H), 5.69 – 5.67 (m, 2H), 5.47 – 5.38 (m, 2H), 5.08 (t, *J* = 9.6 Hz, 1H), 4.86 (dd, *J* = 10.3, 3.7 Hz, 1H), 4.53 (s, 2H), 4.31 – 4.11 (m, 6H), 3.60 (d, *J* = 10.6 Hz, 1H), 3.40 (d, *J* = 10.6 Hz, 1H), 2.13 (s, 3H), 2.12 (s, 3H), 2.09 (s, 3H), 2.04 (s, 6H), 2.01 (s, 3H), 1.96 (s, 3H); ^{13}C NMR (68 MHz, $CDCl_3$) δ 170.8, 170.7, 170.3, 170.1 (2C), 169.9, 169.7, 136.6, 131.7, 129.5, 121.9, 104.4, 89.6, 78.5, 75.6, 74.5, 72.9, 70.2, 70.0, 69.7, 68.2 (2C), 63.4, 61.6, 20.5 and 20.3 (7C); HRMS-ESI (m/z) $[M + Na]^+$ calcd for $C_{33}H_{41}Br^{79}O_{18}Na$ 827.1374, found 827.1390 or calcd for $C_{33}H_{41}Br^{81}O_{18}Na$ 829.1353, found 829.1377.

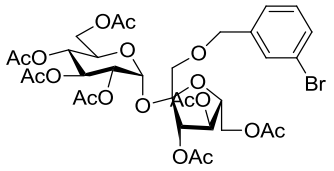

76h. Colorless oil (70.1 mg, 87%): $[\alpha]_D$ +55 (*c* 1 $CHCl_3$); ^1H NMR (270 MHz, $CDCl_3$) δ 7.50 (s, 1H), 7.43 (dt, *J* = 7.2, 1.8 Hz, 1H), 7.29 – 7.20 (m, 2H), 5.71 – 5.68 (m, 2H), 5.47 – 5.39 (m, 2H), 5.08 (t, *J* = 9.6 Hz, 1H), 4.86 (dd, *J* = 10.4, 3.8 Hz, 1H), 4.56 (s, 2H), 4.32 – 4.11 (m, 6H), 3.62 (d, *J* = 10.5 Hz, 1H), 3.42 (d, *J* = 10.5 Hz, 1H), 2.13 (s, 3H), 2.12 (s, 3H), 2.09 (s, 3H), 2.05 (s, 3H), 2.04 (s, 3H), 2.01 (s, 3H), 1.97 (s, 3H); ^{13}C NMR (68 MHz, $CDCl_3$) δ 170.8, 170.7, 170.2, 170.1 (2C), 169.9, 169.6, 137.0, 131.0, 130.6, 130.1, 126.2, 122.6, 104.4, 89.6, 78.5, 75.6, 74.5, 72.8, 70.22, 70.15, 69.7, 68.2 (2C), 63.4, 61.6, 20.50 and 20.47 and 20.3 (7C); HRMS-ESI (m/z) $[M + Na]^+$ calcd for $C_{33}H_{41}Br^{79}O_{18}Na$ 827.1374, found 827.1400 or calcd for $C_{33}H_{41}Br^{81}O_{18}Na$ 829.1353, found 829.1381.

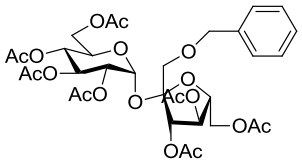

76i. Colorless oil (50.1 mg, 69%): $[\alpha]_D$ +56 (*c* 1 $CHCl_3$); ^1H NMR (270 MHz, $CDCl_3$) δ 7.36 – 7.29 (m, 5H), 5.72 – 5.68 (m, 2H), 5.47 – 5.38 (m, 2H), 5.07 (t, *J* = 9.7 Hz, 1H), 4.86 (dd, *J* = 10.3, 3.7 Hz, 1H), 4.59 (s, 2H), 4.32 – 4.10 (m, 6H), 3.60 (d, *J* = 10.6 Hz, 1H), 3.41 (d, *J* = 10.6 Hz, 1H), 2.11 (s, 6H), 2.08 (s, 3H), 2.03 (s, 6H), 2.00 (s, 3H), 1.94 (s, 3H); ^{13}C NMR (68 MHz, $CDCl_3$) δ 170.8, 170.7, 170.2, 170.1 (2C), 169.9, 169.7, 137.6, 128.5, 127.9, 127.8, 104.5, 89.6, 78.3, 75.6, 74.6, 73.6, 70.2, 69.8 (2C), 68.24, 68.18, 63.5, 61.7, 20.52 and 20.46 and 20.2 (7C); HRMS-ESI (m/z) $[M + Na]^+$ calcd for $C_{33}H_{42}O_{18}Na$ 749.2269, found 749.2257.

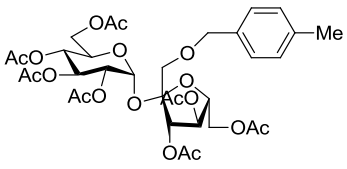

76j. Colorless oil (40.7 mg, 55%): $[\alpha]_D$ +51 (*c* 1 $CHCl_3$); ^1H NMR (270 MHz, $CDCl_3$) δ 7.22 (d, *J* = 8.0 Hz, 2H), 7.15 (d, *J* = 8.0 Hz, 2H), 5.71 – 5.67 (m, 2H), 5.47 – 5.37 (m, 2H), 5.07 (t, *J* = 9.6 Hz, 1H), 4.86 (dd, *J* = 10.4, 3.8 Hz, 1H), 4.54 (s, 2H), 4.31 – 4.10 (m, 6H), 3.56 (d, *J* = 10.6 Hz, 1H), 3.39 (d, *J* = 10.6 Hz, 1H), 2.34 (s, 3H), 2.11 (s, 6H), 2.08 (s, 3H), 2.03 (s, 6H), 2.00 (s, 3H), 1.95 (s, 3H); ^{13}C NMR (68 MHz, $CDCl_3$) δ 170.9, 170.7, 170.3, 170.2 (2C), 169.9, 169.7, 137.7, 134.5, 129.2, 128.0, 104.6, 89.6, 78.4, 75.6, 74.6, 73.5, 70.2, 69.8, 69.6, 68.3, 68.2, 63.5, 61.7, 21.0, 20.54 and 20.48 and 20.3 (7C); HRMS-ESI (m/z) $[M + Na]^+$ calcd for $C_{34}H_{44}O_{18}Na$ 763.2425, found 763.2428.

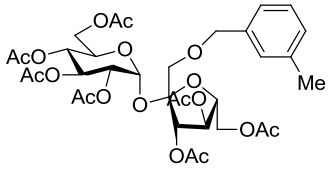

76k. Colorless oil (28.9 mg, 39%): $[\alpha]_D$ +56 (*c* 1 $CHCl_3$); ^1H NMR (270 MHz, $CDCl_3$) δ 7.27 – 7.21 (m, 1H), 7.14 – 7.09 (m, 3H), 5.73 – 5.68 (m, 2H), 5.47 – 5.38 (m, 2H), 5.07 (t, *J* = 9.7 Hz, 1H), 4.86 (dd, *J* = 10.4, 3.7 Hz, 1H), 4.55 (s, 2H), 4.31 – 4.10 (m, 6H), 3.58 (d, *J* = 10.6 Hz, 1H), 3.40 (d, *J* = 10.6 Hz, 1H), 2.35 (s, 3H), 2.12 (s, 3H), 2.11 (s, 3H), 2.08 (s, 3H), 2.03 (s, 6H), 2.00 (s, 3H), 1.94 (s, 3H); ^{13}C NMR (68 MHz, $CDCl_3$) δ 170.8, 170.7, 170.3, 170.2, 170.1, 169.8, 169.7, 138.2, 137.5, 128.7, 128.6, 128.4, 124.9, 104.5, 89.6, 78.4, 75.6, 74.6, 73.7, 70.1, 69.8, 69.7, 68.23, 68.15, 63.5, 61.7, 21.2, 20.51 and 20.46 and 20.3 (7C); HRMS-ESI (m/z) $[M + Na]^+$ calcd for $C_{34}H_{44}O_{18}Na$ 763.2425, found 763.2452.

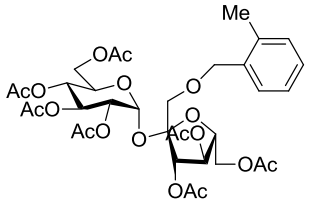

76l. Colorless oil (37.0 mg, 50%): $[\alpha]_D$ +55 (*c* 1 $CHCl_3$); ^1H NMR (270 MHz, $CDCl_3$) δ 7.31 – 7.29 (m, 1H), 7.22 – 7.17 (m, 3H), 5.69 – 5.66 (m, 2H), 5.48 – 5.36 (m, 2H), 5.07

(t, *J* = 9.7 Hz, 1H), 4.86 (dd, *J* = 10.3, 3.7 Hz, 1H), 4.58 (dd, *J* = 20.0, 12.0 Hz, 2H), 4.31 – 4.10 (m, 6H), 3.63 (d, *J* = 10.5 Hz, 1H), 3.43 (d, *J* = 10.5 Hz, 1H), 2.33 (s, 3H), 2.11 (s, 6H), 2.09 (s, 3H), 2.03 (s, 3H), 2.01 (s, 6H), 1.96 (s, 3H); ^{13}C NMR (68 MHz, $CDCl_3$) δ 170.8, 170.7, 170.3, 170.2 (2C), 169.8, 169.7, 136.9, 135.4, 130.4, 128.8, 128.1, 125.8, 104.6, 89.7, 78.5, 75.7, 74.7, 72.0, 70.2, 70.0, 69.8, 68.3, 68.2, 63.5, 61.7, 20.5 and 20.4 and 20.3 (7C), 18.60; HRMS-ESI (m/z) $[M + Na]^+$ calcd for $C_{34}H_{44}O_{18}Na$ 763.2425, found 763.2441.

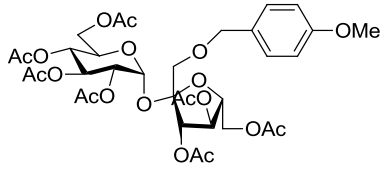

76m. Colorless oil (8.3 mg, 11%): $[\alpha]_D$ +56 (*c* 1 $CHCl_3$); ^{1}H NMR (270 MHz, $CDCl_3$) δ 7.26 (d, *J* = 8.5 Hz, 2H), 6.88 (d, *J* = 8.5 Hz, 2H), 5.71 – 5.67 (m, 2H), 5.47 – 5.37 (m, 2H), 5.07 (t, *J* = 9.5 Hz, 1H), 4.86 (dd, *J* = 10.3, 3.8 Hz, 1H), 4.51 (s, 2H), 4.31 – 4.10 (m, 6H), 3.81 (s, 3H), 3.55 (d, *J* = 10.6 Hz, 1H), 3.38 (d, *J* = 10.6 Hz, 1H), 2.11 (s, 3H), 2.09 (s, 3H), 2.03 (s, 6H), 2.01 (s, 3H), 1.96 (s, 3H); ^{13}C NMR (68 MHz, $CDCl_3$) δ 170.8, 170.7, 170.3, 170.2 (2C), 169.9, 169.7, 159.5, 129.5, 113.9, 104.6, 89.6, 78.4, 75.6, 74.6, 73.3, 70.2, 69.8, 69.4, 68.3, 68.2, 63.5, 61.7, 55.2, 20.6 and 20.5 and 20.4 (7C); HRMS-ESI (m/z) $[M + Na]^+$ calcd for $C_{34}H_{44}O_{19}Na$ 779.2374, found 779.2380.

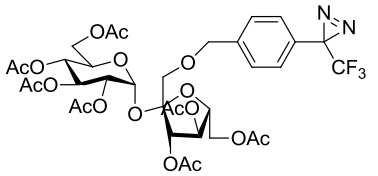

76n. Colorless oil (66.7 mg, 80%): $[\alpha]_D$ +53 (*c* 1 $CHCl_3$); ^{1}H NMR (270 MHz, $CDCl_3$) δ 7.39 (d, *J* = 8.2 Hz, 2H), 7.20 (d, *J* = 8.2 Hz, 2H), 5.70 – 5.68 (m, 2H), 5.47 – 5.39 (m, 2H), 5.08 (t, *J* = 9.3 Hz, 1H), 4.86 (dd, *J* = 9.9, 4.1 Hz, 1H), 4.60 (s, 2H), 4.32 – 4.11 (m, 6H), 3.60 (d, *J* = 10.5 Hz, 1H), 3.41 (d, *J* = 10.5 Hz, 1H), 2.13 (s, 3H), 2.12 (s, 3H), 2.09 (s, 3H), 2.04 (s, 6H), 2.01 (s, 3H), 1.94 (s, 3H); ^{13}C NMR (68 MHz, $CDCl_3$) δ

170.7, 170.6, 170.2, 170.0 (2C), 169.8, 169.6, 139.4, 128.6, 128.0, 126.6, 122.1 (q, J = 275.3 Hz), 104.3, 89.5, 78.4, 75.5, 74.4, 72.7, 70.1 (2C), 69.7, 68.2, 68.1, 63.3, 61.6, 28.2 (q, J = 39.9 Hz), 20.5 and 20.4 and 20.2 (7C); ^{19}F-NMR (470 MHz, $CDCl_3$): δ = -65.28 ppm; HRMS-ESI (m/z) $[M + Na]^+$ calcd for $C_{35}H_{41}N_2O_{18}F_3Na$ 857.2204, found 857.2191.

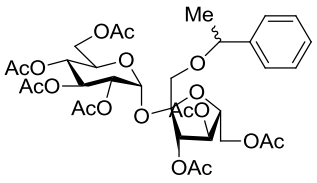

76o. Colorless oil (70.3 mg, 95%, mixture of (*R*)- and (*S*)-isomers): $[\alpha]_D$ +54 (*c* 1 $CHCl_3$); ^{1}H NMR (270 MHz, $CDCl_3$) δ 7.34 – 7.27 (m, 5H), 5.76 – 5.63 (m, 2H), 5.46 – 5.29 (m, 2H), 5.10 – 5.01 (m, 1H), 4.84 (dd, J = 10.3, 3.8 Hz, 1H), 4.50 – 4.41 (m, 1H), 4.33 – 4.05 (m, 6H), 3.49 – 3.42 (m, 1H), 3.27 – 3.17 (m, 1H), 2.18 – 1.86 (m, 21H), 1.46 – 1.43 (m, 3H); ^{13}C NMR (68 MHz, $CDCl_3$) δ 170.8 – 169. 7 (7C), 143.1 and 142.8, 128.64 and 128.59, 127.9 and 127.8, 126.3, 104.8 and 104.7, 89.8 and 89.5, 79.3, 79.2 and 79.0, 78.3, 75.7 and 75.5, 75.2 and 74.7, 70.2 and 70.1, 69.8 and 69.7, 68.3 and 68.20, 68.15 and 68.1, 63.54 and 63.48, 61.6, 23.9 and 23.7, 20.6 – 20.2 (7C); HRMS-ESI (m/z) $[M + Na]^+$ calcd for $C_{34}H_{44}O_{18}Na$ 763.2425, found 763.2443.

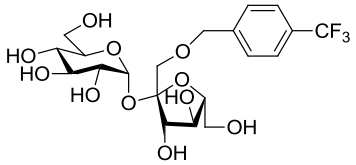

79a. White solid (96.0 mg, 96%): mp 90–92 °C; $[\alpha]_D$ +57 (*c* 1 CH_3OH); ^{1}H NMR (270 MHz, CD_3OD) δ 7.66 (d, J = 8.1 Hz, 2H), 7.58 (d, J = 8.1 Hz, 2H), 5.41 (d, J = 3.8 Hz, 1H), 4.76 (d, J = 12.5 Hz, 1H), 4.69 (d, J = 12.5 Hz, 1H), 4.27 (d, J = 8.5 Hz, 1H), 4.11 – 4.03 (m, 1H), 3.86 – 3.61 (m, 9H), 3.41 (dd, J = 6.4, 3.3 Hz, 1H), 3.37 (s, 1H); ^{13}C NMR (68 MHz, CD_3OD) δ 144.3, 130.8 (q, J = 31.9 Hz), 129.0 (d, J = 2.0 Hz), 126.3 (d, J = 2.6 Hz), 125.8 (q, J = 272.1 Hz), 105.2, 94.0, 83.5, 78.6, 75.3, 74.7, 74.3, 73.7, 73.1,

71.4 (2C), 63.3, 62.2; ^{19}F-NMR (470 MHz, CD_3OD): δ = -64.00 ppm. HRMS-ESI (m/z) $[M + Na]^+$ calcd for $C_{20}H_{27}F_3O_{11}Na$ 523.1403, found 523.1423.

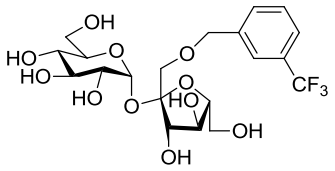

79b. White solid (93.0 mg, 93%): mp 91–93 °C; $[\alpha]_D$ +55 (*c* 1 CH_3OH); ^{1}H NMR (270 MHz, CD_3OD) δ 7.61 – 7.44 (m, 4H), 5.32 (d, *J* = 3.8 Hz, 1H), 4.67 (d, *J* = 12.5 Hz, 1H), 4.60 (d, *J* = 12.5 Hz, 1H), 4.17 (d, *J* = 8.6 Hz, 1H), 4.05 – 3.95 (m, 1H), 3.77 – 3.62 (m, 7H), 3.57 (t, *J* = 10.7 Hz, 2H), 3.33 (dd, *J* = 6.2, 3.5 Hz, 1H), 3.29 (d, *J* = 2.5 Hz, 1H); ^{13}C NMR (68 MHz, CD_3OD) δ 141.2, 132.4, 131.8 (q, *J* = 32.0 Hz), 130.3, 125.8 (q, *J* = 271.4 Hz), 125.4 (q, *J* = 3.8 Hz), 125.2 (q, *J* = 3.8 Hz), 105.2, 94.0, 83.5, 78.6, 75.3, 74.7, 74.3, 73.8, 73.1, 71.4 (2C), 63.3, 62.2; ^{19}F-NMR (470 MHz, CD_3OD): δ = -64.08 ppm. HRMS-ESI (m/z) $[M + Na]^+$ calcd for $C_{20}H_{27}F_3O_{11}Na$ 523.1403, found 523.1395.

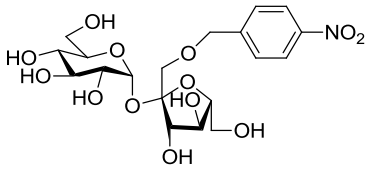

79c. White solid (85.9 mg, 90%): mp 93–95 °C; $[\alpha]_D$ +53 (*c* 1 CH_3OH); ^{1}H NMR (270 MHz, CD_3OD) δ 8.26 (d, *J* = 8.7 Hz, 2H), 7.65 (d, *J* = 8.7 Hz, 2H), 5.42 (d, *J* = 3.7 Hz, 1H), 4.83 (d, *J* = 13.3 Hz, 1H), 4.75 (d, *J* = 13.3 Hz, 1H), 4.27 (d, *J* = 8.5 Hz, 1H), 4.12 – 4.02 (m, 1H), 3.87 – 3.64 (m, 9H), 3.41 (dd, *J* = 8.6, 4.8 Hz, 1H), 3.37 (s, 1H); ^{13}C NMR (68 MHz, CD_3OD) δ 149.0, 147.7, 129.3, 124.6, 105.3, 94.1, 83.7, 78.7, 75.4, 74.8, 74.4, 73.4, 73.2, 71.6, 71.5, 63.4, 62.3; HRMS-ESI (m/z) $[M + Na]^+$ calcd for $C_{19}H_{27}NO_{13}Na$ 500.1380, found 500.1382.

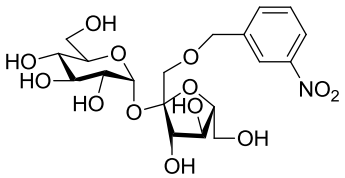

79d. White solid (85.9 mg, 90%): mp 91–93 °C; $[\alpha]_D$ +53 (*c* 1 CH_3OH); ^1H NMR (270 MHz, CD_3OD) δ 8.26 (s, 1H), 8.16 (dd, *J* = 7.9, 1.2 Hz, 1H), 7.79 (d, *J* = 7.9 Hz, 1H), 7.60 (t, *J* = 7.9 Hz, 1H), 5.39 (d, *J* = 3.8 Hz, 1H), 4.77 (d, *J* = 13.0 Hz, 1H), 4.71 (d, *J* = 13.0 Hz, 1H), 4.23 (d, *J* = 8.5 Hz, 1H), 4.07 – 4.01 (m, 1H), 3.85 – 3.60 (m, 9H), 3.38 (dd, *J* = 6.6, 3.1 Hz, 1H), 3.34 (d, *J* = 3.3 Hz, 1H); ^{13}C NMR (68 MHz, CD_3OD) δ 150.0, 142.4, 134.9, 130.8, 123.6, 123.3, 105.3, 94.1, 83.6, 78.7, 75.3, 74.7, 74.4, 73.4, 73.2, 71.5 (2C), 63.3, 62.3; HRMS-ESI (m/z) $[M + Na]^+$ calcd for $C_{19}H_{27}NO_{13}Na$ 500.1380, found 500.1382.

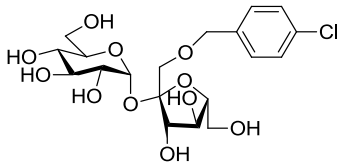

79e. White solid (88.7 mg, 95%): mp 90–92 °C; $[\alpha]_D$ +55 (*c* 1 CH_3OH); ^1H NMR (270 MHz, CD_3OD) δ 7.38 – 7.25 (m, 4H), 5.37 (d, *J* = 3.8 Hz, 1H), 4.62 (d, *J* = 12.2 Hz, 1H), 4.55 (d, *J* = 12.2 Hz, 1H), 4.20 (d, *J* = 8.5 Hz, 1H), 4.05 – 3.99 (m, 1H), 3.82 – 3.55 (m, 9H), 3.37 (dd, *J* = 5.8, 4.0 Hz, 1H), 3.34 (s, 1H); ^{13}C NMR (68 MHz, CD_3OD) δ 138.6, 134.6, 130.5, 129.6, 105.3, 94.1, 83.6, 78.8, 75.4, 74.8, 74.4, 73.8, 73.3, 71.5, 71.2, 63.4, 62.3; HRMS-ESI (m/z) $[M + Na]^+$ calcd for $C_{19}H_{27}Cl^{35}O_{11}Na$ 489.1140, found 489.1116 or calcd for $C_{19}H_{27}Cl^{37}O_{11}Na$ 491.1110, found 491.1086.

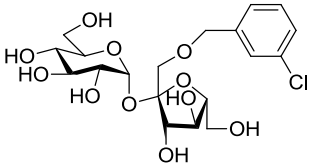

79f. White solid (81.3 mg, 87%): mp 90–92 °C; $[\alpha]_D$ +59 (*c* 1 CH_3OH); ^1H NMR (270 MHz, CD_3OD) δ 7.39 (s, 1H), 7.33 – 7.26 (m, 3H), 5.38 (d, *J* = 3.8 Hz, 1H), 4.64 (d, *J* = 12.2 Hz, 1H), 4.57 (d, *J* = 12.2 Hz, 1H), 4.22 (d, *J* = 8.5 Hz, 1H), 4.11 – 4.00 (m, 1H), 3.83 – 3.56 (m, 9H), 3.38 (dd, *J* = 6.3, 3.4 Hz, 1H), 3.34 (s, 1H); ^{13}C NMR (68 MHz, CD_3OD) δ 142.2, 135.5, 131.1, 128.84, 128.76, 127.1, 105.3, 94.1, 83.6, 78.7, 75.4, 74.8, 74.4, 73.8, 73.2, 71.5, 71.3, 63.4, 62.3; HRMS-ESI (m/z) $[M + Na]^+$ calcd for

$C_{19}H_{27}Cl^{35}O_{11}Na$ 489.1140, found 489.1158 or calcd for $C_{19}H_{27}Cl^{37}O_{11}Na$ 491.1110, found 491.1137.

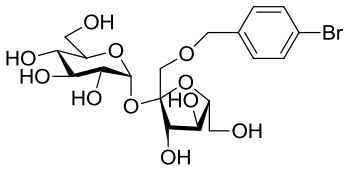

79g. White solid (101.2 mg, 99%): mp 89–91 °C; $[\alpha]_D$ +59 (*c* 1 CH_3OH); ^1H NMR (270 MHz, CD_3OD) δ 7.49 (d, *J* = 8.4 Hz, 2H), 7.29 (d, *J* = 8.4 Hz, 2H), 5.37 (d, *J* = 3.7 Hz, 1H), 4.61 (d, *J* = 12.2 Hz, 1H), 4.54 (d, *J* = 12.2 Hz, 1H), 4.20 (d, *J* = 8.5 Hz, 1H), 4.05 – 3.99 (m, 1H), 3.82 – 3.55 (m, 9H), 3.38 (dd, *J* = 5.8, 4.0 Hz, 1H), 3.34 (s, 1H); ^{13}C NMR (68 MHz, CD_3OD) δ 139.1, 132.7, 130.8, 122.5, 105.3, 94.1, 83.6, 78.8, 75.4, 74.8, 74.4, 73.8, 73.3, 71.5, 71.2, 63.4, 62.3; HRMS-ESI (m/z) $[M + Na]^+$ calcd for $C_{19}H_{27}Br^{79}O_{11}Na$ 533.0634, found 533.0652 or calcd for $C_{19}H_{27}Br^{81}O_{11}Na$ 535.0614, found 535.0634.

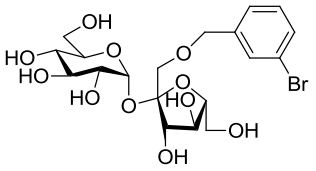

79h. White solid (92.0 mg, 90%): mp 90–92 °C; $[\alpha]_D$ +52 (*c* 1 CH_3OH); ^1H NMR (270 MHz, CD_3OD) δ 7.55 (s, 1H), 7.42 (d, *J* = 7.6 Hz, 1H), 7.34 (d, *J* = 7.6 Hz, 1H), 7.26 (d, *J* = 7.6 Hz, 1H), 5.37 (d, *J* = 3.8 Hz, 1H), 4.63 (d, *J* = 12.3 Hz, 1H), 4.56 (d, *J* = 12.3 Hz, 1H), 4.22 (d, *J* = 8.5 Hz, 1H), 4.11 – 4.00 (m, 1H), 3.83 – 3.55 (m, 9H), 3.38 (dd, *J* = 6.2, 3.6 Hz, 1H), 3.34 (s, 1H); ^{13}C NMR (68 MHz, CD_3OD) δ 142.5, 131.9, 131.8, 131.4, 127.6, 123.5, 105.3, 94.1, 83.6, 78.7, 75.4, 74.8, 74.4, 73.8, 73.3, 71.5, 71.3, 63.4, 62.3; HRMS-ESI (m/z) $[M + Na]^+$ calcd for $C_{19}H_{27}Br^{79}O_{11}Na$ 533.0634, found 533.0663 or calcd for $C_{19}H_{27}Br^{81}O_{11}Na$ 535.0614, found 535.0632.

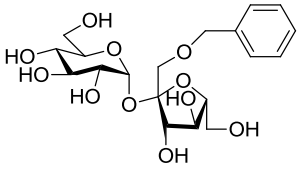

79i. White solid (78.7 mg, 91%): mp 78–80 °C; $[\alpha]_D$ +57 (*c* 1 CH_3OH); ^1H NMR (270 MHz, CD_3OD) δ 7.39 – 7.25 (m, 5H), 5.38 (d, *J* = 3.8 Hz, 1H), 4.64 (d, *J* = 12.0 Hz, 1H), 4.57 (d, *J* = 12.0 Hz, 1H), 4.22 (d, *J* = 8.5 Hz, 1H), 4.07 – 3.98 (m, 1H), 3.83 – 3.56 (m, 9H), 3.38 (dd, *J* = 5.8, 3.9 Hz, 1H), 3.35 (s, 1H); ^{13}C NMR (68 MHz, CD_3OD) δ 139.6, 129.6, 129.0, 128.9, 105.3, 94.1, 83.6, 78.8, 75.4, 74.8, 74.7, 74.4, 73.3, 71.5, 71.2, 63.3, 62.3; HRMS-ESI (m/z) $[M + Na]^+$ calcd for $C_{19}H_{28}O_{11}Na$ 455.1529, found 455.1538.

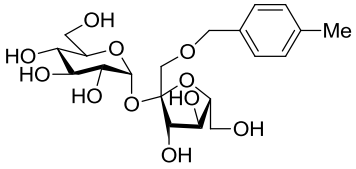

79j. White solid (79.5 mg, 89%): mp 85–87 °C; $[\alpha]_D$ +58 (*c* 1 CH_3OH); ^1H NMR (270 MHz, CD_3OD) δ 7.25 (d, *J* = 7.7 Hz, 2H), 7.15 (d, *J* = 7.7 Hz, 2H), 5.38 (d, *J* = 3.7 Hz, 1H), 4.60 (d, *J* = 11.8 Hz, 1H), 4.53 (d, *J* = 11.8 Hz, 1H), 4.21 (d, *J* = 8.5 Hz, 1H), 4.08 – 4.00 (m, 1H), 3.83 – 3.54 (m, 9H), 3.39 (t, *J* = 4.8 Hz, 1H), 3.35 (brs, 1H), 2.33 (s, 3H); ^{13}C NMR (68 MHz, CD_3OD) δ 138.7, 136.5, 130.1, 129.2, 105.3, 94.0, 83.5, 78.8, 75.4, 74.7, 74.6, 74.3, 73.2, 71.4, 71.0, 63.3, 62.2, 21.1; HRMS-ESI (m/z) $[M + Na]^+$ calcd for $C_{20}H_{30}O_{11}Na$ 469.1686, found 469.1693.

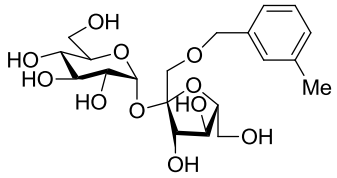

79k. White solid (83.0 mg, 93%): mp 86–88 °C; $[\alpha]_D$ +57 (*c* 1 CH_3OH); ^1H NMR (270 MHz, CD_3OD) δ 7.21 (t, *J* = 7.5 Hz, 1H), 7.17 (s, 1H), 7.14 (d, *J* = 7.5 Hz, 1H), 7.08 (d, *J* = 7.5 Hz, 1H), 5.38 (d, *J* = 3.8 Hz, 1H), 4.60 (d, *J* = 11.8 Hz, 1H), 4.53 (d, *J* = 11.8 Hz, 1H), 4.21 (d, *J* = 8.5 Hz, 1H), 4.06 – 4.00 (m, 1H), 3.83 – 3.54 (m, 9H), 3.38 (dd, *J* = 5.8, 3.9 Hz, 1H), 3.35 (s, 1H), 2.33 (s, 3H); ^{13}C NMR (68 MHz, CD_3OD) δ 139.5, 139.3, 129.7, 129.53, 129.45, 126.1, 105.3, 94.1, 83.5, 78.8, 75.4, 74.8 (2C), 74.4, 73.3, 71.4, 71.1, 63.3, 62.3, 21.4; HRMS-ESI (m/z) $[M + Na]^+$ calcd for $C_{20}H_{30}O_{11}Na$ 469.1686,

found 469.1678.

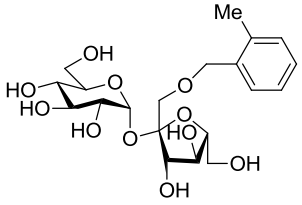

79l. White solid (81.2 mg, 91%): mp 83–85 °C; $[\alpha]_D$ +58 (*c* 0.2 CH_3OH); ^1H NMR (270 MHz, CD_3OD) δ 7.33 – 7.30 (m, 1H), 7.18 – 7.10 (m, 3H), 5.38 (d, *J* = 3.8 Hz, 1H), 4.65 (d, *J* = 11.7 Hz, 1H), 4.57 (d, *J* = 11.7 Hz, 1H), 4.21 (d, *J* = 8.5 Hz, 1H), 4.07 – 3.98 (m, 1H), 3.83 – 3.56 (m, 9H), 3.38 (dd, *J* = 6.1, 3.8 Hz, 1H), 3.34 (s, 1H), 2.34 (s, 3H); ^{13}C NMR (68 MHz, CD_3OD) δ 138.2, 137.4, 131.3, 130.0, 129.1, 126.9, 105.4, 94.1, 83.6, 78.7, 75.5, 74.8, 74.4, 73.3, 73.1, 71.5, 71.1, 63.3, 62.3, 18.9; HRMS-ESI (m/z) $[M + Na]^+$ calcd for $C_{20}H_{30}O_{11}Na$ 469.1686, found 469.1698.

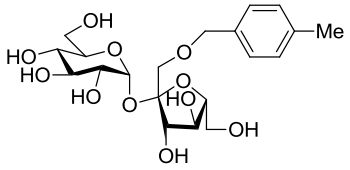

79m. White solid (83.2 mg, 90%): mp 83–85 °C; $[\alpha]_D$ +59 (*c* 1 CH_3OH); ^1H NMR (270 MHz, CD_3OD) δ 7.28 (d, *J* = 8.6 Hz, 2H), 6.89 (d, *J* = 8.6 Hz, 2H), 5.37 (d, *J* = 3.8 Hz, 1H), 4.56 (d, *J* = 11.5 Hz, 1H), 4.49 (d, *J* = 11.5 Hz, 1H), 4.18 (d, *J* = 8.5 Hz, 1H), 4.06 – 3.96 (m, 1H), 3.85 – 3.52 (m, 9H), 3.78 (s, 3H), 3.37 (t, *J* = 4.6 Hz, 1H), 3.34 (s, 1H); ^{13}C NMR (68 MHz, CD_3OD) δ 161.1, 131.5, 130.8, 114.9, 105.3, 94.1, 83.6, 78.9, 75.5, 74.8, 74.41, 74.40, 73.3, 71.5, 70.9, 63.4, 62.3, 55.7; HRMS-ESI (m/z) $[M + Na]^+$ calcd for $C_{20}H_{30}O_{12}Na$ 485.1635, found 485.1645.

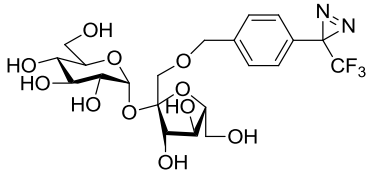

79n. White solid (98.3 mg, 91%): mp 73–75 °C; $[\alpha]_D$ +50 (*c* 1 CH_3OH); ^1H NMR (270 MHz, CD_3OD) δ 7.50 (d, *J* = 8.4 Hz, 2H), 7.25 (d, *J* = 8.4 Hz, 2H), 5.39 (d, *J* = 3.9 Hz,

1H), 4.70 (d, *J* = 12.7 Hz, 1H), 4.63 (d, *J* = 12.7 Hz, 1H), 4.23 (d, *J* = 8.5 Hz, 1H), 4.09 – 3.97 (m, 1H), 3.84 – 3.57 (m, 9H), 3.39 (dd, *J* = 5.7, 2.6 Hz, 1H), 3.35 (s, 1H); ^{13}C NMR (68 MHz, CD_3OD) δ 142.2, 129.4, 129.3, 127.7, 123.8 (q, *J* = 273.7 Hz), 105.2, 94.1, 83.6, 78.7, 75.4, 74.7, 74.4, 73.7, 73.2, 71.4, 71.3, 63.3, 62.3, 29.4 (q, *J* = 40.5 Hz); ^{19}F-NMR (470 MHz, CD_3OD): δ = -67.15 ppm. HRMS-ESI (m/z) $[M + Na]^+$ calcd for $C_{21}H_{27}N_2O_{11}F_3Na$ 563.1465, found 563.1488.

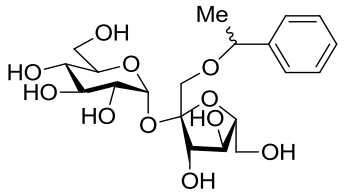

79o. White solid (87.5 mg, 98%, mixture of (*R*)- and (*S*)-isomers): mp 60–62 °C; $[\alpha]_D$ +53 (*c* 1 CH_3OH); ^{1}H NMR (270 MHz, CD_3OD) δ 7.37 – 7.21 (m, 5H), 5.33 (d, *J* = 3.8 Hz, 0.5H) and 5.30 (d, *J* = 3.8 Hz, 0.5H), 4.63 – 4.48 (m, 1H), 4.27 (d, *J* = 8.5 Hz, 0.5H) and 4.15 (d, *J* = 8.5 Hz, 0.5H), 4.01 (t, *J* = 7.9 Hz, 1H), 3.81 – 3.49 (m, 9H), 3.43 – 3.33 (m, 2H), 1.44 – 1.40 (m, 3H); ^{13}C NMR (68 MHz, CD_3OD) δ 145.1 and 145.0, 129.68 and 129.65, 128.7, 127.5 and 127.4, 105.6 and 105.1, 94.03 and 93.96, 83.7 and 83.6, 80.3 and 80.2, 79.2 and 78.6, 75.5 and 75.4, 74.9 and 74.7, 74.4 and 74.3, 73.3 and 73.2, 71.4, 70.1 and 69.2, 63.4 and 63.2, 62.2, 24.4 and 24.2; HRMS-ESI (m/z) $[M + Na]^+$ calcd for $C_{20}H_{30}O_{11}Na$ 469.1686, found 469.1687.

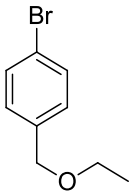

81a. Colorless oil (63.2 mg, 98%): ^{1}H NMR (270 MHz, $CDCl_3$) δ 7.47 (d, *J* = 8.4 Hz, 2H), 7.22 (d, *J* = 8.4 Hz, 2H), 4.45 (s, 2H), 3.53 (q, *J* = 7.0 Hz, 2H), 1.24 (t, *J* = 7.0 Hz, 3H); ^{13}C NMR (68 MHz, $CDCl_3$) δ 137.8, 131.6, 129.4, 121.4, 71.9, 65.9, 15.1; HRMS-ESI (m/z) $[M + H]^+$ calcd for $C_9H_{10}BrO$ 214.9895, found 214.9910.

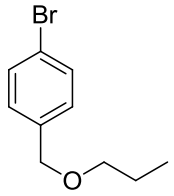

81b.. Colorless oil (65.3 mg, 95%): ^{1}H NMR (270 MHz, $CDCl_3$) δ 7.47 (d, J = 8.4 Hz, 2H), 7.22 (d, J = 8.4 Hz, 2H), 4.45 (s, 2H), 3.42 (t, J = 6.7 Hz, 2H), 1.70 – 1.59 (m, 2H), 0.94 (t, J = 6.7 Hz, 3H); ^{13}C NMR (68 MHz, $CDCl_3$) δ 137.9, 131.5, 129.3, 121.4, 72.2, 72.0, 22.8, 10.5; HRMS-ESI (m/z) $[M + H]^+$ calcd for $C_{10}H_{12}BrO$ 229.0051, found 229.0046.

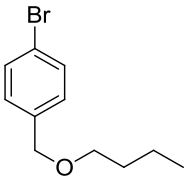

81c. Colorless oil (72.9 mg, 100%): ^{1}H NMR (270 MHz, $CDCl_3$) δ 7.46 (d, J = 8.4 Hz, 2H), 7.21 (d, J = 8.4 Hz, 2H), 4.44 (s, 2H), 3.46 (t, J = 6.5 Hz, 2H), 1.65 – 1.54 (m, 2H), 1.46 – 1.35 (m, 2H), 0.92 (t, J = 6.5 Hz, 3H); ^{13}C NMR (68 MHz, $CDCl_3$) δ 137.9, 131.5, 129.3, 121.3, 72.1, 70.3, 31.7, 19.2, 13.8; HRMS-ESI (m/z) $[M + H]^+$ calcd for $C_{11}H_{14}BrO$ 243.0208, found 243.0189.

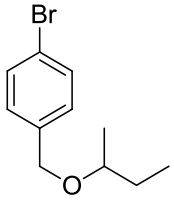

81d. Colorless oil (71.4 mg, 98%): ^{1}H NMR (270 MHz, $CDCl_3$) δ 7.46 (d, J = 8.3 Hz, 2H), 7.23 (d, J = 8.3 Hz, 2H), 4.46 (q, J = 12.1 Hz, 2H), 3.49 – 3.38 (m, 1H), 1.66 – 1.43 (m, 2H), 1.18 (d, J = 6.2 Hz, 3H), 0.92 (t, J = 7.4 Hz, 3H); ^{13}C NMR (68 MHz, $CDCl_3$) δ 138.4, 131.5, 129.3, 121.2, 76.4, 69.5, 29.1, 19.0, 9.7; HRMS-ESI (m/z) $[M + H]^+$ calcd for $C_{11}H_{14}BrO$ 243.0208, found 243.0182.

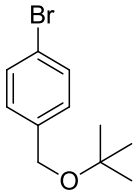

81e. White solid (64.9 mg, 89%): mp 45–47 °C; ^{1}H NMR (270 MHz, $CDCl_3$) δ 7.44 (d, J = 8.4 Hz, 2H), 7.22 (d, J = 8.4 Hz, 2H), 4.39 (s, 2H), 1.28 (s, 9H); ^{13}C NMR (68 MHz, $CDCl_3$) δ 139.1, 131.4, 129.1, 120.9, 73.6, 63.4, 27.6; HRMS-ESI (m/z) $[M + H]^+$ calcd for $C_{11}H_{14}BrO$ 243.0208, found 243.0191.

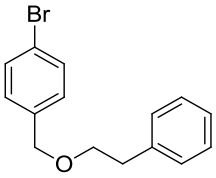

81f. Colorless oil (80.3 mg, 92%): ^{1}H NMR (270 MHz, $CDCl_3$) δ 7.43 (d, J = 8.3 Hz, 2H), 7.28 – 7.13 (m, 7H), 4.46 (s, 2H), 3.67 (t, J = 8.3 Hz, 2H), 2.91 (t, J = 8.3 Hz, 2H); ^{13}C NMR (68 MHz, $CDCl_3$) δ 139.0, 137.6, 131.5, 129.3, 129.0, 128.5, 126.3, 121.4, 72.1, 71.3, 36.3; HRMS-ESI (m/z) $[M + H]^+$ calcd for $C_{15}H_{14}BrO$ 291.0208, found 291.0219.

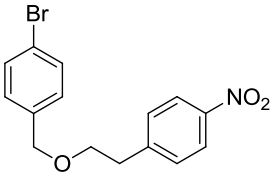

81g. white solid (87.7 mg, 87%): mp 93–95 °C; ^{1}H NMR (270 MHz, $CDCl_3$) δ 8.14 (d, J = 7.2 Hz, 2H), 7.46 – 7.37 (m, 4H), 7.13 (d, J = 7.1 Hz, 2H), 4.45 (s, 2H), 3.72 (t, J = 6.5 Hz, 2H), 3.01 (t, J = 6.2 Hz, 2H); ^{13}C NMR (68 MHz, $CDCl_3$) δ 147.2, 146.8, 137.1, 131.6, 129.8, 129.2, 123.6, 121.6, 72.3, 70.1, 36.1; HRMS-ESI (m/z) $[M + H]^+$ calcd for $C_{15}H_{15}BrNO_3$ 336.0235, found 336.0218.

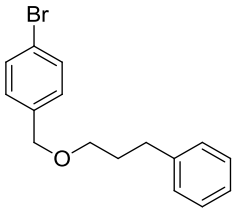

81h. Colorless oil (83.3 mg, 91%): ^{1}H NMR (270 MHz, $CDCl_3$) δ 7.47 (d, J = 8.3 Hz, 2H), 7.30 – 7.16 (m, 7H), 4.44 (s, 2H), 3.47 (t, J = 6.3 Hz, 2H), 2.71 (t, J = 7.5 Hz, 2H), 1.98 – 1.88 (m, 2H); ^{13}C NMR (68 MHz, $CDCl_3$) δ 142.0, 137.8, 131.6, 129.4, 128.6, 128.4, 125.9, 121.4, 72.1, 69.6, 32.3, 31.2; HRMS-ESI (m/z) $[M + H]^+$ calcd for $C_{16}H_{16}BrO$ 305.0364, found 305.0386.

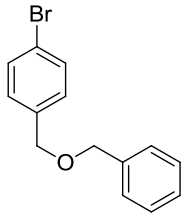

81i. Colorless oil (79.8 mg, 96%): ^{1}H NMR (270 MHz, $CDCl_3$) δ 7.47 (d, J = 8.4 Hz, 2H), 7.36 – 7.30 (m, 5H), 7.24 (d, J = 8.4 Hz, 2H), 4.55 (s, 2H), 4.50 (s, 2H); ^{13}C NMR (68 MHz, $CDCl_3$) δ 138.1, 137.4, 131.6, 129.5, 128.5, 127.9, 121.5, 72.2, 71.3; HRMS-ESI (m/z) $[M + H]^+$ calcd for $C_{14}H_{12}BrO$ 277.0051, found 277.0061.

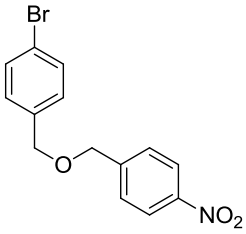

81j. Pale yellow oil (90.8 mg, 94%): ^{1}H NMR (270 MHz, $CDCl_3$) δ 8.22 (d, J = 8.8 Hz, 2H), 7.54 – 7.49 (m, 4H), 7.25 (d, J = 8.8 Hz, 2H), 4.64 (s, 2H), 4.57 (s, 2H); ^{13}C NMR (68 MHz, $CDCl_3$) δ 147.6, 145.7, 136.7, 131.8, 129.5, 127.9, 123.8, 122.0, 72.0, 70.9; HRMS-ESI (m/z) $[M + H]^+$ calcd for $C_{14}H_{13}BrNO_3$ 322.0079, found 322.0084.

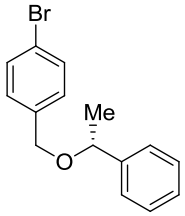

81k. Colorless oil (82.9 mg, 95%): $[\alpha]_D$ +78 (*c* 1 $CHCl_3$); ^{1}H NMR (270 MHz, $CDCl_3$) δ 7.45 (d, *J* = 8.3 Hz, 2H), 7.37 – 7.28 (m, 5H), 7.18 (d, *J* = 8.3 Hz, 2H), 4.48 (q, *J* = 6.5 Hz, 1H), 4.38 (d, *J* = 12.2 Hz, 1H), 4.25 (d, *J* = 12.2 Hz, 1H), 1.48 (d, *J* = 6.5 Hz, 3H); ^{13}C NMR (68 MHz, $CDCl_3$) δ 143.6, 137.8, 131.5, 129.4, 128.6, 127.7, 126.4, 121.4, 69.5, 24.0; HRMS-ESI (m/z) $[M + H]^+$ calcd for $C_{15}H_{14}BrO$ 291.0208, found 291.0197; HPLC (Chiralcel OJ column, *n*-hexane:*i*-PrOH = 85:15, 0.5 mL/min, 210 nm), t_R (major) = 19.45 min, t_R (minor) = 15.08 min; ee = 96%

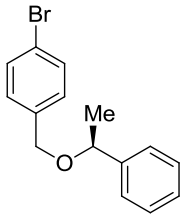

81l. Colorless oil (81.2 mg, 93%): $[\alpha]_D$ -78 (*c* 1 $CHCl_3$); ^{1}H NMR, ^{13}C NMR and HRMS-ESI are identical with **81k**. HPLC (Chiralcel OJ column, *n*-hexane:*i*-PrOH = 85:15, 0.5 mL/min, 210 nm), t_R (major) = 14.99 min, t_R (minor) = 19.45 min; ee = 95%

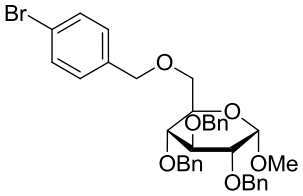

81m. Colorless oil (180.4 mg, 95%): $[\alpha]_D$ +23 (*c* 1 $CHCl_3$); ^{1}H NMR (270 MHz, $CDCl_3$) δ 7.42 (d, *J* = 8.4 Hz, 2H), 7.34 – 7.12 (m, 17H), 4.98 (d, *J* = 10.9 Hz, 1H), 4.87 – 4.38 (m, 8H), 3.98 (t, *J* = 9.2 Hz, 1H), 3.77 – 3.62 (m, 4H), 3.55 (dd, *J* = 9.6, 3.6 Hz, 1H) 3.37 (s, 3H); ^{13}C NMR (68 MHz, $CDCl_3$) δ 138.9, 138.32, 138.26, 137.1, 131.6, 129.5, 128.6, 128.5, 128.2, 128.1, 128.0, 127.8, 127.7, 121.6, 98.2, 82.1, 79.9, 77.7, 75.8, 75.0, 73.4, 72.6, 70.0, 68.7, 55.1; HRMS-ESI (m/z) $[M + Na]^+$ calcd for $C_{35}H_{37}BrO_6Na$

657.1651, found 657.1677.

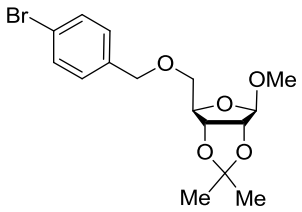

81n. Colorless oil (91.8 mg, 82%): $[\alpha]_D$ -45 (*c* 1 $CHCl_3$); ^1H NMR (270 MHz, $CDCl_3$) δ 7.47 (d, *J* = 8.3 Hz, 2H), 7.22 (d, *J* = 8.3 Hz, 2H), 4.96 (s, 1H), 4.67 (d, *J* = 5.9 Hz, 1H), 4.57 (d, *J* = 5.9 Hz, 1H), 4.50 (s, 2H), 4.39 – 4.33 (m, 1H), 3.54 – 3.41 (m, 2H), 3.29 (s, 3H), 1.48 (s, 3H), 1.31 (s, 3H); ^{13}C NMR (68 MHz, $CDCl_3$) δ 137.2, 131.6, 129.3, 121.6, 112.5, 109.4, 85.1, 82.1, 72.5, 71.2, 54.8, 26.4, 24.9; HRMS-ESI (m/z) $[M + Na]^+$ calcd for $C_{16}H_{21}BrO_5Na$ 397.0450, found 397.0432.

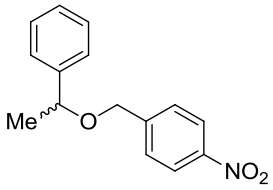

81o. Colorless oil (71.7 mg, 93%, mixture of (*R*)- and (*S*)-isomers): ^1H NMR (270 MHz, $CDCl_3$) δ 8.19 (d, *J* = 8.6 Hz, 2H), 7.48 (d, *J* = 8.6 Hz, 2H), 7.38 – 7.31 (m, 5H), 4.56 – 4.40 (m, 3H), 1.53 (d, *J* = 6.5 Hz, 3H); ^{13}C NMR (68 MHz, $CDCl_3$) δ 147.4, 146.5, 143.1, 128.7, 127.9, 127.8, 126.3, 123.6, 78.2, 69.1, 23.9; HRMS-ESI (m/z) $[M + Na]^+$ calcd for $C_{15}H_{15}NO_3Na$ 280.0950, found 280.0970.

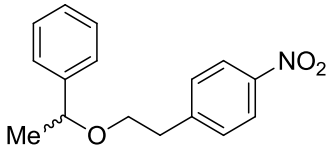

81p. Colorless oil (73.2 mg, 90%, mixture of (*R*)- and (*S*)-isomers): ^1H NMR (270 MHz, $CDCl_3$) δ 8.13 (d, *J* = 8.7 Hz, 2H), 7.36 – 7.19 (m, 7H), 4.37 (q, *J* = 6.5 Hz, 1H), 3.55 (t, *J* = 6.5 Hz, 2H), 2.95 (t, *J* = 6.5 Hz, 2H), 1.40 (d, *J* = 6.5 Hz, 3H); ^{13}C NMR (68 MHz, $CDCl_3$) δ 147.5, 146.7, 143.6, 129.9, 128.5, 127.6, 126.2, 123.5, 78.4, 68.3, 36.3, 23.8; HRMS-ESI (m/z) $[M + K]^+$ calcd for $C_{16}H_{17}NO_3K$ 310.0846, found 310.0832.

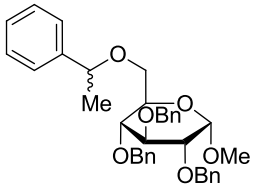

81q. Colorless oil (156.8 mg, 92%, mixture of (*R*)- and (*S*)-isomers): $_D$ +18 (*c* 1 $CHCl_3$); ^{1}H NMR (270 MHz, $CDCl_3$) δ 7.34 – 7.17 (m, 20H), 4.98 (d, *J* = 10.8 Hz, 1H), 4.90 – 4.77 (m, 3H), 4.69 – 4.55 (m, 3H), 4.32 (q, *J* = 6.5 Hz, 1H), 3.98 (t, *J* = 9.5 Hz, 1H), 3.71 – 3.51 (m, 4H), 3.44 (dd, *J* = 10.6, 4.1 Hz, 1H), 3.35 (s, 3H), 1.42 (d, *J* = 6.5 Hz, 3H); ^{13}C NMR (68 MHz, $CDCl_3$) δ 143.7, 138.9, 138.5, 138.4, 128.5, 128.2, 128.1, 128.0, 127.9, 127.8, 127.7, 127.5, 126.3, 98.1, 82.3, 79.9, 79.0, 77.8, 75.7, 75.0, 73.3, 70.2, 67.4, 55.0, 24.0; HRMS-ESI (m/z) $[M + Na]^+$ calcd for $C_{36}H_{40}O_6Na$ 591.2723, found 591.2728.

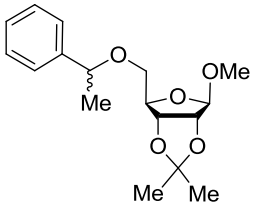

81r. Colorless oil (83.2 mg, 90%, mixture of (*R*)- and (*S*)-isomers): $_D$ -43 (*c* 1 $CHCl_3$); ^{1}H NMR (270 MHz, $CDCl_3$) δ 7.34 – 7.26 (m, 5H), 4.93 (d, *J* = 3.6 Hz, 1H), 4.72 – 4.55 (m, 1H), 4.43 – 4.28 (m, 2H), 3.40 – 3.30 (m, 2H), 3.28 – 3.22 (m, 3H), 1.48 – 1.43 (m, 6H), 1.33 – 1.31 (m, 3H); ^{13}C NMR (68 MHz, $CDCl_3$) δ 143.7 and 143.6, 128.5, 127.6, 126.3, 126.2, 112.4, 109.3, 85.5 and 85.4, 85.2, 82.3 and 82.1, 78.6 and 78.4, 69.6 and 69.5, 54.7 and 54.6, 26.4, 25.0, 24.0 and 23.9; HRMS-ESI (m/z) $[M + Na]^+$ calcd for $C_{17}H_{24}O_5Na$ 331.1521, found 331.1519.

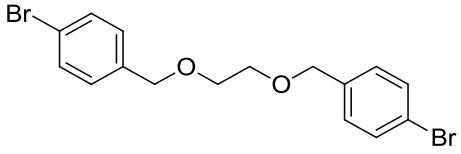

81s. White solid (111.6 mg, 93%): mp 49–51 °C; ^{1}H NMR (270 MHz, $CDCl_3$) δ 7.47 (d, *J* = 8.3 Hz, 4H), 7.22 (d, *J* = 8.3 Hz, 4H), 4.52 (s, 4H), 3.64 (s, 4H); ^{13}C NMR (68 MHz,

$CDCl_3$) δ 137.4, 131.6, 129.4, 121.5, 72.5, 69.6; HRMS-ESI (m/z) $[M + Na]^+$ calcd for $C_{16}H_{16}Br_2O_2Na$ 422.9394, found 422.9382.

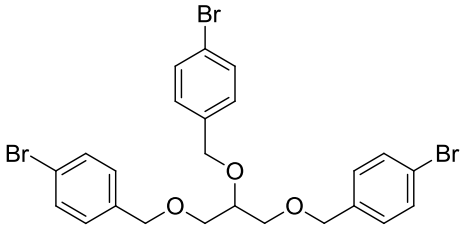

81t. Colorless oil (145.6 mg, 81%): ^{1}H NMR (270 MHz, $CDCl_3$) δ 7.49 – 7.43 (m, 6H), 7.25 – 7.15 (m, 6H), 4.62 (s, 2H), 4.47 (s, 4H), 3.80 – 3.72 (m, 1H), 3.59 (d, J = 4.6 Hz, 4H); ^{13}C NMR (68 MHz, $CDCl_3$) δ 137.7, 137.3, 131.6, 131.5, 129.4, 129.3, 121.6, 121.5, 72.6, 71.5, 70.3; HRMS-ESI (m/z) $[M + Na]^+$ calcd for $C_{24}H_{23}Br_3O_3Na$ 620.9075, found 620.9046.

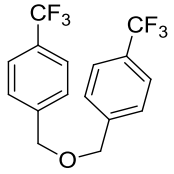

77a. Colorless oil: ^{1}H NMR (270 MHz, $CDCl_3$) δ 7.62 (d, J = 8.0 Hz, 4H), 7.48 (d, J = 8.0 Hz, 4H), 4.63 (s, 4H); ^{13}C NMR (68 MHz, $CDCl_3$) δ 142.1, 130.1 (q, J = 32.2 Hz), 127.7, 125.5 (q, J = 3.7 Hz), 124.2 (q, J = 271.9 Hz), 71.6; ^{19}F-NMR (470 MHz, $CDCl_3$): δ = -62.52 ppm; HRMS-ESI (m/z) $[M + H]^+$ calcd for $C_{16}H_{13}OF_6$ 335.0871, found 335.0894.

6.4 Conclusions

In conclusion, a cosolvent-promoted O-benzylation strategy was developed in this work. It can not only improve the reaction solubility but also increase the reaction yield. In the cosolvent, the byproducts derived from benzyl bromides are greatly inhibited and the carbohydrates are highly soluble in it. Regardless of the relatively low yield of 1'-hydroxyl of sucrose, the benzylation yield can reach 95%. The

benzylation mechanism with primary and secondary benzyl bromides were elaborated, respectively. With this strategy in hand, we successfully prepared a photoreactive 1'-sucrose derivative which acts as a promising reagent to investigate sucrose in photoaffinity labeling. Further investigation indicated that the cosolvent-promoted strategy are suitable for many substrates such and commonly used alcohol, glucose, ribose as well as polyols.

Conclusions

PAL is a useful strategy to investigate the interaction between ligands and receptors. Under the UV irradiation, it is feasible to find out the corresponding targets or binding site which are of great importance for understanding our physiological activity and drug design. Among of the three major photophores used in the field of PAL, TPD has emerged as the most promising one due to its many advantages. The works of my thesis were mainly performed around TPD. Here, we presented a significantly effective one-pot synthesis of TPD from the corresponding tosyloxime, introduced a novel method to prepare deuterated cross-linkable aromatic α-amino acids, described the metabolic study of photoreactive phenylalanines in the presence of *Klebsiella* sp. CK6, reported an effective synthetic procedure for photoreactive saccharin as well as the corresponding gustatory receptor assay, and developed a crucial cosolvent-promoted O-benzylation strategy with Ag_2O which can be used in both of the carbohydrate and synthetic field. In consideration of the great significance of TPD as well as TPD-based photoaffinity labeling probes, many excellent works will spring up in the future.

References

1. Singh, A.; Thornton, E. R.; Westheimer, F. H., The photolysis of diazoacetylchymotrypsin. *J. Biol. Chem.* **1962**, *237*, 3006-3008.

2. Fleet, G. W. J.; Porter, R. R.; Knowles, J. R., Affinity labelling of antibodies with aryl nitrene as reactive group. *Nature* **1969**, *224*, 511-512.

3. Galardy, R. E.; Craig, L. C.; Jamieson, J. D.; Printz, M. P., Photoaffinity labeling of peptide hormone binding sites. *J. Biol. Chem.* **1974**, *249*, 3510-3518.

4. Paulsen, S. R., 3.3-Dialkyl-diazacyclopropen-(1). *Angew. Chem.* **1960**, *72*, 781-782.

5. Kumar, N. S.; Braun, M. P.; Chaudhary, A. G.; Young, R. N., Synthesis of a tritium-labeled photo-affinity probe based on an atypical leukotriene biosynthesis inhibitor. *J. Labelled Compd. Rad.* **2011,** *54*, 43-50.

6. Wallrabe, H.; Periasamy, A., Imaging protein molecules using FRET and FLIM microscopy. *Curr. Opin. Biotech.* **2005,** *16*, 19-27.

7. Wold, F., [1] Affinity labeling-An overview. *Methods Enzymol.* **1977**, *46*, 3-14.

8. Hulce, J. J.; Cognetta, A. B.; Niphakis, M. J.; Tully, S. E.; Cravatt, B. F., Proteome-wide mapping of cholesterol-interacting proteins in mammalian cells. *Nat. Methods.* **2013**, *10*, 259-264.

9. Bayer, E. A.; Wilchek, M., Eight international symposium on affinity chromatography and biological recognition application of avidin-biotin technology to affinity-based separations. *J. Chromatogr. A* **1990**, *510*, 3-11.

10. Sinz, A., Investigation of protein-ligand interactions by mass spectrometry. *ChemMedChem* **2007**, *2*, 425-431.

11. Platz, M. S., Comparison of phenylcarbene and phenylnitrene. *Acc. Chem. Res.* **1995,** *28*, 487-492.

12. Karney, W. L.; Borden, W. T., Why does *o*-fluorine substitution raise the barrier to ring expansion of phenylnitrene? *J. Am. Chem. Soc.* **1997**, *119*, 3347-3350.

13. Prestwich, G. D.; Dormán, G.; Elliott, J. T.; Marecak, D. M.; Chaudhary, A., Benzophenone photoprobes for phosphoinositides, peptides and drugs. *Photochem. Photobiol.* **1997**, *65*, 222-234.

14. Moss, R. A., Diazirines: Carbene precursors par excellence. *Acc. Chem. Res.* **2006**, *39*, 267-272.

15. Brunner, J.; Senn, H.; Richards, F. M., 3-Trifluoromethyl-3-phenyldiazirine. A new carbene generating group for photolabeling reagents. *J. Biol. Chem.* **1980**, *255*, 3313-3318.

16. Das, J., Aliphatic diazirines as photoaffinity probes for proteins: Recent

developments. *Chem. Rev.* **2011**, *111*, 4405-4417.

17. Ford, F.; Yuzawa, T.; Platz, M. S.; Matzinger, S.; Fülscher, M., Rearrangement of dimethylcarbene to propene: study by laser flash photolysis and *ab initio* molecular orbital theory. *J. Am. Chem. Soc.* **1998**, *120*, 4430-4438.

18. Hashimoto, M.; Hatanaka, Y., Practical conditions for photoaffinity labeling with 3-trifluoromethyl-3-phenyldiazirine photophore. *Anal. Biochem.* **2006**, *348*, 154-156.

19. Erni, B.; Khorana, H. G., Fatty acids containing photoactivable carbene precursors. Synthesis and photochemical properties of 3,3-bis(1,1-difluorohexyl)diazirine and 3-(1,1-difluorooctyl)-3*H*-diazirine. *J. Am. Chem. Soc.* **1980**, *102*, 3888-3896.

20. Akasaka, T.; Liu, M. T. H.; Niino, Y.; Maeda, Y.; Wakahara, T.; Okamura, M.; Kobayashi, K.; Nagase, S., Photolysis of diazirines in the presence of C_{60}: A chemical probe for carbene/diazomethane partitioning. *J. Am. Chem. Soc.* **2000**, *122*, 7134-7135.

21. Wakahara, T.; Niino, Y.; Kato, T.; Maeda, Y.; Akasaka, T.; Liu, M. T. H.; Kobayashi, K.; Nagase, S., A nonspectroscopic method to determine the photolytic decomposition pathways of 3-chloro-3-alkyldiazirine: Carbene, diazo and rearrangement in excited state. *J. Am. Chem. Soc.* **2002**, *124*, 9465-9468.

22. Al-Omari, M.; Banert, K.; Hagedorn, M., Bi-3*H*-diazirin-3-yls as precursors of highly strained cycloalkynes. *Angew. Chem. Int. Ed.* **2006**, *45*, 309-311.

23. Vila-Perelló, M.; Pratt, M. R.; Tulin, F.; Muir, T. W., Covalent capture of phospho-dependent protein oligomerization by site-specific incorporation of a diazirine photo-cross-linker. *J. Am. Chem. Soc.* **2007**, *129*, 8068-8069.

24. Song, Z.; Zhang, Q., Fluorous aryldiazirine photoaffinity labeling reagents. *Org. Lett.* **2009**, *11*, 4882-4885.

25. Delfino, J. M.; Schreiber, S. L.; Richards, F. M., Design, synthesis, and properties of a photoactivatable membrane-spanning phospholipidic probe. *J. Am. Chem. Soc.* **1993**, *115*, 3458-3474.

26. Burkard, N.; Bender, T.; Westmeier, J.; Nardmann, C.; Huss, M.; Wieczorek, H.; Grond, S.; von Zezschwitz, P., New fluorous photoaffinity labels (F-PAL) and their application in V-ATPase inhibition studies. *Eur. J. Org. Chem.* **2010**, *2010*, 2176-2181.

27. Kumar, N. S.; Young, R. N., Design and synthesis of an all-in-one 3-(1,1-difluoroprop-2-ynyl)-3*H*-diazirin-3-yl functional group for photo-affinity labeling. *Bioorg. Med. Chem.* **2009**, *17*, 5388-5395.

28. Sánchez Carrera, S.; Kerdelhué, J.-L.; Langenwalter, K. J.; Brown, N.; Warmuth, R., Inner-phase reaction dynamics: The influence of hemicarcerand polarizability and shape on the potential energy surface of an inner-phase reaction. *Eur. J. Org. Chem.* **2005**, *2005*, 2239-2249.

29. Wang, L.; Murai, Y.; Yoshida, T.; Ishida, A.; Masuda, K.; Sakihama, Y.;

Hashidoko, Y.; Hatanaka, Y.; Hashimoto, M., Alternative one-pot synthesis of (trifluoromethyl)phenyldiazirines from tosyloxime derivatives: Application for new synthesis of optically pure diazirinylphenylalanines for photoaffinity labeling. *Org. Lett.* **2015**, *17*, 616-619.

30. Murai, Y.; Wang, L.; Masuda, K.; Sakihama, Y.; Hashidoko, Y.; Hatanaka, Y.; Hashimoto, M., Rapid and controllable hydrogen/deuterium exchange on aromatic rings of α-amino acids and peptides. *Eur. J. Org. Chem.* **2013**, *2013*, 5111-5116.

31. Wang, L.; Murai, Y.; Yoshida, T.; Okamoto, M.; Masuda, K.; Sakihama, Y.; Hashidoko, Y.; Hatanaka, Y.; Hashimoto, M., Hydrogen/deuterium exchange of cross-linkable α-amino acid derivatives in deuterated triflic acid. *Biosci. Biotech. Biochem.* **2014**, *78*, 1129-1134.

32. Wang, L.; Hisano, W.; Murai, Y.; Sakurai, M.; Muto, Y.; Ikemoto, H.; Okamoto, M.; Murotani, T.; Isoda, R.; Kim, D.; Sakihama, Y.; Sitepu, I.; Hashidoko, Y.; Hatanaka, Y.; Hashimoto, M., Distinct metabolites for photoreactive $_{L}$-phenylalanine derivatives in *Klebsiella* sp. CK6 isolated from rhizosphere of a wild dipterocarp sapling. *Molecules* **2013**, *18*, 8393-8401.

33. Wang, L.; Yoshida, T.; Muto, Y.; Murai, Y.; Tachrim, Z. P.; Ishida, A.; Nakagawa, S.; Sakihama, Y.; Hashidoko, Y.; Masuda, K.; Hatanaka, Y.; Hashimoto, M., Synthesis of diazirine-based photoreactive saccharin derivatives for the photoaffinity labeling of gustatory receptors. *Eur. J. Org. Chem.* **2015**, *2015*, 3129-3134.

34. Wang, L.; Hashidoko, Y.; Hashimoto, M., Cosolvent-promoted O-benzylation with silver(I) oxide: Synthesis of 1′-benzylated sucrose derivatives, mechanistic studies, and scope investigation. *J. Org. Chem.* **2016**, *81*, 4464-4474.

35. Coulter, L. V.; Sinclair, J. R.; Cole, A. G.; Roper, G. C., The heat capacity, entropy and heat content of sodium smide from 15 to 300 °K. The thermodynamics of amide ion in liquid ammonia. *J. Am. Chem. Soc.* **1959**, *81*, 2986-2989.

36. Fernelius, W. C.; Bowman, G. B., Ammonolysis in liquid ammonia. *Chem. Rev.* **1940**, *26*, 3-48.

37. Hatanaka, Y.; Hashimoto, M.; Kurihara, H.; Nakayama, H.; Kanaoka, Y., A novel family of aromatic diazirines for photoaffinity labeling. *J. Org. Chem.* **1994**, *59*, 383-387.

38. Hatanaka, Y.; Hashimoto, M.; Nakayama, H.; Kanaoka, Y., Syntheses of nitro-substituted aryl diazirines. An entry to chromogenic carbene precursors for photoaffinity labeling. *Chem. Pharm. Bull.* **1994**, *42*, 826-831.

39. Hashimoto, M.; Hatanaka, Y., Recent progress in diazirine-based photoaffinity labeling. *Eur. J. Org. Chem.* **2008**, *2008*, 2513-2523.

40. Smith, R. A. G.; Knowles, J. R., The preparation and photolysis of 3-aryl-3*H*-diazirines. *J. Chem. Soc., Perkin Trans. 2* **1975**, 686-694.

41. Nassal, M., 4'-(1-Azi-2,2,2-trifluoroethyl)phenylalanine, a photolabile

carbene-generating analog of phenylalanine. *J. Am. Chem. Soc.* **1984**, *106*, 7540-7545.

42. Fishwick, C. W. G.; Sanderson, J. M.; Findlay, J. B. C., An efficient route to S-N-(9-fluorenylmethoxycarbonyl)-4′-(1-azi-2,2,2-trifluoroethyl)phenylalanine. *Tetrahedron Lett.* **1994**, *35*, 4611-4614.

43. Hashimoto, M.; Hatanaka, Y.; Sadakane, Y.; Nabeta, K., Synthesis of tag introducible (3-trifluoromethyl)phenyldiazirine based photoreactive phenylalanine. *Bioorg. Med. Chem. Lett.* **2002**, *12*, 2507-2510.

44. Nakashima, H.; Hashimoto, M.; Sadakane, Y.; Tomohiro, T.; Hatanaka, Y., Simple and versatile method for tagging phenyldiazirine photophores. *J. Am. Chem. Soc.* **2006**, *128*, 15092-15093.

45. Masuda, K.; Koizumi, A.; Misaka, T.; Hatanaka, Y.; Abe, K.; Tanaka, T.; Ishiguro, M.; Hashimoto, M., Photoactive ligands probing the sweet taste receptor. Design and synthesis of highly potent diazirinyl $_{D}$-phenylalanine derivatives. *Bioorg. Med. Chem. Lett.* **2010**, *20*, 1081-1083.

46. Fillion, D.; Deraët, M.; Holleran, B. J.; Escher, E., Stereospecific synthesis of a carbene-generating angiotensin II analogue for comparative photoaffinity labeling: Improved incorporation and absence of methionine selectivity. *J. Med. Chem.* **2006**, *49*, 2200-2209.

47. Arsene, C. G.; Ohlendorf, R.; Burkitt, W.; Pritchard, C.; Henrion, A.; O'Connor, G.; Bunk, D. M.; Güttler, B., Protein quantification by isotope dilution mass spectrometry of proteolytic fragments: Cleavage rate and accuracy. *Anal. Chem.* **2008**, *80*, 4154-4160.

48. Hasegawa, H.; Akagawa, N.; Shinohara, Y.; Baba, S., Synthesis of [2,6-$^{3}H_{2}$-Tyr^{1}]leucine-enkephalin. *J. Chem. Soc., Perkin Trans. 1*, **1990**, 2085-2088.

49. Atzrodt, J.; Derdau, V.; Fey, T.; Zimmermann, J., The renaissance of H/D exchange. *Angew. Chem. Int. Ed.* **2007**, *46*, 7744-7765.

50. Wang, L.; Murai, Y.; Yoshida, T.; Okamoto, M.; Tachrim, Z.; Hashidoko, Y.; Hashimoto, M., Utilization of acidic *α*-amino acids as acyl donors: An effective stereo-controllable synthesis of aryl-keto *α*-amino acids and their derivatives. *Molecules* **2014**, *19*, 6349.

51. Murashige, R.; Hayashi, Y.; Hashimoto, M., Asymmetric and efficient synthesis of homophenylalanine derivatives via Friedel-Crafts reaction with trifluoromethanesulfonic acid. *Tetrahedron Lett.* **2008**, *49*, 6566-6568.

52. Paramelle, D.; Miralles, G.; Subra, G.; Martinez, J., Chemical cross-linkers for protein structure studies by mass spectrometry. *Proteomics* **2013**, *13*, 438-456.

53. Burdine, L.; Gillette, T. G.; Lin, H.-J.; Kodadek, T., Periodate-triggered cross-linking of DOPA-containing peptide-protein complexes. *J. Am. Chem. Soc.* **2004**, *126*, 11442-11443.

54. Kotzyba-Hibert, F.; Kapfer, I.; Goeldner, M., Recent trends in photoaffinity

labeling. *Angew. Chem. Int. Ed.* **1995**, *34*, 1296-1312.

55. Olah, G. A.; Ramaiah, P.; Wang, Q.; Prakash, G. K. S., Triflic acid catalyzed phenylamination of aromatics with phenyl azide. *J. Org. Chem.* **1993**, *58*, 6900-6901.

56. Moss, R. A.; Fedé, J.-M.; Yan, S., SbF_5-Mediated reactions of oxafluorodiazirines. *Org. Lett.* **2001**, *3*, 2305-2308.

57. Murai, Y.; Masuda, K.; Ogasawara, Y.; Wang, L.; Hashidoko, Y.; Hatanaka, Y.; Iwata, S.; Kobayashi, T.; Hashimoto, M., Synthesis of photoreactive 2-phenethylamine derivatives-synthesis of adenosine derivatives enabling functional analysis of adenosine receptors by photoaffinity labeling. *Eur. J. Org. Chem.* **2013**, *2013*, 2428-2433.

58. Rahman, A.; Sitepu, I. R.; Tang, S.-Y.; Hashidoko, Y., Salkowski's reagent test as a primary screening index for functionalities of rhizobacteria isolated from wild dipterocarp saplings growing naturally on medium-strongly acidic tropical peat soil. *Biosci. Biotech. Biochem.* **2010**, *74*, 2202-2208.

59. Kaneshiro, T.; Nicholson, J. J., Tryptophan catabolism by tan variants isolated from enrichment cultures of bradyrhizobia. *Curr. Microbiol.* **1989**, *18*, 57-60.

60. Li, X.; Staszewski, L.; Xu, H.; Durick, K.; Zoller, M.; Adler, E., Human receptors for sweet and umami taste. *Proc. Natl. Acad. Sci. USA* **2002**, *99*, 4692-6.

61. Moeker, J.; Peat, T. S.; Bornaghi, L. F.; Vullo, D.; Supuran, C. T.; Poulsen, S.-A., Cyclic secondary sulfonamides: Unusually good inhibitors of cancer-related carbonic anhydrase enzymes. *J. Med. Chem.* **2014**, *57*, 3522-3531.

62. Suami, T.; Hough, L.; Machinami, T.; Saito, T.; Nakamura, K., Molecular mechanisms of sweet taste 8: saccharin, acesulfame-K, cyclamate and their derivatives. *Food Chem.* **1998**, *63*, 391-396.

63.Murai, Y.; Masuda, K.; Sakihama, Y.; Hashidoko, Y.; Hatanaka, Y.; Hashimoto, M., Comprehensive synthesis of photoreactive (3-trifluoromethyl)diazirinyl indole derivatives from 5- and 6- trifluoroacetylindoles for photoaffinity labeling. *J. Org. Chem.* **2012**, *77*, 8581-8587.

64. Hosoya, T.; Hiramatsu, T.; Ikemoto, T.; Nakanishi, M.; Aoyama, H.; Hosoya, A.; Iwata, T.; Maruyama, K.; Endo, M.; Suzuki, M., Novel bifunctional probe for radioisotope-free photoaffinity labeling: Compact structure comprised of photospecific ligand ligation and detectable tag anchoring units. *Org. Biomol. Chem.* **2004**, *2*, 637-641.

65. Murashige, R.; Murai, Y.; Hatanaka, Y.; Hashimoto, M., Effective synthesis of optically active trifluoromethyldiazirinyl homophenylalanine and aroylalanine derivatives with the Friedel-Crafts reaction in triflic acid. *Biosci. Biotech. Biochem.* **2009**, *73*, 1377-1380.

66. Ueda, T.; Ugawa, S.; Yamamura, H.; Imaizumi, Y.; Shimada, S., Functional interaction between T2R taste receptors and G-protein α subunits expressed in taste

receptor cells. *J. Neurosci.* **2003**, *23*, 7376-7380.

67. Kuhn, C.; Bufe, B.; Winnig, M.; Hofmann, T.; Frank, O.; Behrens, M.; Lewtschenko, T.; Slack, J. P.; Ward, C. D.; Meyerhof, W., Bitter taste receptors for saccharin and acesulfame K. *J. Neurosci.* **2004**, *24*, 10260-10265.

68. Hill, K.; Rhode, O., Sugar-based surfactants for consumer products and technical applications. *Lipid/Fett* **1999**, *101*, 25-33.

69. Lewandowski, B.; Jarosz, S., Amino-acid templated assembly of sucrose-derived macrocycles. *Org. Lett.* **2010**, *12*, 2532-2535.

70. Toda, M.; Takagaki, A.; Okamura, M.; Kondo, J. N.; Hayashi, S.; Domen, K.; Hara, M., Green chemistry: Biodiesel made with sugar catalyst. *Nature* **2005**, *438*, 178-178.

71. Polat, T.; Mohammadi, M.; Linhardt, R. J., Synthesis of sulfosucrose derivatives for evaluation as regulators of fibroblast growth factor activity. *Tetrahedron Lett.* **2002**, *43*, 8047-8049.

72. Lichtner, F. T.; Spanswick, R. M., Sucrose uptake by developing soybean cotyledons. *Plant Physiol.* **1981**, *68*, 693-698.

73. Card, P. J.; Hitz, W. D., Synthesis of 1'-deoxy-1'-fluorosucrose via sucrose synthetase mediated coupling of 1-deoxy-1-fluorofructose with uridine diphosphate glucose. *J. Am. Chem. Soc.* **1984,** *106*, 5348-5350.

74. Card, P. J.; Hitz, W. D.; Ripp, K. G., Chemoenzymic syntheses of fructose-modified sucroses via multienzyme systems. Some topographical aspects of the binding of sucrose to a sucrose carrier protein. *J. Am. Chem. Soc.* **1986**, *108*, 158-161.

75. Hitz, W. D.; Card, P. J.; Ripp, K. G., Substrate recognition by a sucrose transporting protein. *J. Biol. Chem.* **1986**, *261*, 11986-11991.

76. Chauvin, C.; Plusquellec, D., A new chemoenzymatic synthesis of 6'-O-acylsucroses. *Tetrahedron Lett.* **1991**, *32*, 3495-3498.

77. Jarosz, S.; Mach, M., Regio- and stereoselective transformations of sucrose at the terminal positions. *Eur. J. Org. Chem.* **2002**, *2002*, 769-780.

78. Clode, D. M.; McHale, D.; Sheridan, J. B.; Birch, G. G.; Rathbone, E. B., Partial benzoylation of sucrose. *Carbohydr. Res.* **1985**, *139*, 141-146.

79. Wuts, P. G. M.; Greene, T. W., Protection for the hydroxyl group, including 1,2- and 1,3-diols. *Greene's protective groups in organic synthesis*, 4th ed.; John Wiley & Sons: Hoboken, NJ, 2007; p102.

80. Arihara, R.; Kakita, K.; Yamada, K.; Nakamura, S.; Hashimoto, S., Synthesis of the tetrasaccharide repeating unit from *Acinetobacter baumannii* serogroup O18 capitalizing on phosphorus-containing leaving groups. *J. Org. Chem.* **2015**, *80*, 4278-4288.

81. Sharif, E. U.; Wang, H. Y.; Akhmedov, N. G.; O'Doherty, G. A., Merremoside

D: *de novo* synthesis of the purported structure, NMR analysis, and comparison of spectral data. *Org. Lett.* **2014**, *16*, 492-5.

82. Zulueta, M. M. L.; Zhong, Y.-Q.; Hung, S.-C., Synthesis of $_{L}$-hexoses and their related biomolecules. *Chem. Commun.* **2013,** *49*, 3275-3287.

83. Rankin, G. M.; Maxwell-Cameron, I.; Painter, G. F.; Larsen, D. S., The dimethoxyphenylbenzyl protecting group: an alternative to the *p*-methoxybenzyl group for protection of carbohydrates. *J. Org. Chem.* **2013**, *78*, 5264-72.

84. Ghosh, R.; Maity, J. K.; Achari, B.; Mandal, S. B., Locked nucleosides based on oxabicyclo[3.2.1]octane and oxabicyclo[2.2.1]heptane skeletons. *J. Org. Chem.* **2010**, *75*, 2419-2422.

85. Ermolenko, L.; Sasaki, N. A., Diastereoselective synthesis of all eight $_{L}$-hexoses from $_{L}$-ascorbic acid. *J. Org. Chem.* **2006**, *71*, 693-703.

86. Bessières, B.; Morin, C., Iodomethyl group as a hydroxymethyl synthetic equivalent: Application to the syntheses of $_{D}$-*manno*-hept-2-ulose and $_{L}$-fructose derivatives. *J. Org. Chem.* **2003**, *68*, 4100-4103.

87. Tamigney Kenfack, M.; Blériot, Y.; Gauthier, C., Intramolecular aglycon delivery enables the synthesis of 6-deoxy-*β*-$_{D}$-*manno*-heptosides as fragments of *Burkholderia pseudomallei* and *Burkholderia mallei* capsular polysaccharide. *J. Org. Chem.* **2014**, *79*, 4615-4634.

88. Ribes, C.; Falomir, E.; Carda, M.; Marco, J. A., Short, Stereoselective synthesis of the naturally occurring pyrrolidine radicamine B and a formal synthesis of nectrisine. *J. Org. Chem.* **2008**, *73*, 7779-7782.

89. Barros, M. T.; Maycock, C. D.; Thomassigny, C., Preparation of sucrose heptaesters unsubstituted at the C-1 hydroxy group of the fructose moiety via selective O-desilylation. *Carbohydr. Res.* **2000,** *328*, 419-423.

90. Li, Y.-L.; Wu, Y.-L., Synthesis and glycosylation of thio-$_{D}$-fructofuranoside donors. *Tetrahedron Lett.* **1996**, *37*, 7413-7416.

91. Chang, K.-Y.; Wu, S.-H.; Wang, K.-T., Regioselective enzymic deacetylation of octa-O-acetyl-sucrose: Preparation of hepta-O-acetylsucroses. *Carbohyd. Res.* **1991**, *222*, 121-129.

92. Tsunekawa, Y.; Masuda, K.; Muto, M.; Muto, Y.; Murai, Y.; Hashidoko, Y.; Orikasa, Y.; Oda, Y.; Hatanaka, Y.; Hashimoto, M., Chemo-enzymatic synthesis of 1'-photoreactive sucrose derivatives via ether linkage. *Heterocycles* **2012**, *84*, 283-290.

93. Smallwood, I. M., *Handbook of organic solvent properties*; Amold: London, 1996.

94. Wong, F. M.; Chan, Y. M.; Chen, D. X.; Wu, W. Convenient one-pot synthesis of *trans*-1,2-diaryloxiranes from the directcoupling of benzyl halides. *Tetrahedron Lett*. **2010**, 51, 6649–6650.

95. Wang, L.; Yoshida, T.; Okamoto, M.; Sakihama, Y.; Hashidoko, Y.;

Hashimoto, M., 2,3-Bis(4-(3-(trifluoromethyl)-3*H*-diazirin-3-yl)phenyl)oxirane, *Molbank,* **2014**, M816.

96. Lanterna, A. E.; Elhage, A.; Scaiano, J. C., Heterogeneous photocatalytic C-C coupling: mechanism of plasmon-mediated reductive dimerization of benzyl bromides by supported gold nanoparticles. *Catal. Sci. Technol.* **2015**, *5*, 4336-4340.

97. Arnold, P. L.; Scarisbrick, A. C.; Blake, A. J.; Wilson, C., Chelating alkoxy-*N*-heterocyclic carbene complexes of silver and copper. *Chem. Commun.* **2001**, 2340-2341.